EXERGY ANALYSIS OF THE URBAN WATER CYCLE: A CASE STUDY OF BRASÍLIA, BRAZIL

VALTRUDES PEREIRA FRANCO

DOCTORAL THESIS IN MECHANICAL SCIENCES

DIRECTOR: PROF. EDGAR AMARAL SILVEIRA, PhD

BRASÍLIA, DECEMBER/2025

UNIVERSITY OF BRASILIA

FACULTY OF TECHNOLOGY

DEPARTMENT OF MECHANICAL ENGINEERING

POSTGRADUATE PROGRAM IN MECHANICAL SCIENCES

UNIVERSIDADE DE BRASÍLIA

FACULDADE DE TECNOLOGIA

DEPARTAMENTO DE ENGENHARIA MECÂNICA

PROGRAMA DE PÓS-GRADUAÇÃO EM CIÊNCIAS MECÂNICAS

ANÁLISE EXERGÉTICA DO CICLO DA ÁGUA URBANA: ESTUDO DE CASO BRASÍLIA, BRASIL

VALTRUDES PEREIRA FRANCO

TESE DE DOUTORADO SUBMETIDA AO PROGRAMA DE PÓS-GRADUAÇÃO EM CIÊNCIAS MECÂNICAS DO DEPARTAMENTO DE ENGENHARIA MECÂNICA, FACULDADE DE TECNOLOGIA, UNIVERSIDADE DE BRASÍLIA (ENM/FT/UnB), COMO PARTE DOS REQUISITOS NECESSÁRIOS À OBTENÇÃO DO TÍTULO DE DOUTOR EM CIÊNCIAS MECÂNICAS, ÁREA DE CONCENTRAÇÃO ENERGIA E AMBIENTE.

APROVADA PELA BANCA EXAMINADORA:

Prof. **Edgar Amaral Silveira**, PhD. PCMEC/ENM/FT/UnB	Orientador	_____
Prof. **Silvio de Oliveira Júnior,** PhD. EPUSP/PME/USP	Examinador Externo	_____
Prof. **Sérgio Botelho de Oliveira,** PhD. DEPT. 2/IFGO	Examinador Externo	_____
Prof. **Mario Benjamim B. Siqueira**, PhD. PCMEC/ENM/FT/UnB	Examinador Interno	_____
Prof. **Flamínio Levy Neto**, PhD. PCMEC/ENM/FT/UnB	Examinador Suplente	_____

DECLARAÇÃO DE ORIGINALIDADE

Declaro que esta Tese resulta do meu próprio esforço e que os trabalhos de outros estão devidamente referenciados e reconhecidos.

CATALOGING DATA

Franco, Valtrudes Pereira

Exergy Analysis of the Urban Water Cycle: A Case Study of Brasília, Brazil. Director: Prof. Edgar Amaral Silveira, PhD. Brasília, 2025. 148 p.

Doctoral thesis in Mechanical Sciences. University of Brasília, 2025.

1. Exergetic analysis; 2. Urban water cycle; 3. Optimization; 4. Energy and water depletion; 5. Environmental impacts.

I Silveira, Edgar A. II. ENM/FT/UnB.

BIBLIOGRAPHIC REFERENCE

FRANCO, V. P. 2025. **Exergetic analysis of the urban water cycle: A case study of Brasília, Brazil**. Departament of Mechanical Engeneering/Faculty of Tecnology/University of Brasília. Brasília, Federal District, Brazil. 148p.

E-mail: valtrudes@gmail.com

_____

Valtrudes P. Franco

"We are comparable to dwarfs standing on the shoulders of giants (the Ancients): we therefore see more than they saw and we see farther than they did. What is the reason for this? It is neither the sharpness of our eyesight nor the superiority of our height, but because we are carried and lifted up by the great stature of giants".

Bernard de Chartrer (1130-1160)

*"*The highest among us is nothing more than someone nearest of the hollowness and uncertainty of everything".

Fernando Pessoa (1888-1935)

"Pray and work, pretending that this life is a day of weeding under a hot sun, which sometimes takes longer to pass, but always does. And you can still have many good moments of joy…

Everyone has their time and their turn: you will have yours".

João Guimarães Rosa (1908-1967)

Good quality water is like health or freedom: it only has value when it runs out.

João Guimarães Rosa (1908-1967)

ACKNOWLEDGEMENTS

To the University of Brasília, through the Postgraduate Program in Mechanical Sciences (PCMEC), for the opportunity to carry out this work;

To my advisor, Prof. Edgar Amaral Silveira, for his competence and dedication, and to Prof. Armando de Azevedo Caldeira Pires, my initial advisor;

To Profs. Flamínio Levy Neto, Sergio Botelho, Silvio de Oliveira Junior, and Mario Benjamim for the virtuosity of the examining board; Profs. Taygoara Felamingo de Oliveira and Eder Lima de Albuquerque for their encouragement and support for my continuation in the program, and to Profs. Jair Dinoah and Katia Azevedo for motivating the completion of this work;

To my colleagues at CAESB for their support, encouragement, and operational data on the CAU systems in Brasília;

Finally, to my family and friends who understood, were supportive of the effort to complete this doctorate, and cheered for its completion.

Thank you all.

AGRADECIMENTOS

À Universidade de Brasília, através do Programa de Pós-Graduação em Ciências Mecânicas (PCMEC), pela oportunidade de realizar este trabalho;

Ao meu orientador Prof. Edgar Amaral Silveira pela competência e dedicação como tal e ao Prof. Armando de Azevedo Caldeira Pires, orientador inicial;

Aos Profs. Flamínio Levy Neto, Sergio Botelho, Silvio de Oliveira Junior e Mario Benjamim pelo virtuosismo da banca examinadora; Profs. Taygoara Felamingo de Oliveira e Eder Lima de Albuquerque pelo incentivo e apoio à minha continuidade no programa, e aos Profs. Jair Dinoah e Katia Azevedo por motivarem a conclusão deste trabalho;

Aos Colegas da CAESB pelo apoio, estímulo e dados operacionais dos sistemas do CAU de Brasília;

Finalmente, aos meus familiares e amigos que compreenderam, foram solidários ao esforço para realizar este doutoramento e torceram pela conclusão.

Grato a todos.

ABSTRACT

Urban water supply and sewage systems must operate in a way that guarantees service to the population, optimizing the consumption of resources, environmental impacts, and energy depletion. Seeking to contribute to this goal, this thesis studied the applicability and reliability of exergy analysis as a diagnostic tool in the urban water cycle systems of Brasília, Federal District, Brazil. A bibliometric review conducted in the Scopus and Web of Science databases revealed a growing interest in applying the concept of exergy to the exergy-urban water nexus in water cycle systems and formed the basis for the study's methodology. Using operational data from both systems provided by CAESB, the steady-state processes were modeled, and mass, energy, and exergy balances were performed. In the city's water supply system, 2,461 m^3 s^{-1} of raw water are collected, 17.6% are lost in the distribution of treated water, and 72.1% return to the environment, closing the water balance. The electricity demand is 10.68 MW, with an energy intensity of 4.34 kWh m^{-3} and a specific energy of 3.6 W $inhabitant^{-1}$. Raw water pumping dominates the thermodynamic profile, where approximately 60% of the total exergy is destroyed and efficiencies range between 59.8% and 76.1%. At the water treatment plant, the exergy efficiency is 7.6%, with 53.6% of the incoming exergy related to chemical reagents, of which 82.9% is destroyed by internal irreversibilities. In treated water distribution, the exergy efficiency of pumping is 70.7%, and losses represent 43%, equivalent to 260 kW of useful pumping exergy. In the sewage system, wastewater treatment is the most dissipative stage of the cycle due to biochemical oxidation. The overall exergy efficiency of the Brasília's UWC remained around 69–70% throughout the operational chain. Analyses indicated that strategies such as modernization of old pumps, reduction of treated water losses, and recovery of biogas generated in wastewater treatment plants (WWTPs) can significantly improve the operational performance of the both systems and the exergy efficiency of the cycle. The exergy analysis method, combined with the evaluation of process emissions, proved effective in identifying bottlenecks, guiding operational improvements, and promoting more rational use of resources. Finally, the study offers a replicable quantitative methodology capable of identifying critical points, supporting optimization actions, and contributing to the reduction of environmental impacts on the urban water cycle.

KEYWORDS: Exergy analysis; urban water cycle; optimization; energy and water depletions.

RESUMO

Os sistemas de abastecimento de água e de esgotamento sanitário do ciclo da água urbana (CAU) devem operar de forma a garantir atendimento à população, otimizando o consumo de insumos, impactos ambientais e depleções de energia. Buscando contribuir neste sentido, na presente tese foi estudada a aplicabilidade e a confiabilidade da análise exergética como ferramenta de diagnóstico nos sistemas do CAU de Brasília, Distrito Federal, Brasil. Revisão bibliométrica feita nas bases Scopus e Web of Science revelou um crescente interesse da aplicação do conceito de exergia ao nexo exergia–água urbana nos sistemas do ciclo e embasou a metodologia do estudo. Com dados operacionais de ambos sistemas fornecidos pela CAESB, foram modelados os processos em regime permanente e efetuados os balanços de massa, energia e exergia. No sistema de abastecimento da cidade, 2,461 $m^3\ s^{-1}$ de água bruta são captados, 17,6% são perdidos na distribuição de água tratada e 72,1% retornaram ao meio ambiente, fechando o balanço hídrico CAU. A demanda de eletricidade é de 10,68 MW, com intensidade energética de 4,34 kWh m^{-3} e energia específica 3,6 W habitante^{-1}. O bombeamento de água bruta domina o perfil termodinâmico, onde cerca de 60% da exergia total é destruída e eficiências entre 59,8% e 76,1%. Na ETA, a eficiência exergética é 7,6%, sendo 53,6% da exergia de entrada relativa a reagentes químicos da qual 82,9% é destruída por irreversibilidades internas. Na distribuição de água tratada, a eficiência exergética do bombeamento é 70,7% e as perdas representam 43%, equivalendo a 260 kW da exergia útil de bombeamento. No sistema de esgotamento sanitário, o tratamento de efluentes é a etapa mais dissipativa do ciclo devido à oxidação bioquímica. A eficiência exergética global do CAU de Brasília, manteve-se em torno de 69–70% ao longo da cadeia operacional. As análises indicaram que estratégias como modernização de bombas antigas, redução de perdas de água tratada e recuperação do biogás gerado nas ETEs podem melhorar significativamente o desempenho operacional dos sistemas e a eficiência exergética do ciclo. O método da análise exergética, aliada à avaliação das emissões dos processos, mostrou-se eficaz para identificar gargalos, orientar melhorias operacionais e promover o uso mais racional de recursos. Por fim, o estudo oferece uma metodologia quantitativa replicável, capaz de identificar pontos críticos, subsidiar ações de otimização e contribuir para a redução de impactos ambientais no ciclo da água urbana.

PALAVRAS-CHAVE: Análise exergética; ciclo da água urbana; otimização; depleções de energia e água.

SUMMARY

PRESENTATION OF THE THESIS STRUCTURE

This thesis presents the conceptual and methodological framework that underpins the exergetic analysis of the urban water cycle (UWC) applied to the case of Brasília, Brazil, addressed through two scientific articles that constitute the analytical core of the work, and is structured by the following two main chapters.

Chapter One brings together the essential elements that provide the conceptual and methodological basis necessary for understanding the models, indicators, and procedures employed. This foundation is structured around three main components:

• Introduction: contextualizes the problem, presents the scientific and operational relevance of applying exergy analysis to the UWC, and defines the general and specific objectives of the research.

• State of the Art: encompasses the bibliometric and systematic review on the exergy–urban water nexus, covering studies applied to water supply and wastewater systems as well as the literature related to greenhouse gas (GHG) emissions in sanitation processes.

• General Considerations, Limitations and Perspectives: this section, concluding Chapter One, provides an interpretative synthesis of the results obtained in the two articles that compose the thesis. It highlights the main insights of the research, the environmental implications identified, the aspects requiring improvement, and the methodological limitations that influence the interpretation of the findings. By synthesizing these elements, the section bridges the theoretical foundations and practical application, guiding the reader toward the developments presented in Chapter Two.

Chapter Two comprises the two scientific articles developed as part of the thesis. The first article presents the exergy analysis of the Brasília water supply system, examining the thermodynamic performance of the abstraction, treatment, pumping, and distribution stages. The second article, already published in an international journal (https://doi.org/10.1016/j.jclepro.2025.146057), provides the exergy and environmental assessment of the wastewater system, with emphasis on biological processes, GHG emissions, and resource recovery potential.

Finally, supplementary materials are provided, including operational data, exergy calculations, equipment selection information, and other elements that ensure the research's rigor, transparency, and reproducibility.

CHAPTER ONE

1 INTRODUCTION

The expansion of scientific knowledge, particularly from the nineteenth century onward, laid the foundation for the development of technologies based on petroleum and electricity for powering machines, new modes of transportation, industrial and agricultural production, the exploitation of natural resources, communication systems, heating, cooling, and lighting. These advances enabled increased food production, greater availability of consumer goods, improvements in urban infrastructure, health, and education, thereby transforming the economic and social foundations of humanity.

Despite the occurrence of wars, epidemics, and natural disasters during this period, technological progress, the availability of new energy sources, and the intensive exploitation of natural resources (such as freshwater, minerals, metals, and timber) contributed to global population growth from an estimated 1.3 billion inhabitants in 1850 to 8.09 billion in 2025, concentrated mainly in urban areas. Conversely, climate change has been triggering environmental alterations and reducing the availability of natural resources, especially freshwater, which is essential for human and animal hydration, food production, and other anthropogenic activities (UN, 2025). The sustainability of cities, in addition to basic inputs, fundamentally depends on water supply and wastewater systems, which constitute the urban water cycle (UWC), illustrated by the Fig. 1.1.

The operation of these systems requires chemical products, materials, fuels, and specialized labor as inputs, as well as significant amounts of electricity for abstracting raw water from surface or groundwater sources, transporting it to water treatment plants (WTPs), and performing the treatment, conveyance, storage, and distribution of potable water to consumers (blue color in Fig. 1.1). Subsequently, wastewater must be collected from residential, commercial, and industrial users, conveyed to wastewater treatment plants (WWTPs), and discharged as treated effluents and solid residues in a manner that causes minimal environmental impact (brown and grey colors in Fig. 1.1), thereby preserving public health and the environment. According to ANA (2022), 80% of water supplied becomes wastewater, treated or not, which is discharged into water bodies where nature struggles to restore it to its original potable state.

Wastewater is the liquid residual resulting from domestic and industrial discharges, infiltration water, and parasitic stormwater inflows into the sewerage system, with its quantity and characteristics varying according to water consumption, season of the year, day of the week, time of the day, and place of origin, according to Brazilian Norm NBR 9648 (1986).

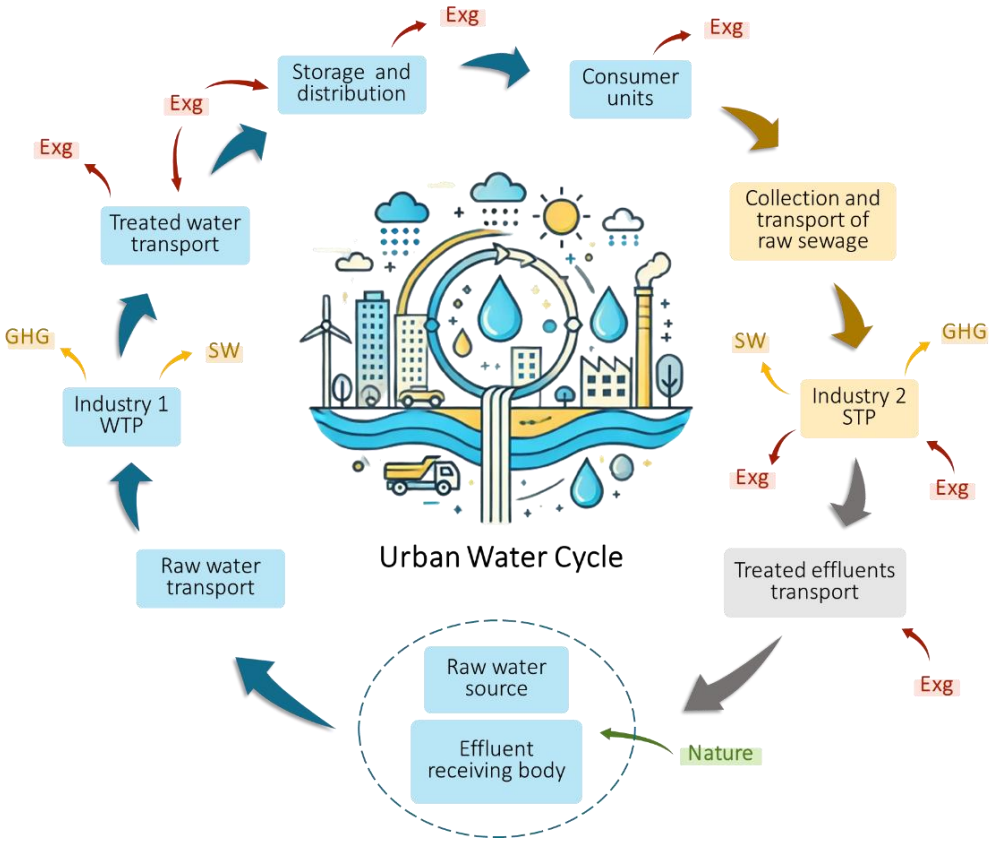

Figure 1.1 – General model of the conventional urban water cycle and the associated flows of solid waste (SW), (GHG), and exergy (EXG). Source: the Author.

Water supply systems generally consume the largest share of electricity and inputs within the urban water cycle, a condition exacerbated by the high levels of treated water losses. For example, in 2022 the national average loss of treated urban water in Brazil reached 37.8%, according to the SNIS (2023), resulting in proportional depletions of electricity, chemicals and other treatment inputs, in addition to avoidable environmental impacts. In that year, water supply systems consumed 12.6 TWh of electricity - about 2.47% of the 509.6 TWh of electricity consumed in the country, according to the 2025 National Energy Balance (EPE, 2025), and the losses amounted to 4.76 TWh.

These factors highlight the need for more effective and optimized operational control of water and wastewater systems. Moreover, although nearly all Brazilian municipalities have water supply systems, there remains a substantial deficit in wastewater collection and treatment infrastructure. Even where such systems exist, the quality of treatment is often inadequate, resulting in significant sanitary and environmental impacts (SNIS, 2023). Thus, assessing the nexus among energy, water, inputs, materials, and waste through reliable methods capable of quantifying and locating depletions, optimizing installed capacity, and identifying opportunities for performance improvement contributes to mitigating freshwater scarcity and preserving water sources, the environment, and public health.

One well-established assessment method is the analysis of open thermodynamic systems based on the two laws of thermodynamics, or energy-exergy analysis, which allows for comparison and quantification of exergy relationships relative to an ideal case, the exergy efficiency of processes, the identification of recoverable exergy (where and how energy consumption can be reduced), the technological potential, and the environmental and economic improvements. Therefore, it enhances process optimization and constitutes a more precise analytical tool.

The conventional UWC is an open thermodynamic system characterized by intensive energy, environmental, and economic interactions, making it suitable for such an analytical approach.

The literature review indicates a growing number of scientific articles applying exergy analysis to seawater desalination plants for urban supply, WWTPs, and river water quality assessments, with results validating the method's applicability in these contexts. However, no studies were found applying the methodology simultaneously to both systems of the conventional UWC, services typically provided by urban sanitation utilities. This gap presents an opportunity to evaluate the method's effectiveness and reliability in optimizing and mitigating depletions of water, energy, inputs, emissions, and environmental impacts within the operational processes of the cycle.

The central hypothesis of this thesis is that exergy analysis, when systematically applied to the processes of the conventional UWC, is capable of accurately identifying where and how energy, water, chemical inputs, and environmental quality are depleted, thus providing a more precise and comprehensive basis for optimizing operational performance in water and wastewater systems. Under this hypothesis, exergy offers a unified thermodynamic–environmental metric able to reveal inefficiencies that are not fully captured by traditional energy, hydraulic, or operational indicators.

Based on this premise, the research seeks to answer the following guiding questions:

- Where along the UWC do the main exergy depletions occur, and what operational, hydraulic, or biological mechanisms drive them?
- To what extent can exergy efficiency and destroyed exergy quantify environmental impacts associated with water treatment, wastewater treatment, and resource consumption?
- How do usual and optimized operating conditions compare in terms of exergy performance, emissions, and resource use?
- Which process failures or inefficiencies represent the greatest opportunities for

improving the energy–environmental performance of the UWC?

- Can exergy analysis be consolidated as a reliable and practical management tool for water and sanitation utilities?

This hypothesis and its guiding questions establish the scientific foundation for the objectives of the thesis and orient the development of the models, indicators, and analytical procedures presented in the following sections. To investigate this hypothesis, dedicated process models were developed for both subsystems of the UWC, enabling the systematic application of exergy analysis across the abstraction, treatment, distribution, collection, and wastewater treatment stages. These models were subsequently validated through a comprehensive case study of the conventional UWC of Brasília (15°47'41.033"S and 47°52'57.151"W), Federal District, Brazil, ensuring coherence between the theoretical framework and the real operational conditions of the systems.

1.1 General Objective

To consolidate and validate the application of exergy analysis to the processes of the conventional UWC, to quantify and mitigate depletions of energy, water, chemical inputs, and environmental impacts, and to support the optimization of operational performance in water and wastewater systems.

1.2 Specific Objectives

a) To develop and apply thermodynamic–environmental models and indicators capable of characterizing exergy flows, depletions, and environmental implications in the systems of the conventional UWC.

b) To calculate and compare exergy efficiency, destroyed exergy, and associated environmental impacts under usual and optimized operating conditions, encompassing WTPs and WWTPs.

c) To diagnose operational inefficiencies and process failures, identifying where and how exergy destruction, resource consumption, losses, and emissions occur, and to propose improvements that enhance the energy and environmental performance of the UWC.

2 ESTATE OF THE ART

2.1 Systematic Literature Review on the Exergy–Urban Water Nexus

To support the development of this thesis, a systematic literature review was conducted focusing on studies that relate exergy, water, and environmental performance to the drinking water supply and wastewater systems of the conventional UWC. The objective was to evaluate

the maturity of existing approaches, the models and methods employed, their temporal evolution, and their scientific relevance, while avoiding methodological inconsistencies in the application of exergy analysis.

The search for publications was conducted in the curated databases Web of Science (WoS) and Scopus, using keyword sets and logical operators to exclude articles outside the study's scope. To organize and map the retrieved publications before the bibliometric analysis, the post-processing tools of each database and the Science Mapping Analysis Tool (SciMAT) software, version 1.1.04, were used, according to the recommendations of Cobo et al. (2012) and the methodological procedures described by Pegorin; Theisen (2019).

2.1.1 Search Terms and Retrieved Results

Initial searches using the keywords (exerg AND water) * in WoS and Scopus for the period 1997–2022 returned 6,414 and 5,889 references, respectively, including articles, conference papers, review articles, book chapters, editorials, and books. These volumes rendered an objective and targeted analysis unfeasible.

To refine the dataset and eliminate publications outside the scope of the research, the following logical expression was applied: (exerg*AND water) AND ("urban water" OR "urban water cycle" OR "drink* water" OR "fresh water" OR "potable water" OR "water quality indicators" OR sewer* OR sewage OR wastewater OR sanitation) AND NOT (desalin* OR distil* OR solar OR osmosis OR heat* OR cooling OR power OR boiling OR coal OR combustion OR drying OR hydrogen OR soil OR landscape OR lakes OR wetland* OR industrial OR strogen).

After refinement, the number of publications was reduced to 38 (WoS) and 47 (Scopus), totaling 85 articles up to 2022. A subsequent search in 2023 using the same terms identified 3 additional articles in WoS and 5 in Scopus, leading to a final dataset of 93 publications.

2.1.2 Pre-processing of Results

Figure 2.1(a) presents the annual distribution of the 93 articles published between 1997 and 2023 in the Scopus and WoS databases, highlighting the growing scientific interest in the exergy–urban water nexus.

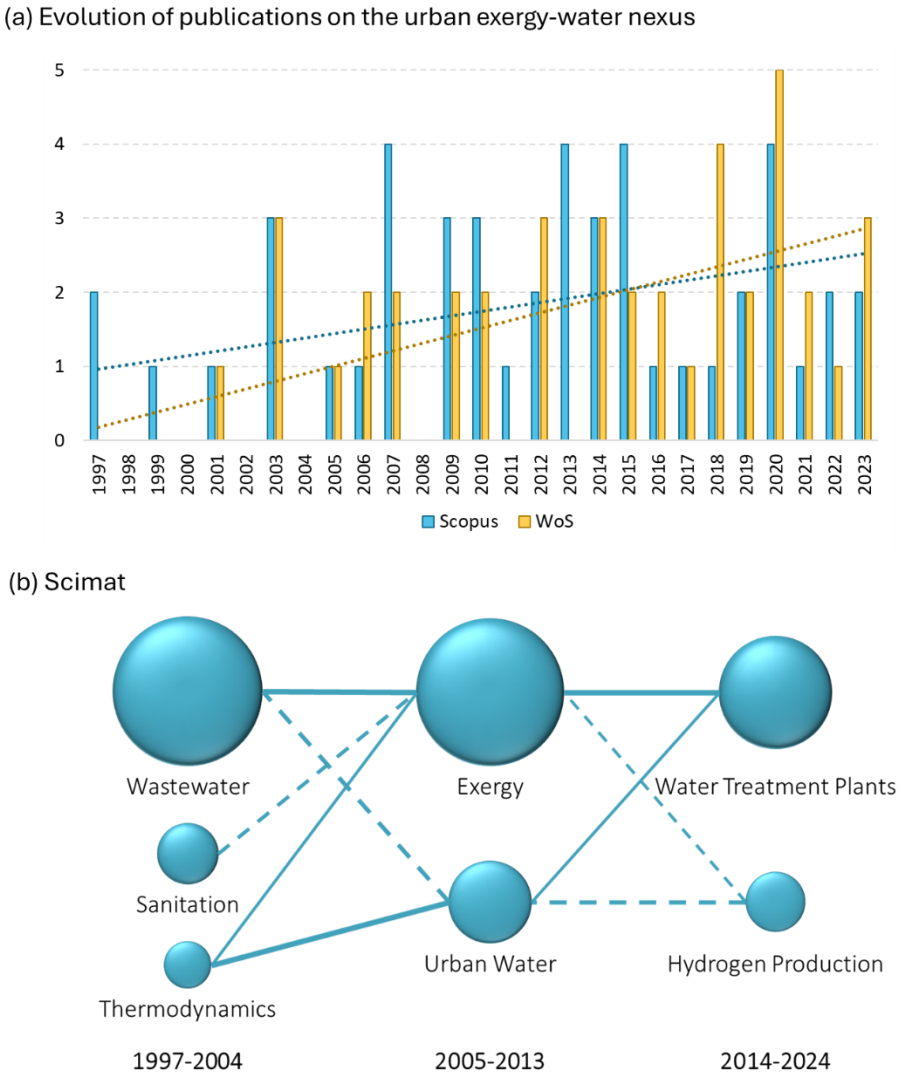

Figure 2.1 – (a) Annual evolution of publications related to the exergy–urban water nexus according to Scopus and WoS databases for the final keywords. (b) maps of the main themes in publications between 1997 and 2023 based on the h-index method. Source: Author and SciMAT.

Subsequently, the abstracts of all retrieved articles were screened for relevance, adherence to the exergy–urban water nexus, and alignment with the thesis objectives. Duplicate articles across databases and studies that, despite mentioning exergy, water, or wastewater, clearly addressed topics outside the scope were excluded. As a result, out of the 93 initial articles, 63 were removed, leaving 30 articles eligible for bibliometric and thematic analysis.

2.1.3 Configuration, Normalization, and Thematic Network Mapping

The 30 selected articles were analyzed using SciMAT with the h-index configuration, divided into three intervals: 1997–2004, 2005–2013, and 2014–2023. This approach enabled the evaluation of author productivity, article impact (citation counts), and the evolution of thematic clusters associated with the "Exergy–Urban Water" relationship. Figure 2.1(b) shows

the thematic evolution map for the three periods.

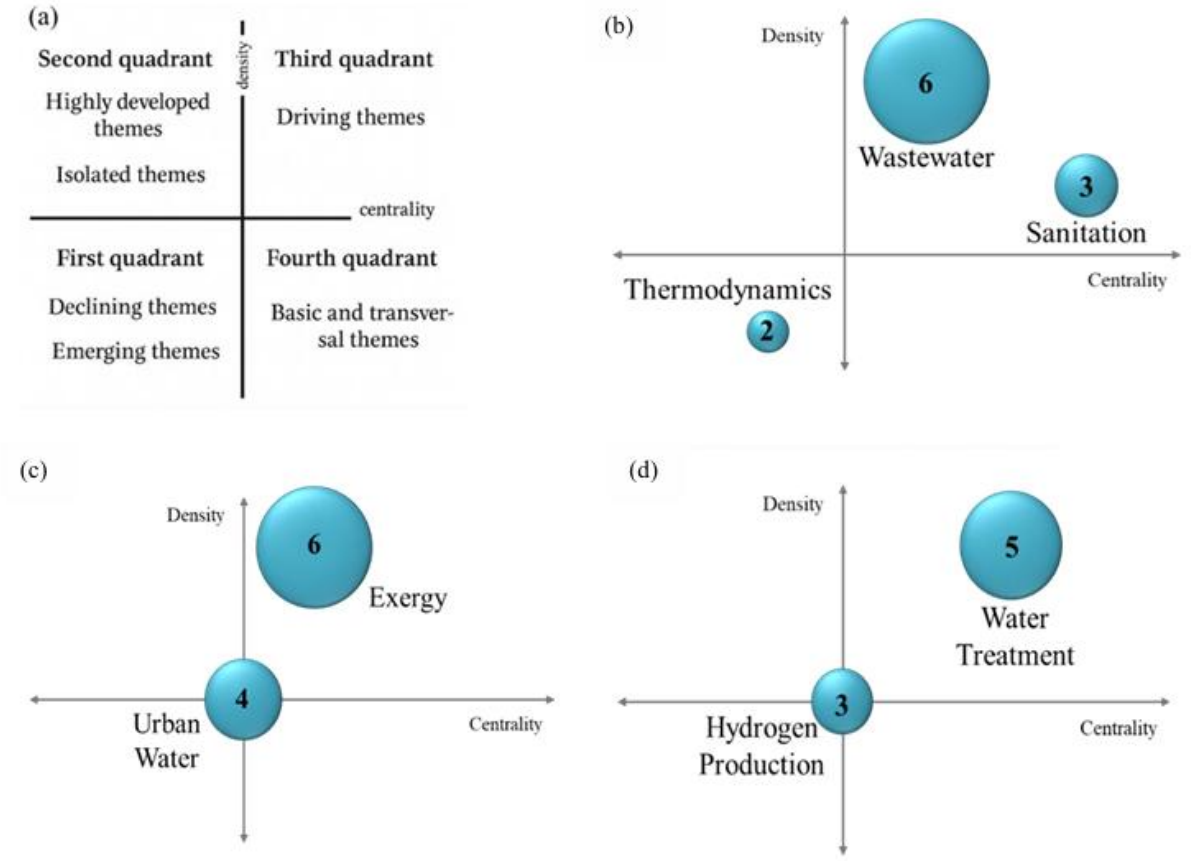

Figure 2.2 – (a) Strategic diagram of themes. The vertical axis, density, represents the internal cohesion of the cluster, and the horizontal axis, centrality, reflects the cluster's interactions with other clusters, indicating its relevance to the broader research field. (b) Strategic diagram for keywords in 1997–2004. (c) Strategic diagram for keywords in 2005–2013. (d) Strategic diagram for keywords in 2014–2023. Source: SciMAT.

A total of eight clustering tests were required to obtain a thematic grouping that reliably represented the exergy–urban water nexus. The overlap map revealed that among the 17 initial themes with strong presence between 1997 and 2004, 5 disappeared or significantly decreased, while 12 remained in 2005–2013. In this second period, 3 new themes were added and 3 were discontinued. In the third period (2014–2023), 12 themes persisted, and 4 new themes emerged. Across the entire timeline, 7 new themes were incorporated and 8 declined, resulting in 16 active themes by 2023. Figure 2.2(a) presents the strategic diagram (density vs. centrality) of the thematic clusters. Meanwhile, Figures 2.2(b), 2.2(c), and 2.2(d) display the strategic diagrams for each period.

In the 1997–2004 period, “Wastewater” and “Sanitation” emerged as motor themes, strongly linked to “Exergy” and “WWTPs,” while “Thermodynamics” appeared associated

with “Optimization” and “Urban Water.”

In 2005–2013, the motor theme shifted to “Exergy,” connected to “WWTPs,” “Sewage,” “Drinking Water Treatment Plants (DWTPs),” and “Environment,” whereas “Urban Water” emerged as a central linking theme.

In 2014–2023, “DWTPs” became the dominant theme, linked to “Exergy,” “Urban Water,” “Water,” “WWTPs,” “Wastewater,” and “Energy,” while “Hydrogen Production” appeared as a central theme related to energy recovery processes in WWTPs.

2.1.4 Exergy- and Urban Water–Related Articles

Of the 30 articles associated with the thematic clusters, the following were excluded for addressing content outside the scope of this thesis, despite their partial relevance: Austoni *et al*. (2007); Li *et al.* (2009); Marcuello *et al.* (2012); Wasilievski *et al.* (2018); Aydin *et al.* (2021); Zeng *et al.* (2017); Chatzipaschali; Stamatis (2015) e Rodríguez-Merchan *et al.* (2019)

During 1997–2004, “Exergy” was strongly associated with “Wastewater Treatment Plants,” as shown in the studies by Dewulf *et al.* (2001), Wilsenach *et al.* (2003), Hellström, (1999), Armando *et al* (2003), Hellström (2003), Hellström; Kärrman (1997), Ptasinski *et al.* (1997)

In 2005–2013, the theme evolved toward “Urban Water,” with notable contributions from Huang et al. (2007) and Martinez; Uche (2010) and later returned to WWTP-related applications Lamas *et al.* (2009), Lamas *et al.* (2010), Khosravi; Panjeshahi; Atei (2013), Lamas, (2013), Oliveira Jr (2013), Mora Bejarano; Oliveira Jr, (2008), Mora Bejarano (2009), Mora Bejarano; Oliveira Jr (2005).

From 2014–2023, the exergy theme connected strongly to “Drinking Water Treatment Plants” and urban supply systems Bilgen; Bulut (2014), Bylka; Mróz (2020) and Rodríguez-Merchan *et al.* (2021), as well as to environmental and effluent-quality indicators in WWTPs Abusoglu *et al*. (2017) and Fitzsimons *et al.* (2016).

Several studies within the dataset addressed exergy applied to source-water or receiving-water quality, including Armando *et al.* (2003), Huang *et al.* (2007), Rodríguez-Merchan *et al.* (2019) and Stanek *et al.* (2017) focused specifically on urban drinking water in Chile, comparing desalinated water, surface withdrawals, and deep groundwater. Bylka; Mróz (2020) examined a generic urban water distribution system.

After filtering out papers outside the thesis's scope, the systematic review identified the studies most closely aligned with the exergy–urban water nexus and its environmental dimension. For the drinking water supply subsystem, the most relevant contributions were those

of Bylka; Mróz (2020), Rodríguez-Merchan *et al.* (2021) and Stanek *et al.* (2017). For wastewater systems, the key studies were Fitzsimons *et al. (*2016), Hellström (1999), Khosravi; Panjeshahi; Atei (2013), Mora Bejarano; Oliveira Jr. (2008) and Wilsenach *et al.* (2003).

Consistent with the discussion in Chapter 1, the systematic review confirmed that no existing study addressed, in a sequential and integrated manner, all stages and processes of both drinking water supply and wastewater treatment within a conventional Urban Water Cycle. This conceptual and methodological gap substantiates the need for the integrated exergy analysis developed in this thesis.

The articles selected in this section reflect the current state of the art in the exergy analysis of UWS systems, serving as the basis for the systematic analysis of the exergy–water nexus in both the drinking water supply system and the wastewater system.

2.1.5 Exergy–water nexus in urban water supply

The studies related to the water–exergy nexus in potable water supply systems are detailed in this section. In order to highlight the critical role of water resources in regions of Chile, Rodríguez-Merchan *et al.* (2021) used the cumulative exergy consumption indicator (CE_{xC}), Equation (2.1), defined as the sum of the exergy of all resources required to provide a service or product, as proposed by Szargut (2005), assigning it to freshwater and to the energy required by system installations throughout their entire life cycle.

$$CE_xC_{l,k} = \frac{\sum_{i,j}(Ex_{E_{i,j}} + Ex_{W_{i,j}})}{F_u} \quad (2.1)$$

Here, $Ex_{E_{i,j}}$ ($MJ_{ex}\ m^{-3}$) are associated with the energy of treated water and $Ex_{W_{i,j}}$ (MJ_{ex}) with the water entering the system, either directly (i) or indirectly (j), depending on the type of pumping (l) and treatment technology (k). Fu is the functional unit for treated water (1 m^3).

The authors also employed the WSI metric (water stress index), defined as the ratio between total water use and availability, as well as the BWF (blue water footprint). The indicator $CE_xC_{l,k}$ accounts for the exergies related to the energy consumed in potable water supply ($E_{i,j}$) and water production ($W_{i,j}$), as proposed by Dincer; Rosen (2013). The exergy of the electricity consumed corresponds to the energy required in the pumping and water treatment stages, following the approach used by Szargut (2005). The exergy of the annual water flow estimated for treatment in WTPs is determined using Equation (2.1), neglecting the potential, kinetic and physical energies of the water flow relative to the reference environment, resulting in only the chemical component ($Ex_{W_{i,j}}$) from Equation (2.2).

$$Ex_w = Ex_w^0 \times m_w \tag{2.2}$$

Here, Ex_w is the chemical exergy rate contained in water flows ($MJ_{ex}\ year^{-1}$); Ex_w^0 is the standard chemical exergy of freshwater (5×10^{-8} $MJ_{ex}\ m^{-3}$), following Szargut (2005), and m_w is the annual flow of pumped water reaching the WTP ($m^3\ year^{-1}$).

Thus, the high values obtained for CE_xC result from the higher consumption of water and energy, increasing the pressure on these resources and reducing the efficiency of the water–energy nexus.

The water bodies or water resources of an urban water supply system and a WTP were evaluated exergetically by Bylka; Mróz (2020) using QGIS and Python scripts, based on the Gouy–Stodola Theorem and the model presented by Stanek *et al.* (2017). Their approach relies on the specific exergy of water (E_{H_2O}), given by Equations (2.3).

$$E_{H_2O} = E_t + E_m + E_{ch,f} + E_{ch,c} + E_k + E_p \tag{2.3}$$

where E_t is thermal exergy (J); E_m is mechanical exergy (J); $E_{ch,f}$ is chemical exergy (J); $E_{ch,c}$ is concentration exergy (J); E_k is kinetic exergy (J); and E_p is potential exergy (J). Using quantitative flow components and qualitative components of total specific exergy (temperature, pressure, elevation, velocity, concentration, composition, and liquid incompressibility), they calculated exergy destruction in transformations of chemical reactions, heat transfer processes, mass flow, hydraulic friction, mechanical friction, diffusion, and the irreversibility associated with entropy generation. The expanded physical and chemical terms of this equation result in Equation (2.4).

$$\begin{aligned} E_{H_2O} = {} & c_{pH_2O}\left[T - T_0 - T_0 \ln\left(\frac{T}{T_0}\right)\right] + v_{H_2O}(p - p_0) \\ & + \left[\sum_i y_i\,(\Delta G_{fi} + \sum_e n_e E_{ch,n_e})_i\right]_p + RT_0 \sum_i x_i \ln\left(\frac{a_i}{a_0}\right) \\ & + \frac{1}{2}\left(\frac{C^2 - c_0^2}{1000}\right) + g(z - z_0) \end{aligned} \tag{2.4}$$

where c_{pH_2O} is the specific heat at constant pressure; T and T_0 are the absolute temperatures of the water and the reference environment (K); v_{H_2O} is the specific volume of water ($m^3\ kg^{-1}$); p and p_0 are the system and reference pressures (Pa); y_i is the number of moles of substance i divided by the total mass of the solution; ΔG_{fi} is the standard Gibbs free energy of formation of species i; n_e is the number of moles of element e forming species i, E_{ch,n_e} is

the specific chemical exergy of element e (J mol^{-1}), ; x_i is the molar fraction of species i; $a_i$and $a_0$are the activities of species i in the system and in the reference environment; R is the universal gas constant (J mol^{-1} K^{-1}); C and $C_0$are the velocities of the water stream and the reference state (m s^{-1}); z and z_0 denote the elevations of the stream and reference level (m); and g is the gravitational acceleration (m s^{-2}). The subscript 0 indicates the thermodynamic properties of the reference water environment.

Chemical, thermal, and potential terms may be estimated or disregarded when applied, for example, to river water. The total exergy of a water resource (E_{H_2O}) represents the minimum energy required to restore it relative to a reference environment (RE), such as seawater, since both are part of the natural water cycle. Organic matter cannot be neglected. Freshwater exhibits two unusual physical characteristics: its distinct composition, which differs from the surrounding environment, and its specific distribution, which defines its concentration level; both intrinsic properties can be assessed through exergy analysis.

Mass and exergy balances within control volumes, applying Equation (2.4) to the inlet and outlet of water sources, pumps, pipelines, WTP devices, storage tanks, distribution network nodes and valves, show that the greatest exergy destruction occurs due to excessive pressure in the water distribution networks and in the WTP pumps. Exergy analysis proves more precise and useful for evaluating and planning the modernization of supply systems compared to conventional energy-based methods.

Stanek *et al.* (2017) evaluated the different exergy components of a water body and their relevance depending on the system or process in which water is used. A new reference environment was introduced to achieve a more accurate assessment of the chemical exergy of these resources, reaffirming the value of water for the planet. The goal of the assessment was to restore the natural state of water bodies according to European environmental legislation. Moreover, they discussed the most practical way to include the chemical exergy of organic matter in water bodies, highlighting its importance particularly in surface waters.

2.1.6 Exergy–wastewater nexus

Wilsenach *et al.* (2003) argue that the exergy analysis of the integrated management of potable water, surface water, energy, and nutrient assets reveals pathways to make wastewater management more sustainable, providing an effective method to quantify different recoverable resources such as energy and nutrients. Diluting wastewater does not reduce pollution; it merely destroys exergy and increases the cost of effluent treatment. Therefore, wastewater streams should be kept as concentrated as possible, which facilitates the recovery of energy and valuable minerals, such as the recovery of struvite (magnesium–ammonium–phosphate crystals) from

urine and the treatment of ammonium-rich streams. A gradual shift toward nutrient removal and recovery can be incorporated into existing WWTPs, minimizing exergy losses and making water and waste management more efficient and sustainable.

Three different wastewater treatment systems in Sweden were analyzed exergetically by Hellström (1999). The first consisted of conventional sewage collection, nitrogen removal, biological and residual chemical treatment, anaerobic digestion, and sludge dewatering. The second included separate collection of urine and feces in specific toilets, with conventional treatment of the remaining domestic wastewater. The third system separated urine and blackwater (feces, flush water and toilet paper) into distinct fractions, with treatment either centrally at WWTP or on-site.

Urine, which contains approximately 80% of nitrogen and 50% of phosphorus excreted by humans, is separated and stored by gravity in underground tanks adjacent to buildings. It is later collected and transported by trucks to nearby farms for agricultural use. Blackwater is collected via low-pressure vacuum systems and stored in dedicated tanks, then transported either through a higher-pressure system or by trucks to anaerobic digesters at WWTP for treatment and methane production. Promising results indicate that urine separation combined with enhanced chemical or biological phosphorus removal increases the overall efficiency of nutrient removal from wastewater. The general exergy analysis model for organic matter and nutrients follows the logic:

Inputs: (a) wastewater (organic matter and nutrients); (b) WWTP operation (including wastewater and solids transport, chemicals, electricity, etc.); (c) waste transport (fuel).

System: wastewater collection and treatment processes.

Outputs: (a) waste (biosolids, urine, methane gas, etc.); (b) losses (discharge to receiving bodies).

Total exergy was lower when urine and feces were separated at the source compared to the conventional nutrient-recovery treatment system. Significant exergy consumption occurs in the transport and dispersion of urine, although this can be reduced when source separation is adopted. The highest potential for exergy recovery arises from the increased number of useful residuals; conversely, exergy recovery decreases when wastewater is excessively diluted or when the urban population is large.

In the exergy balance of the model, given by Equation (2.5), modified from Equation (2.3), the total exergy destroyed in the treatment process (E_T) is the difference between the

exergy entering the system (E_e), or the exergy contained in wastewater (E_{es}), the exergy added to operate the treatment unit (E_{ro}), the exergy required for waste transport (E_{tr}), the exergy at the system outlet (E_s), the exergy discharged into receiving water bodies (E_n), the exergy of useful residues (E_{ru}) in dewatered sludge and the exergy of nutrients and methane gas produced (E_n):

$$E_T = E_e - E_s = (E_{es} + E_{ro} + E_{tr}) - (E_{ru} + E_n) \quad (2.5)$$

The study by Mora Bejarano; Oliveira Jr (2009) evaluated two wastewater treatment plants in São Paulo using the environmental exergy efficiency index ($\eta_{env,ex}$) and the total environmental pollution rate ($R_{pol,t}$), given by Equations (2.6) and (2.7), originally proposed by Kotas (1985) and applied by Makarytchev (1997) and Mora Bejarano; Oliveira Jr (2004). Considering negligible temperature variations of the liquid wastewater, negligible difference in geometric elevation between inlet and outlet, and negligible flow velocity changes in the WWTP, mechanical exergy (thermal, potential, and kinetic) was neglected. Thus, environmental sustainability indicators were determined based solely on the chemical exergy of organic matter, nutrients, coagulants, produced sludge and toxic metals.

The theoretical potential for future improvements in a natural resource treatment process is indicated by environmental exergy efficiency ($\eta_{env,ex}$), given by Equation (2.6):

$$\eta_{env,ex} = \frac{E_{prod}}{E_{nat,res} + E_{prep} + E_{Deact} + E_{Disp}} \quad (2.6)$$

where E_{prod} is the exergy of the process associated with useful effect; $E_{nat,res}$ is the exergy of the natural resource consumed in the process; E_{prep} is the exergy required for natural resource extraction and preparation; E_{Deact} is the exergy of additional natural resources destroyed during waste deactivation; and E_{Disp} is the exergy related to waste disposal. All terms are expressed in kW.

The environmental pollution rate, Equation (2.7), defined as the ratio between the exergy associated with the process wastes (contained in solids, rejected heat, emissions and the exergies defined above) and the exergy of the useful effect (E_{prod}), is also expressed in kW:

$$R_{pol,t} = \frac{E_{waste} + E_{Deact}}{E_{prod}} \quad (2.7)$$

The results of the exergy and environmental performance, as well as the exergy destruction in the processes of the two WWTPs analyzed by Mora Bejarano; Oliveira Jr (2009), indicated that the environmental exergy efficiency ($\eta_{env,ex}$) of both plants is reduced due to the

high electricity consumption required to obtain the final product, the non-utilization of methane as a fuel, and the lack of use of sludge for agricultural purposes. Otherwise, efficiency would increase and the pollution rate would decrease. Thus, the analysis of the exergy required for wastewater residue deactivation is a useful tool that quantifies and optimizes the environmental impact and performance of energy conversion processes and offers insights for economic assessments, although it remains limited for evaluating toxicity and the biological quality of substances.

The thermodynamic efficiency of the Qods wastewater treatment plant in Iran, which treats sewage from 85,000 inhabitants, was evaluated by Khosravi; Panjeshahi; Atei (2013) after modifications to the primary and secondary clarifiers and to the effluent quality. The assessment was based on the qualitative chemical exergy of biochemical oxygen demand (BOD) and chemical oxygen demand (COD) in wastewater and on the sustainability indicator for the treatment system ($\eta_{env,ex}$ and $R_{pol,t}$).

The plant follows a conventional configuration, consisting of preliminary treatment with screens, primary treatment in primary clarifiers, secondary treatment in aeration tanks and secondary clarifiers, followed by sand filters, chlorination units, and sludge treatment units. The environmental exergy efficiency ($\eta_{env,ex}$) increased from 0.14 to 0.36, and the total pollution rate ($R_{pol,t}$) decreased from 6.14 to 1.79, demonstrating the expected improvement resulting from the modifications. If the sludge is used as a fertilizer, $\eta_{env,ex}$ increases even further and $R_{pol,t}$ decreases, although harmful effects are not captured by environmental indicators.

In Ireland, the study of two WWTPs with similar scale, discharge requirements, and treatment technologies, conducted by Fitzsimons *et al.* (2016), applied exergy analysis of simultaneous wastewater quality data and consumed resources as a useful analytical approach for decision-making benchmarking models. Equation (2.8), originally proposed by Kotas (1985) , was applied to determine the rational exergy efficiency (REE), defined as the ratio between the exergy flows of the desired output and the required inputs, including electricity and other contributions necessary to produce the desired effect.

$$REE = \frac{Ex_{ef}}{Ex_{el} + Ex_{in} + Ex_{TN,TP,in} - Ex_{L} - Ex_{TN,TP,out}} \quad (2.8)$$

where Ex_{el} is the electrical exergy; Ex_{in} is the exergy contained in the influent wastewater; $Ex_{TN,TP,in}$ is the influent nitrogen and phosphorus exergy; Ex_{L} is the exergy

contained in the sludge; and $Ex_{TN,TP,out}$ is the effluent nitrogen and phosphorus exergy, all expressed in kW.

The results of Fitzsimons *et al.* (2016) showed that, even in the presence of significantly different exergy destruction and exergy efficiency values, exergy destruction remains a useful tool for comparing the overall performance of WWTPs. In Plant 1, the REE was 27.5%, whereas in Plant 2 it reached 40.2%, attributed to differences in the composition and quality of the influent wastewater.

2.2 GHG emissions in UWC

In the current context of climate change, sanitation utilities must also adapt to carbon and GHG emission-reduction strategies, in accordance with the GHG Protocol, a set of widely used international standards for measuring and managing greenhouse gas emissions in companies and organizations.(FGV, 2024), as shown in Table 2.1, since such emissions are inevitably produced during system operations.

The protocol defines three types of GHG emissions, categorized as Scope I, II or III, applicable to companies and organizations that operate production systems, including sanitation utilities. Therefore, emissions must be assessed to support the development of mitigation policies.

Table 2.1. Classification of emissions according to the GHG Protocol.

Scope	Type of emission	Definition
I	Direct emissions	Results from operations that are owned or controlled by the reporting company or organization
II	Indirect emissions	Originating from purchased or consumed electricity, steam, heating or cooling by the reporting entity
III	Other indirect emissions	Not included in Scope II and occurring along the value chain of the reporting organization, including upstream and downstream emissions

Source: FGV (2024).

In drinking water supply systems, indirect emissions mainly arise from the electricity consumed, while direct emissions are associated with fuel used in transportation.

In wastewater systems, in addition to indirect emissions from physical processes, direct emissions during treatment at WWTPs constitute the main mechanisms of GHG production, occurring under aerobic, anoxic, and anaerobic conditions, as shown in Table 2.2.

Table 2.2. Gas formation reactions during wastewater treatment in WWTPs.

Conditions	Reactions
Aerobic	$C_6H_{12}O_6 + 6O_2 \rightarrow 6CO_2 + 6H_2O$
Anoxic – nitrate reduction (denitrification)	$2NO_3^- + 2H^+ \rightarrow N_2 + 2.5O_2 + H_2O$
Anaerobic – sulfate reduction	$CH_3OOH + SO_4^{2-} + 2H^+ \rightarrow H_2S + 2H_2O + 2CO_2$
Anaerobic – CO_2 reduction (hydrogenotrophic methanogenesis)	$4H_2 + CO_2 \rightarrow CH_4 + 2H_2O$
Anaerobic – acetotrophic methanogenesis	$CH_3OOH \rightarrow CH_4 + CO_2$

Source: von Sperling (2007).

The main direct emissions during treatment processes are attributed to water vapor $(H_2O)_v$, carbon dioxide (CO_2), methane (CH_4) and nitrous oxide (N_2O). Water vapor absorbs and emits more radiation but has a short atmospheric lifetime because it condenses, reducing its long-term impact. The other gases have longer-lasting atmospheric effects and must be quantified.

The CO_2 is generated in aerobic and anaerobic fermentation reactions, from vehicle fuel used to transport sludge and by direct combustion at WWTP. Although aeration produces substantial CO_2, these emissions originate from biogenic sources linked to the natural carbon cycle and are disregarded in GHG inventories under Intergovernmental Panel on Climate Change (IPCC, 2006). Accordingly, CO_2 from these sources is also disregarded in this assessment.

Indirect CO_2 emissions are associated with the electricity production used in treatment processes and are calculated using the annual average emission factor (FMA) for CO_2, shown in Table 2.3 and published by the Brazilian Ministry of Science, Technology, and Innovation (MCT, 2024).

Table 2.3. Annual average CO_2 emission factor associated with electricity produced by the Brazilian interconnected power system.

Year	2020	2021	2022	2023	Average
FMA (kg CO_2/kWh)	0.0617	0.1264	0.0426	0.0385	0.0673

Source: (MCT, 2024).

The methane (CH_4) results from the anaerobic decomposition of organic matter during effluent treatment and sludge management. It has a global warming potential 27 times greater than CO_2 according to the IPCC. To reduce this impact, methane is typically flared or used as a fuel to generate electricity or mechanical energy.

The N_2O is produced from the degradation of nitrogenous compounds (nitrates and proteins) during aeration. It is an intermediate product of nitrification and denitrification processes, influenced by operational parameters such as pH, temperature, dissolved oxygen and

nitrite (NO_2^-) concentration. Daudt (2019) notes that studies on N_2O emissions from WWTPs are still incipient in Brazil, but interest in quantifying and reporting N_2O emissions is increasing. Emission rates vary widely due to treatment technologies, operational conditions, applied loads, altitude, and climate, with no consensus on their actual impact or mitigation strategies. Until more robust methods are established, N_2O emissions continue to be estimated using the IPCC method, Equation (2.9):

$$E_{N_2O,WWTP} = P.G_{WWTP}.FD_{i-c}.F_{E(WWTP)} \quad (2.9)$$

where $E_{N_2O,WWTP}$ is nitrous oxide emission (kg N_2O $year^{-1}$); $P$is the population served by the WWTP; G_{WWTP} is the utilization rate (%); FD_{i-c} is the industrial–commercial discharge factor (standard value 1.25 according to Ribeiro (2017) and Metcalf & Eddy (2003)); and $F_{E(WWTP)}$ is the individual N_2O emission factor (3.2 g N_2O $person^{-1}$ $year^{-1}$), defined by Cziepel; Crill; Harriss (1995) , resulting in Equation (2.10):

$$E_{N_2O_{WWTP}} = P.G_{WWTP}.(1.25).(3.2) \quad (2.10)$$

Ribeiro (2017) and Daudt (2019) emphasize that the IPCC method is imprecise because it relies exclusively on the study of Cziepel; Crill; Harriss, (1995) conducted at the New Hampshire activated sludge WWTP without biological nitrogen removal, one of the earliest N_2O monitoring studies and still used as the IPCC reference.

Table 2.4 lists Brazilian authors who reported N_2O emission factors FE_{WWTP} higher than the IPCC method for WWTPs using similar treatment technologies, attributed to the factors discussed above. Daudt (2019) reported a high value (219.69 g N_2O $person^{-1}$ $year^{-1}$) in an experimental reactor (LABEFLU) at Universidade Federal de Santa Catarina (UFSC), which differs substantially from real municipal WWTP conditions and was therefore excluded from this analysis.

Ribeiro (2017) and Cziepel; Crill; Harriss (1995), note that, in activated sludge WWTPs without biological nitrogen removal, approximately 90 percent of N_2O is produced in aerated and non-aerated tanks, sand basins, aeration units and sludge storage tanks, like values reported by Brotto *et al.* (2010) in nutrient-removal WWTPs in metropolitan Rio de Janeiro.

Table 2.4. N_2O emission factors in wastewater treatment processes.

References	g $\boldsymbol{N_2O\ pers^{-1}\ year^{-1}}$	g$\boldsymbol{N_2O\ L_{affl}^{-1}}$	*g$\boldsymbol{N_2O}$-N $\boldsymbol{gN_{WW}^{-1}}$
Brotto (2011)	8.1	8.03 10^{-5}	0.12
De Mello *et al.* (2011)	8.8	8.00 10^{-5}	0.11
Brotto *et al.* (2010)	13	9.00 10^{-5}	0.14
Ribeiro (2017) [1]	3	3.0 10^{-5}	0.04
Ribeiro (2017) [2]	13.8	1.2 10^{-4}	0.26
Ribeiro (2017) [3]	19.6	1.9 10^{-4}	0.3
Brotto *et al.* (2015)	8.1	8.03 10^{-5}	–
Daudt (2019)	219.69	–	–
IPCC (2006)	3.2	–	–
Cziepel; Crill; Harriss, (1995)	3.2	3.2 10^{-5}	0.035
Ahn *et al.* (2010)	–	–	(0.01–1.8)
Aboobakar *et al.* (2013)	–	–	(0.077–0.217)
Yoshida *et al.* (2014)	8.1	8.03 10^{-5}	0.12

*Based on influent TKN load. ([1]) Sampled on 18/05/2010; ([2]) 17/02/2011; ([3]) 30/06/2011. N_{WW} is the Nitrogen in Wastewater. Source: Brotto (2011) and Ribeiro (2017).

3 GENERAL CONSIDERATIONS, LIMITATIONS AND PERSPECTIVES

3.1 Thesis structure and synthesis of results

The thesis was structured to evaluate, in an integrated manner, the applicability and reliability of exergy analysis as a diagnostic, optimization, and decision-support tool for the Brasília UWC. Chapter One established the conceptual and methodological foundations required for the development of the work, presenting the context, the general and specific objectives, the scientific gap identified in the literature, and the central research hypothesis. Subsequently, the systematic review characterized the state of the art of the exergy–urban water nexus, highlighting the growing relevance of the topic, the absence of studies that simultaneously integrate water supply and wastewater systems, and therefore the pertinence of the approach adopted.

Chapter Two materialized this proposal through two complementary scientific articles that sequentially analyze from an exergetic perspective the two fundamental subsystems of the UWC: the WSS and the wastewater system.

The first article examined the thermodynamic performance of the WSS: raw water abstraction, treatment, pumping, and potable water distribution. The second article, already published internationally, analyzed the biological wastewater treatment processes, GHG emissions, the irreversibilities associated with biochemical oxidation, and the potential for resource recovery. Together, these studies form a coherent and integrated analytical body,

enabling the interpretation of the UWC as a single open system from a thermodynamic standpoint.

Based on the results obtained in the articles, the thesis successfully addressed the guiding questions presented in the introduction. The systematic application of exergy analysis made it possible to accurately identify where and why the main depletions of energy, water, and inputs occur throughout the cycle. In the WSS, raw water pumping was found to dominate both energy use and exergy destruction, while at the water treatment plant, most of the incoming exergy is associated with chemical reagents and is destroyed due to internal irreversibilities. In the wastewater system, the biological stages emerged as the most dissipative, corroborating the entropic nature of biochemical degradation processes.

It has also been shown that exergy analysis is capable of consistently quantifying the environmental impacts associated with the UWC, particularly by relating destroyed exergy to GHG formation and natural resource consumption. The comparison between usual and optimized operating conditions, carried out in both articles, revealed significant potential for improving overall exergetic performance, especially through the modernization of old pumps, the reduction of treated-water losses, and the energy recovery of biogas generated in WWTPs.

These findings allow the conclusion that the central hypothesis of the thesis was validated: exergy analysis, when systematically and integrative applied to the processes of the urban water cycle, is indeed capable of identifying and quantifying depletions of energy, water, inputs, and environmental quality, offering more precise indicators than traditional energy, hydraulic, or operational metrics. The methodology adopted demonstrated internal coherence, thermodynamic consistency, and the ability to support technological, operational, and environmental improvements in sanitation utilities.

Thus, the contributions achieved by the thesis confirm the relevance and robustness of the exergo-environmental approach as a tool for management, diagnosis, and planning in the urban sanitation sector. The two articles that compose Part Two complement and reinforce each other, forming an integrated and innovative assessment of Brasília UWC, aligned with the scientific gaps identified in the systematic review and with the objectives defined in Part One.

In this way, the thesis offers a replicable method, a solid analytical foundation, and a set of evidence that strengthens the adoption of optimization and sustainability strategies in urban water systems.

3.2 Perspectives and suggestions for new research

The analyses developed in this thesis demonstrated that the systems of Brasília UWC,

although fulfilling their essential role in protecting public health and mitigating environmental impacts on Lake Paranoá, require significant amounts of energy and inputs. The identification of the main exergy depletions and inefficiency points reveals substantial opportunities for technological and operational improvements, reinforcing the usefulness of the analyses performed and opening promising avenues for future developments.

In the WSS, exergy depletions were found to be primarily associated with equipment inefficiencies, operational conditions, and treated water losses. This indicates potential for improvement through pump modernization, rationalization of input use, and enhanced loss control.

Similarly, in the wastewater system, exergy recovery through the direct combustion of biogas produced at WWTPs and the agricultural use of dewatered sludge represent promising strategies to add energetic and environmental value to the generated residues.

The application of exergy analysis and environmental assessment proved effective in meeting the general objective of this study, identifying relationships among energy flows, resource use, and environmental impacts associated with UWC systems. However, the research naturally faced limitations inherent to the complexity of the systems analyzed.

Thus, further research may expand and refine the findings presented here, and the most relevant suggestions observed during the study include:

a). Detailed application of the method to specific process components.

Further analyses focusing on specific sections of the systems—considering relationships among the life cycle of machinery, pipelines, materials, and components of water and wastewater networks, as well as aspects such as service life and wear—can deepen the understanding of critical points and consolidate exergy as a decision-support tool.

b). Evaluation under variable operational conditions

The present thesis relied on data representing steady-state conditions. Future studies may assess exergy behavior under transient scenarios, including seasonal variations, consumption peaks, and rainfall events, enabling a more dynamic interpretation of system performance.

c). Comparison among units with different technological configurations

CAESB operates multiple supply and wastewater treatment units with distinct technological arrangements. Replicating the methodology in these additional facilities can allow comparisons among technologies and expand the applicability of the results.

d). Expansion of exergy and environmental analysis to other systems in the Federal District

Given the availability of operational data, extending the approach to additional UWC subsystems in the Federal District can generate a broader and more robust assessment, strengthening the institutional use of exergy and environmental analysis.

e). Development and evaluation of technological modernization scenarios

Because the study revealed clear opportunities for improvement, future work may simulate modernization scenarios, such as replacing aging pumps, implementing advanced automation, enhancing loss control, and improving energy efficiency in WTPs and WWTPs.

f) Integration of exergy, economics, and environmental analyses

Deepening the relationships among exergy, operational costs, and environmental impacts may substantially contribute to investment planning in sanitation utilities, guiding decisions toward more efficient alternatives with lower energy and environmental burdens.

g). Expanded assessment of circularity and material and energy flows

The recovery of biogas and sludge highlighted in this study may be complemented by systematic evaluations of circularity potential, enhancing the understanding of resource recovery and closed-loop strategies within UWC management.

h). Development of integrated indicators for decision-making

The results of this thesis create opportunities for formulating composite indicators combining exergy, input use, operational losses, and emissions. Such indicators may support strategic planning and the prioritization of interventions in sanitation systems.

i). Evaluation of the effects of regulatory parameters and public policies

Given the central role of regulatory frameworks in the sanitation sector, future studies may examine how regulatory changes influence exergy and environmental performance, enabling better alignment between technological alternatives and policy requirements.

Under these perspectives, the work developed in this thesis opens a broad range of possibilities for continuation and deepening, capable of advancing thermodynamic and environmental understanding of the urban water cycle and strengthening its use as a strategic tool for planning and managing sanitation systems.

GENERAL REFERENCES

ABUSOGLU, A.; ZAHI, E.; KUTLAR, A. DEMIR, S. **Exergy Analyses of Green Hydrogen Production Methods from Biogas-based Electricity and Sewage Sludge**. International Journal Of Hydrogen Energy 42:16 10986-10996 (2017).

AGÊNCIA REGULADORA DE ÁGUAS, ENERGIA E SANEAMENTO BÁSICO DO DISTRITO FEDERAL (ADASA). Abastecimento de água e esgotamento sanitário. Painéis informativos. **Serviço de abastecimento de água.** Disponível em https://www.adasa.df.gov.br/areas-de-atuacao/abastecimento-de-agua-e-esgoto. Acesso em 15/08/2022.

ARMANDO, G. M.; ALEJANDRO, Z. A.; BARBARA, G. R.; HUGO, R. H. V. **On an Exergy Efficiency Definition of a Wastewater Treatment Plant**. International Journal of Thermodynamics 6:4 169-176 (2003).

ARVIZU, F. J. L. **Tratamiento anaeróbio aerobio de las águas residuales de las instalaciones del IIE**. 1996. Disponível em http://www.iie.org.mx/publica/bolso96/aplica.htm. Acesso em 24/01/2017.

ASSOCIAÇÃO BRASILEIRA DE NORMAS TÉCNICAS (ABNT). **NBR 9648: Estudos de Concepção de Sistemas de Esgoto Sanitário. Procedimento.** Rio de Janeiro, 5 p, 1986.

_____. **NBR 6400: Bombas Hidráulicas de Fluxo (Classe C) - Ensaios de Desempenho e Cavitação**. Rio de Janeiro, 26 p, 1989.

AUSTONI, M.; GIORDANI, G.; VIAROLI, P.; ZALDIVAR, J. M. **Application of Specific Exergy to Macrophytes as an Integrated Index of Environmental Quality for Coastal Lagoons**. Ecological Indicators 7:2 229-238 (2007).

AYDIN, M. I.; KARACA, A. E.; QURESHY, A. M. M. I.; DINCER, I. **A Comparative Review on Clean Hydrogen Production from Wastewaters**. Journal of Environmental Management. 279 (2021).

BARBOSA, A.S. Peregrinos do cerrado. **Rev. do Museu de Arqueologia e Etnologia**. São Paulo, 5: 159-193, 1995.

BATISTA, L.F. **Lodos gerados nas estações de tratamento de esgotos no distrito federal: um estudo de sua aptidão para o condicionamento, utilização e disposição final**. Dissertação. ENC/FT/UnB. 197p. Brasília, DF. 2015.

BEJAN, A.; TSATSARONIS, G.; MORAN, M. **Thermal design and optimization**. 3th ed. John Wiley and Sons, New York, 1996. 542 p.

BILGEN, S.; BULUT, V. N. **Investigation or the Chemical Exergy and Water Quality of the Galyan River, Trabzon, Turkey**. Energy Sources, Part. A Recovery, Utilizations and Environmental Effects 36:23 2595-2602 (2014)

BRASIL. AGÊNCIA NACIONAL DE ÁGUAS (ANA). Atlas de Esgotos. **Despoluição de bacias hidrográficas**. http://www3.ana.gov.br/portal/ANA/panorama-das-aguas/quantidade-da-agua. Acessado em 17/11/2023.

_____. Relatório da conjuntura de recursos hídricos do Brasil 2022. **Qualidade e quantidade de água**. https://relatorio-conjuntura-ana-2021.webflow.io/capitulos/quanti-quali. Acessado em 17/02/2022.

_____. MINISTÉRIO DAS CIDADES. Sistema Nacional de Informações sobre Saneamento (SNIS) . **Diagnóstico Anual de Água e Esgoto 2023.** Disponível em Diagnósticos SNIS — Ministério das Cidades. Acessado em 28/10/2025.

_____. MINISTÉRIO DE MINAS E ENERGIA. Empresa de Pesquisa Energética (EPE).

Balanço Energético Nacional 2025. Relatório Síntese 2025**.** Disponível em Balanço Energético Nacional - BEN. Acessado em 20/10/2025.

_____. MINISTÉRIO DA CIÊNCIA, TECNOLOGIA E INOVAÇÃO (MCTI). **Fatores de emissão de CO_2 pela geração de energia elétrica no Sistema Interligado Nacional do Brasil - Ano Base 2023**. Disponível em: https://www.gov.br/mcti/pt-br/acompanhe-o-mcti/sirene/dados-e-ferramentas/fatores-de-emissao. Acesso em 20/02/2024

BROTTO, A. C. **Fatores de controle das emissões de óxido nitroso (NO_2) em tanque de aeração de estação de tratamento de esgoto**. Dissertação. 73pp. UFF. Niterói, RJ. 2011.

BYLKA, J.; MRÓZ, T. **Exergy evaluation of a water distribution system**. Energies 13:23. 2020.

CHATZIPASCHALI, A. A.; STAMATIS, A. G. **Exergetic and Economic Analysis of a Cheese Whey Wastewater Anaerobic Treatment Plant with a Cogeneration System**. Desalination and Water Treatment 56:5 1223-1230 (2015).

CHERNICHARO, C. A. L. **Reatores anaeróbios**, 2ª ed. atualizada e ampliada. 379 p. Editora UFMG. ISBN-13: 978-8542300172. Belo Horizonte, Minas Gerais. 2016.

CLIMATEMPO. **Climatologia em Brasilia, BR.** Disponível em https://www.climatempo.com.br/climatologia/61/brasilia-df. Acesso em 06/09/2024.

COBO, M. J.; LÓPEZ-HERRERA, A. G.; HERRERA-VIEDMA, E.; HERRERA, F. **SciMAT: A new science mapping analysis software tool**. Journal of the American Society for Information Science and Technology, v. 63, n. 8, p. 1609–1630, 2012. Disponível em: https://www.researchgate.net/publication/230760570_SciMAT_A_new_science_mapping_analysis_software_tool. Acesso em 02/01/2022.

COMPANHIA AMBIENTAL DO ESTADO DE SÃO PAULO (CETESB). **Emissões veiculares no estado de São Paulo 2022.** Série Relatórios/CETESB, ISSN 0103-4103. São Paulo, SP. 2023. Disponível em: https://cetesb.sp.gov.br/veicular/relatorios-e-publicacoes/, Acesso em 08/12/2024.

COMPANHIA DE SANEAMENTO AMBIENTAL DO DISTRITO FEDERAL (CAESB). **Sinopse do sistema de abastecimento de água do Distrito Federal (SIÁGUA).** 22a. Ed. 147p. Brasília, DF. 2014a.

_____ **Sinopse do sistema de esgotamento sanitário do Distrito Federal (SIESG)**. 27a. Ed. 169p. Brasília, DF. 2014b.

_____ **Plano diretor de água e esgotos de Brasília – PDAE/DF - 2019**. Vol. I. Disponível em https://www2.caesb.df.gov.br/acoes-e-programas.html. Acesso em 17/09/2022.

_____. **Estações de Tratamento de água da CAESB**. Disponível em https://atlas.caesb.df.gov.br/portal/apps/storymaps/stories/8d0c7820730c4be98a637c3e59522f6b. Acesso em 14/10/2022.

_____. **Relatório de indicadores de desempenho 2023**. Disponível em https://www.caesb.df.gov.br/indicadores-e-resultados. Acesso em 15/08/2023.

_____. **Relatório da Administração CAESB 2023**. Disponível em https://www.caesb.df.gov.br/relatorio-anual-da-administracao/.pdf. Acesso em 07/09/2024.

CZEPIEL, P.; CRILL, P.; HARRISS, R. Nitrous oxide emissions from municipal wastewater treatment. **Environmental Science and Technology**, v. 29, p. 2352-2356, 1995.

DAUDT, G. C. **Emissões de NO_2 e de CO_2 por um reator em bateladas sequenciais com lodo granular aeróbio no tratamento de esgoto sanitário.** Tese. 182 pp. UFSC. Florianópolis, SC. 2019.

DEWULF, J.; VAN LANGENHOVE, H.; DIRCKX, J. **Exergy Analysis in the Assessment of the Sustainability of Waste Gas Treatment Systems**. Science of the Total Environment 273:1-3 41-52 (2001).

DINCER, I.; ROSEN, M. A. **Exergy, energy, environment and sustainable development**. Elsevier. 1st ed., 454 p., 2007.

DINCER, I., ROSEN, M. A. **Exergy: energy, environment and sustainable development**. Elsevier Ltd. 2nd ed. 2013.

EPA. UNITED STATES ENVIRONMENTAL PROTECTION AGENCY. **GHG Emission Factors Hub**. Disponível em: https://www.epa.gov/climateleadership/ghg-emission-factors-hub. Acesso em 27/04/2025.

FAGERIA, N. K.; STONE, L. F. **Manejo da acidez dos solos de cerrado e de várzea do Brasil**. Santo Antônio de Goiás: Embrapa Arroz e Feijão. Documento. 92p. 1999.

FITZSIMONS, L.; HORRIGAN, M.; MCNAMARA, G.; DOHERTY, E.; PHELAN, T.; CORCORAN, B.; DELAURÉ, Y.; CLIFFORD, E. **Benchmarking the thermodynamic performance of Irish municipal wastewater treatment plants using exergy analysis**. Journal of Cleaner Production 131, 387-398. 2016.

FITZSIMONS, L.; HORRIGAN, M.; MCNAMARA, G.; DOHERTY, E.; PHELAN, T.; CORCORAN, B.; DELAURÉ, Y.; CLIFFORD, E. **Assessing the Thermodynamic Performance of Irish Municipal Wastewater Treatment Plants Using Exergy Analysis: A Potential Benchmarking Approach**. Journal of Cleaner Production131: 387-398 (2016).

FUNDAÇÃO GETÚLIO VARGAS (FGV). **Programa Brasileiro GHG Protocol**. Disponível em https://eaesp.fgv.br/centros/centro-estudos-sustentabilidade/projetos/programa-brasileiro-ghg-protocol. Acesso em: 29/01/2024.

GONG, M. & WALL, G. On exergy and sustainable development – Part 2: Indicators and methods. **Exergy, An International Journal**. Vol. 1 (4), 2001, p. 217-233.

HAMEUS, J.; HELLSTRÖM, D.; JOHANSSON, E. **A study of a urine separation system in an ecological village in northern Sweden**. Water Science Technology, UK, 35, 153. 1997.

HELLSTRÖM, D.; KÄRRMAN, E. **Exergy Analysis and Nutrient Flows of Various Sewerage Systems**. Water Science and Technology 35:9 135-144 (1997).

HELLSTRÖM, D. **Exergy analysis: a comparison of source separation systems and conventional treatment systems**. Water Environment Research 71:7, 1354-1363. 1999.

HELSSTRÖM, D. **Exergy Analysis of Nutrient Recovery Processes**. Water Science and Technology 48:1 27-36(2003).

HUANG, L. Q.; CHEN, G. Q.; ZHANG, Y.; CHEN, B. LUAN, S. J. **Exergy as a Unified Measure of Water Quality.** Communications in Nonlinear Science and Numerical Simulation, 12-5 663-672 (2007).

KHOSRAVI, S.; PANJESHAHI, M. H.; ATAEI, A. **Application of exergy analysis for quantification and optimization of the environmental performance in wastewater treatment plants**. International Journal of Exergy 12:1, 119-138. 2013.

INTERGOVERNAMENTAL PANEL ON CLIMATE CHANGE (IPCC). **2006 IPCC Guidelines for National Greenhouse Gas Inventories**. Vol 5 – Waste. Chapter 6 - Wastewater Treatment and Discharge. IGES – Institute for Global Environmental Strategies. 2023. Kanagawa, Japan. Disponível em https://www.ipcc-nggip.iges.or.jp/public/2006gl/index.html. Acessado em 15/12/2023.

JANNATKHAH, J. NAJAFI, B. GHAEBI, H. Energy and exergy analysis of combined PRC-ERC system for biodiesel-fed diesel engine waste heat recovery. Energy Conversion and Management, v. 209, n. 112658, 2019.

JONSSON, H.; STENSTROM, T.-A.; SVENSSON, J.; SUNDIN, A. **Source separated urine-nutrient and heavy metal content, water saving and faecal contamination**. Water Science Technology, UK. 35, 145. 1997.

KOTAS, T. J. **The exergy method of thermal plant analysis**. Editora Butterworths, London, 296p, 1985.

LAMAS, W. D. Q.; SILVEIRA, J. L.; GIACAGLIA, G. E. O.; REIS, L. O. M. **Development of a Methodology for Cost Determination of Wastewater Treatment Based on Functional Diagram**. Applied Thermal Engineering 29:10 2061-2071 (2009).

LAMAS, W. D. Q.; SILVEIRA, J. L.; OSCARE GIACAGLIA, G. E.; MATTOS DOS REIS, L. O. **Thermoeconomic Analysis Applied to an Alternative Wastewater Treatment**. Renewable Energy 35:10 2288-2296 (2010).

LAMAS, W. D. Q. **Fuzzy Thermoeconomic Optimization Applied to a Small Waste Water Treatment Plant**. Renewable and Sustainable Energy Reviews 19: 214-219, 2013.

LI, F.; BAE, M. J.; KWON, Y. S.; CHUNG, N.; HWANG, S. J.; PARK, H. K.; KONG, D.S.; PARK, Y.S **Ecological Exergy as an Indicator of Land-use Impacts on Functional Guilds in River Ecosystems**. Ecological Modelling 252:1 53-62, 2009.

LOBATO, L. C. S. **Aproveitamento energético de biogás gerado em reatores UASB tratando esgoto doméstico.** Tese. 182 pp. UFMG. Belo Horizonte, MG. 2011.

LOPES, T. R. **Caracterização do esgoto sanitário e lodo proveniente de reator anaeróbio e de lagoas de estabilização para avaliação da eficiência na remoção de contaminantes**. Dissertação, UTFPR, Medianeira, PR, 123 pp, 2015.

MARCUELLO, J. U.; GRACIA, A. M.; ALVAREZ, B. C.; CAPILLA, A. V. **Advances in the Distribution of Environmental Cost of Water Bodies Through the Exergy Concept in the Ebro River.** 25th International Conference on Efficiency, Cost, Optimization and Simulation of Energy Conversion Systems and Processes. Ecos 2012 40-57 (2012).

MAKARYTCHEV, S. V. **Environmental impact analysis of ACFB-based gas and power cogeneration**, Energy, Vol. 23, No. 9, pp. 711–717. 1997.

MARTINEZ, A.; UCHE, J. **Chemical exergy assessment of organic matter in a water flow**. *Energy*, Vol. 35, pp.77–84. 2010.

METCALF; EDDY Inc. **Wastewater Engineering: Treatment and Reuse**. 4th ed, McGraw Hill, New York. ISBN 0070418780, 9780070418783.1818 p. 2003.

MORA BEJARANO, C. H.; OLIVEIRA, JR. S. **Exergy efficiency as a measure of the environmental impact of energy conversion processes.** 17th International Conference on Efficiency, Costs, Optimization and Environmental Impact of Energy Systems - ECOS 2004. Guanajuato, Mexico. 423-431. ISBN-968-489-027-3. 2004.

MORA BEJARANO, C. H.; DE OLIVEIRA JR, S. **Environmental Exergy Analysis of Wastewater Treatment Plants**. 18th International Conference on Efficiency, Cost, Optimization, Simulation, and Environmental Impact of Energy Systems - ECOS 2005, 85-92. 2005.

MORA BEJARANO, C. H. **Avaliação exergoecológica de processos de tratamento de esgoto.** Tese. 147pp. EPUSP/USP. São Paulo, SP. 2009.

MORAN, M. J.; SHAPIRO, N. H.; BOETTNER, D.D.; BAILEY, M. B. **Fundamentals of engineering thermodynamics**. 9th ed. John Wiley and Sons. NJ, USA. 875 pp. 2018.

OLIVEIRA JR., S. **Exergy Analysis and Environmental Impact**. Green Energy and Technology 63, 281-303 (2013).

ORTIZ, P. A. S.; FLÓREZ-ORREGO, D. A. **Exergia – Conceituação e Aplicação**. DEM. EPUSP/USP. 2013. Disponível em https://www.academia.edu/3315176/Exergia Conceituação e Aplicação DOI_10.13140_RG.2.1.1088.8804. Acesso em 21/09/2023.

OWEN, F. W. **Energy in wastewater treatment**. ISBN-10: 0132776650. Ed. Prentice-Hall. 320p. New Jersey, 1982.

PEGORIN, M. C.; THEISEN, M. C. **Planejamento urbano e adaptação às mudanças climáticas: revisão de literatura no contexto de cidades resilientes**. In: XII Convención sobre Medio Ambiente e Desarollo por la Integración y Cooperación para la Sostenibilidad. Habana, Cuba, 1-5 julio 2019. Disponível em: https://www.researchgate.net/publication/342703198_PLANEJAMENTO_URBANO_E_ADAPTACAO_AS_MUDANCAS_CLIMATICAS_revisao_de_literatura_no_contexto_de_cidades_resilientes. Acessado em 02/01/2022.

PERRY, R. H., & GREEN, D. W. **Perry's Chemical Engineers' Handbook**. Ed. Mc-Graw-Hill: Knovel. 7th edition. 1997.

POSSETTI, G. R. C., RIETOW, J. C., LOBATO, L. C. S., AISSE, M. M., CHERNICHARO, C. A. L., 2021. **Parte A: Avanços nas ferramentas e técnicas para estimativa de produção e tratamento de biogás em ETEs com reatores anaeróbios. Nota Técnica 2 – Programa computacional de estimative de produção de biogás em reatores UASB - ProBio 2.0**. Cadernos Técnicos Eng Sanit Ambient | v.1 n.1 | 2021 | 21-34. https://doi.org/10.5327/276455760101004

PTASINSKI, K. J.; SCHOLTEN, H. J.; WEEKERS, A. G. W.; KERKHOF, P. J. A. M. **Energy and Exergy Analysis of the Sewage Sludge Incineration and Gasification Processes**. Proceedings of the International Conference on Thermodynamic Analysis and Improvement of Energy Systems, Taies'97, 445-452 (1997).

RIBEIRO, R. P. **Emissões de óxido nitroso em diferentes condições operacionais de sistemas de tratamento de esgotos por lodos ativados em escala real e de bancada**. Tese. 121 pp. UFF. Niterói, RJ. 2017.

ROBERTS, E. **Water Quality Control Handbook**, McGraw Hill, NY. 2007.

RODRÍGUEZ-MERCHAN, V.; ULLOA, TESSER, C.; CASAS LEDóN, Y. **Evaluation of the Water-Energy-Land Nexus (WELN) Using Exergy Based Indicators: The Chilean Electricity System Case**. Energies 13:1 (2019).

RODRÍGUEZ-MERCHAN, V.; ULLOA-ESSER, C.; BAEZA, C.; CASAS LEDÓN, Y. **Evaluation of the water–energy nexus in the treatment of urban drinking water in Chile through exergy and environmental indicators**. Journal of Cleaner Production 317: 2021.

ROSEN, M. A. Energy crisis or exergy crisis? **Exergy, an International Journal**. Vol 2, p.125-127, 2002.

SHIRMER, F. **Comparação de indicadores de eficiência energética e exergética em duas indústrias do setor sucroalcooleiro**. 2006. 81f. Dissertação (Mestrado). Universidade Estadual do Oeste do Paraná (UNIOESTE). Cascavel, PR. 2006.

SCHUURMAN, F.; SILVA, L. C. **Prevenção na formação de gás sulfídrico em esgoto sanitário**. Revista TAE, Ed. 15, outubro/novembro 2023.

SILVA, S. R. **Análise exergética e o uso de recursos em processos biotecnológicos: modelagem e otimização de variáveis de processo**. Tese. 138 p. Escola de Engenharia, UFMG. Belo Horizonte, MG. 2021.

SOUZA, A. M. T.; SOARES, L. N.; CORDEIRO, L. A. **Análise exergética e termoeconomia aplicadas a processos**. ISBN-10 8582290918. Ed. PUC Minas. 1a. Ed. 235 p. Belo Horizonte, MG. 2019.

STANEK, W.; VALERO, A.; UCHE, J.; CALVO, G. **Thermodynamic methods to evaluate resources**. Green Energy and Technology. Chap. 6.5, 156-165. 2017.

SZARGUT, J. **Chemical exergies of the elements**. Applied Energy, Vol. 32, pp.269–286. 1988.

SZARGUT, J.; MORRIS, D.R.; STEWARD, F.R. **Exergy analysis of thermal, chemical, and metallurgical processes**. New York: Hemisphere Publishing Co, 332p. 1988.

SZARGUT, J. **Exergy method: Technical and Ecological Applications**. WIT Press Co, UK. 1st Ed. 161 p. 2005. Referência cruzada.

TAI, S., MATSUSHIGE, K., GODA, T. **Chemical exergy of organic matter in wastewater**. Int. J. Environ. Stud. 3-4, p 301-315. 1986.

UNITED NATIONS (UN). **Causes and Effects of Climate Change.** Available in: https://www.un.org/en/climatechange/science/causes-effects-climate-change. Accessed on 12/22/2025:

VELÁSQUEZ, H. I.; RUIZ, A. A.; OLIVEIRA Jr, S. Ethanol production process from banana fruit and its lignocellulosic residues: Exergy and environmental analysis. In: The 21^{th} Intenational Conference on Efficuency, Costs, Optimization, Simulation and Environmental Impacto of Energy Systems. Krakow, 2008. **Proceedings**. Zaklad Graficzny Politechniki Slaskiej. Krakow-Gliwice, Poland, 2008. v.1 p.209-216

Von SPERLING, M**. Princípios do tratamento biológico de águas residuárias: Introdução à qualidade das águas e ao tratamento de esgotos**. Belo Horizonte, MG. Segrac, v.1, 234 p, 1996.

Von SPERLING, M. **Basic Principles of Wastewater Treatment.** In: Biological wastewater treatment series, vol. 2. IWA Publishing. London, UK. 2007.

WALL, G. **Exergy – A useful concept within resource accounting.** Institute of Theoretical Physics, University of Göteborg, Sweden, 1977. Disponível em http://exergy.se/goran/thesis/paper1/paper1.html. Acessado em 22/11/2023.

WASILIEVSKI, S. ROTH, E.; MINKE, R. STEINMETZ, H. **Evaluation of Different Clinophtilolite Zeolite as Adsorbent for Ammonium Removal from Highly Concentrated Syntetic Wastewater**. Water (Switzerland) 10:5-9 (2018).

WILSENACH, J. A.; MAURER, M.; LARSEN, T. A.; VAN LOOSDRECHT, M. C. M. **From waste treatment to integrated resource management**. Water Science and Technology 48:1, 1-9. 2003.

ZENG, D.; WU, Z.; HUANG, W.; CHEN, Y. **Energy Quality Factor of Materials Conversion and Energy Quality Reference System**. Applied Energy 185, 768-778 (2017).

CHAPTER TWO – ARTICLES

FIRST ARTICLE: TOWARDS SUSTAINABLE URBAN WATER MANAGEMENT: A THERMODYNAMIC–ENVIRONMENTAL NEXUS APPROACH

Valtrudes Pereira Franco [a], Giulia Cruz Lamas [a], Mário Benjamim Baptista de Siqueira [a], Sérgio Botelho de Oliveira [b], Flamínio Levy Neto [a], Armando Caldeira-Pires [a], Edgar A. Silveira [a*]

a. University of Brasília (UnB), Mechanical Sciences Graduate Program, Laboratory of Energy and Environment, Brasília (DF), Brazil.
b. Federal Institute of Goiás (IFG), Department of Chemistry, Goiânia (GO), Brazil.

* Corresponding author
E-mail: edgar.silveira@unb.br

ABSTRACT

Urban water systems are among the most energy-intensive components of municipal infrastructure, yet their thermodynamic performance remains poorly quantified. This study develops an integrated Water–Exergy–Environment Nexus to evaluate the complete urban water cycle (UWC) of Brasília, Brazil, encompassing raw-water abstraction, treatment, distribution, and wastewater management. Operational data from the local utility (CAESB) were used to establish steady-state mass, energy, and exergy balances across all subsystems. The results show a total raw-water abstraction of 2.461 $m^3\ s^{-1}$, with distribution losses of 17.6 % and a return-to-environment ratio of 72.1 %, confirming the hydraulic closure of the system. The total electricity demand reached 10.68 MW, corresponding to an energy intensity of 4.34 kWh m^{-3} and a specific demand of 3.6 W $inhabitant^{-1}$. Exergy analysis revealed that the Raw-Water Pumping Systems dominate the thermodynamic profile, accounting for 60 % of total energy use and exhibiting efficiencies between 59.8 % and 76.1 %. The Water Treatment Plant displayed the lowest exergetic efficiency (7.6 %), with 53.6 % of its input exergy derived from chemical reagents and 82.9 % destroyed by internal irreversibilities. The Treated-Water Pumping System achieved 70.7 % efficiency, while wastewater treatment remained at the most dissipative stage due to biochemical oxidation. The overall exergy efficiency of Brasília's UWC was approximately 69–70 %, consistent across the supply chain. Retrofitting aging pumps and recovering biogas from sludge digestion could significantly enhance performance. The proposed framework provides a replicable thermodynamic–environmental methodology for identifying hotspots, optimizing resource use, and guiding low-carbon strategies toward sustainable urban water management.

KEYWORDS: Urban water cycle; Exergy analysis; Thermodynamic efficiency; Water–energy nexus; Sustainable urban management.

INDEX SUMMARY

UWC	Urban Water Cycle	η_p	Pump hydraulic efficiency
WSS	Water Supply System	η_m	Motor efficiency
WWTP	Wastewater Treatment Plant	η_{mp}	Overall motor–pump efficiency
WTP	Water Treatment Plant	$cos\ \varphi$	Power factor of electric motor
TWPS	Treated Water Pumping System	E_{el}	Electrical exergy input
RWPS	Raw Water Pumping System	W_{hyd}	Hydraulic power output (kW)
LCA	Life Cycle Assessment	E_{ch}	Chemical exergy input
GHG	Greenhouse Gas	E_{mech}	Mechanical exergy input
SDGs	Sustainable Development Goals	E_{total}	Total exergy input
CAESB	Companhia de Saneamento Ambiental do Distrito Federal	E_{out}	Output exergy (useful + losses)
CExC	Cumulative Exergy Consumption	E_{sludge}	Exergy of sludge stream (kW)
TEC	Thermo-Ecological Cost	$E_{reagent}$	Exergy of reagents (kW)
SNIS	Brazilian National Sanitation Information System	$E_{effluent}$	Exergy of treated effluent (kW)
ANVISA	National Health Surveillance Agency	V	Velocity of flow (m s^{-1})
WEAP	Water Evaluation and Planning model	η_{sys}	Global system efficiency
EE	Exergy Efficiency	ψ_{WTP}	Exergetic efficiency of Water Treatment Plant
GWP	Global Warming Potential	ψ_{RWPS}	Exergetic efficiency of Raw Water Pumping System
SD	Sustainable Development	ψ_{TWPS}	Exergetic efficiency of Treated Water Pumping System
$\dot{X}E_{in}$	Input exergy rate (kW)	ψ_{WWTP}	Exergetic efficiency of Wastewater Treatment Plant
$\dot{X}E_{useful}$	Useful exergy rate (kW)	χ_{rec}	Recoverable exergy fraction
$\dot{X}E_{loss}$	Recoverable exergy losses (kW)	θ	Temperature (°C or K)
$\dot{X}E_{dest}$	Destroyed exergy rate (kW)	Δx	Fractional water loss in network
ψ	Exergy efficiency	$E_{input\ total}$	Total exergy supplied to the UWC (kW)
φ	Chemical-to-total input ratio	$E_{destroyed_{total}}$	Total exergy destroyed within UWC (kW)
ξ	Exergy destruction ratio	E_{loss_total}	Total recoverable exergy losses in UWC (kW)
η	Efficiency (pump, motor or overall)	ψ_{total}	Overall exergy efficiency of the UWC
P	Power (kW)	BOD	Biochemical Oxygen Demand
ρ	Density of water (kg m^{-3})	COD	Chemical Oxygen Demand
g	Gravitational acceleration (m s^{-2})	PAC	Polyaluminum chloride
Q	Volumetric flow rate (m^3 s^{-1})	$Ca(OH)_2$	Calcium hydroxide (lime)
H	Total dynamic or manometric head (m)	H_2SiF_6	Fluosilicic acid
$\dot{m}$	Mass flow rate (kg s^{-1})	Cl_2	Chlorine gas
$b°_{ch}$	Standard specific chemical exergy (kJ g^{-1})	CO_2	Carbon dioxide
x_i	Mass fraction of component i in mixture	CH_4	Methane
T_0	Reference temperature (K)	O_2	Oxygen
P_0	Reference pressure (atm)	NH_4^+	Ammonium ion
ΔS_{gen}	Entropy generation (kJ K^{-1})	NO_3^-	Nitrate ion
W_{el}	Electrical power input (kW)	WHO	World Health Organization

1 INTRODUCTION

Rapid urbanization and population growth have significantly increased global demand for energy, water, and food, intensifying environmental pressures and resource scarcity. Recent studies highlight the vulnerability of urban systems to interconnected crises of resource depletion, climate change, and water scarcity, particularly in fast-growing cities where water and energy demand are closely coupled (García-Sánchez, Güereca, 2019; Huang et al., 2023). Urban sustainability, therefore, depends strongly on the efficiency of water supply systems (WSS) within the broader urban water cycle (UWC), which encompasses abstraction, treatment, distribution, consumption, and wastewater recovery processes (Rodríguez-Merchan et al., 2021).

The UWC is a complex network requiring substantial inputs of electricity, chemicals, and fuels. The operational performance of these systems directly affects water security, service reliability, and energy efficiency.

In Brazil, despite widespread access to potable water, significant gaps remain in water treatment infrastructure and operational efficiency. National data indicate that WSS consumed 12.6 TWh in 2022, accounting for 2.15% of national electricity use.

Additionally, 37.8% of treated water was lost through leakages, leading to wasted resources and unnecessary emissions (SNIS, 2023). These inefficiencies highlight the urgent need for integrated evaluations of energy–water–environmental interactions, capable of guiding optimization strategies and reducing environmental impacts.

Although traditional energy assessments provide a first approximation of system performance, they fail to capture the quality of energy flows and the degree of irreversibility inherent to transformation processes. In contrast, exergy analysis quantifies both the quantity and the quality of energy, enabling identification of inefficiencies and comparison between real and ideal processes (Fitzsimons et al., 2016).

Its application to WSS offers a deeper understanding of thermodynamic losses and resource degradation, supporting more sustainable water–energy management practices. Table 1 summarizes representative studies applying exergy analysis to water systems.

As shown in Table 1, exergy-based approaches have been increasingly applied to different components of the urban water cycle, yet their scope and integration remain limited. Studies in Mexico (García-Sánchez, Güereca, 2019) and China (He et al., 2019; Huang et al., 2023) highlighted the interdependence between water and energy systems, emphasizing the rapid rise of electricity demand in urban water management.

Table 1. Summary of studies applying exergy-based approaches to urban water and wastewater systems

Location/year	Analysis	Main Contributions	Ref.
Mexico, 2019	Environmental and social life cycle assessment (LCA) of urban water systems	Evaluated environmental and social impacts of the complete urban water cycle in Mexico City, integrating abstraction, treatment, distribution, and wastewater management to identify sustainability hotspots.	(García-Sánchez and Güereca, 2019)
China, 2019	Energy balance across the complete urban water cycle	Quantified the total electricity demand for Beijing's water production, distribution, consumption, and recycling. Demonstrated a 215 % increase in water-related energy use between 2005–2015.	(He et al., 2019)
Poland, 2020	Exergy balance and hydraulic modeling of water distribution networks	Developed a model for mechanical and potential exergy evaluation in urban water networks using EPANET and QGIS–Python scripts, identifying exergy destruction from friction losses and overpressure.	(Bylka and Mróz, 2020a)
Chile, 2021	Exergy analysis combined with LCA in drinking water systems	Integrated cumulative exergy consumption (CExC) with water stress and blue water footprint indicators to assess the water–energy nexus and highlight the thermodynamic cost of freshwater supply.	(Rodríguez-Merchan et al., 2021)
China, 2023	Water–energy nexus modeling for urban water supply systems	Assessed energy demand of water abstraction, treatment, and distribution using a WEAP-based nexus model for Beijing; identified optimization measures for reducing urban energy intensity.	(Huang et al., 2023)
Brazil, 2025	Exergy analysis, GHG quantification, and LCA applied to WWTPs	Focused exclusively on Brasília's North and South WWTPs. Found that >97 % of total input exergy was destroyed—mainly from unutilized methane (55–60 %) and electricity (28–31 %). Proposed biogas recovery scenarios improving exergy efficiency up to +129 %.	(Franco et al., 2025)
Brazil	Integrated mass, energy, exergy, and GHG analysis of the complete UWC (WSS + WWTP)	Extends the scope of Franco et al. (2025) from WWTPs to the entire urban water system of Brasília, integrating abstraction, treatment, distribution, consumption, and wastewater management within the Water–Exergy–Environment Nexus framework.	This study

In Europe and South America, analyses by Bylka, Mróz (2020a) and Rodríguez-Merchan et al. (2021) demonstrated how exergy metrics can reveal mechanical losses, thermodynamic irreversibilities, and environmental trade-offs in distribution and treatment systems. More recently Franco et al. (2025) quantified exergy destruction and GHG emissions in Brasília's wastewater treatment plants, demonstrating the potential for efficiency gains through biogas recovery. Collectively, these studies highlight important methodological advances but remain confined to partial segments of the urban water cycle.

Therefore, a unified framework that simultaneously quantifies energy, exergy, and potential emissions across both water-supply and wastewater systems is still lacking – gap that this study seeks to fill.

This study assesses the system boundaries beyond wastewater treatment to encompass the entire UWC of Brasília, Brazil. The proposed Water–Exergy–Environment Nexus integrates energy and mass balance and exergy analysis, covering raw-water abstraction, pumping, treatment, distribution, consumption, and wastewater management.

The main objective is to quantify the thermodynamic and environmental performance of Brasília's urban water cycle, identifying systemic inefficiencies and resource-recovery potential that support the transition toward sustainable and low-carbon urban water management.

The methodology is replicable and scalable, providing a robust foundation for achieving SDGs 6, 7, 11, and 13 through data-driven decision-making in the urban water sector.

2 METHODOLOGY

The analysis follows sequential and interdependent steps: i) System definition and data collection, comprising the delineation of operational boundaries and the acquisition of design and operational parameters; ii) Exergy analysis, based on mass and energy balances to quantify the exergy flows and irreversibilities at each stage of the WSS; and iii) GHG assessment.

Figure 1(a) shows the flowchart of the conventional water supply system evaluated in this study. Operational and design data, including raw water intake, treated and distributed water, energy consumption, chemical reagents for treatment, and residual sludge, were described and quantified to perform the exergy analysis of each case.

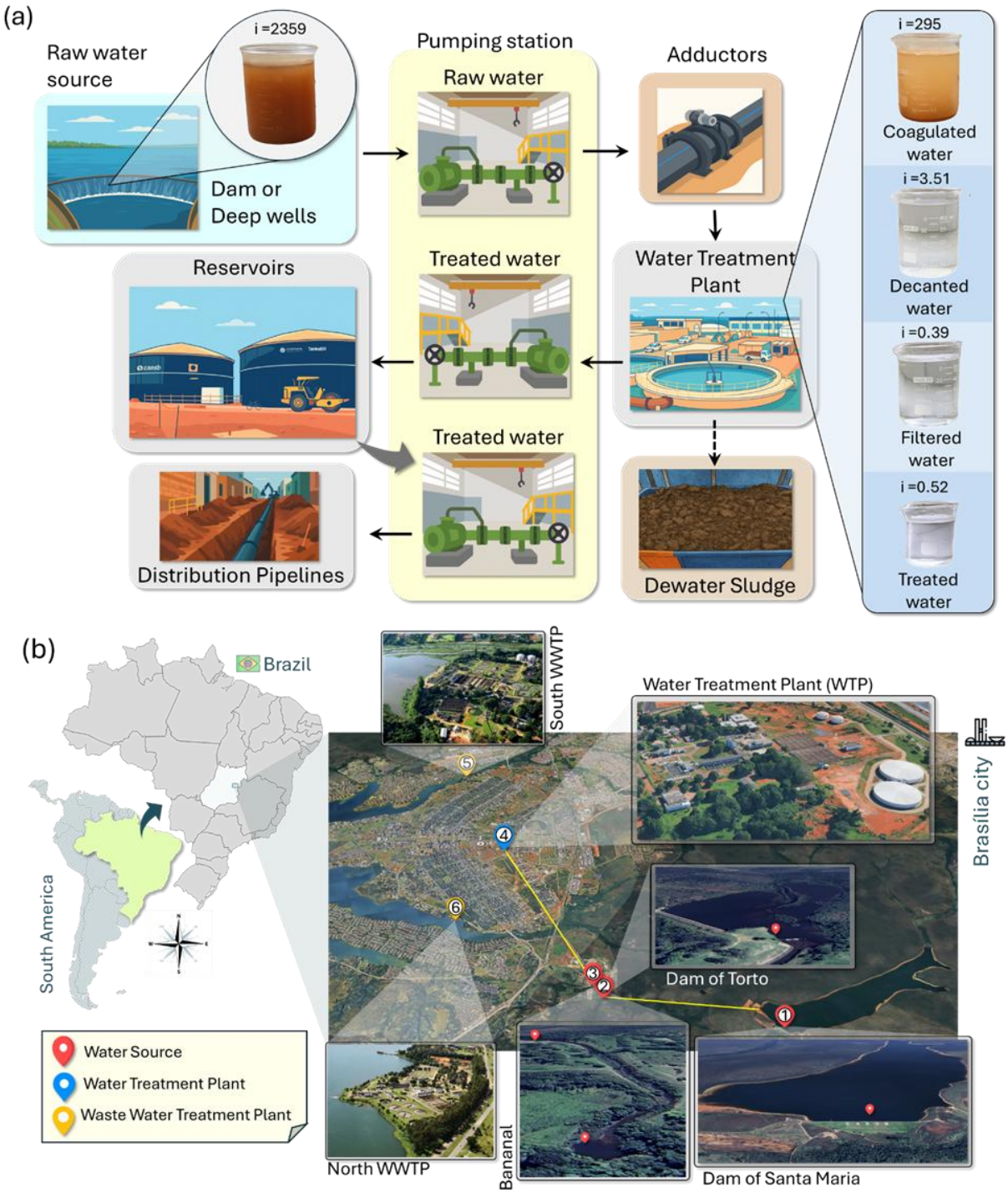

Figure 1. (a) Brasília's UWS characteristics and treatment process. (b) Brasilia map indicating raw water collection, WTP and WWTP locations. Adapted from (CAESB, 2024)).

2.1 WSS description

2.1.1 Raw water collection

Figure 1(b) shows the location of raw water collection in Brasília's map. Raw water is collected from dams of Santa Maria (red indicator – 1, 15°40′08″S, 47°57′12″W, altitude 1,072 m) and Torto (red indicator – 2, 15°41′42″S and 47°54′53″W, altitude 1,026 m), run-of-river from the Bananal (red indicator – 3,15°43'41.1"S, 47°54'36.4"W, altitude 1,009.6m), located at

Brasília National Park.

Figure 1(b) also shows Brasilia city's lake, Paranoá Lake. Located at an altitude of 1,000.24 m, the lake is fed by the Torto, Santa Maria and Bananal streams, among others, and receives approximately 1,776 L s^{-1} of treated effluent from the Brasília South (yellow indicator – 5, 15°50'35.972"S; 47°54'33.063"W) and Brasília North (yellow indicator – 6, 15°44'34.200"S; 47°52'42.754"W) WWTPs. Beyond its hydrological role, Lake Paranoá serves as a climatic regulator, a reservoir for a small hydroelectric plant, and a key recreational area for the local population.

2.1.2 Raw water pumping stations (RWPS)

The collected raw water is pumped to RWPS and conveyed through pipelines to the WTP for processing (blue indicator – 4 in Figure 1(b), 15°46´37.769"S and 47°54´23.721"W). WTP supplies approximately 367,000 residents in the city's neighborhoods. The electrical, hydraulic, and mechanical parameters obtained from (CAESB, 2024) include suction pressure, discharge pressure, flow rate, rotational speed, and electrical variables such as voltage, current, and power factor. These data are summarized in Tables S1.1, S2.1 and S3.1 of the Supplementary Material (SM), along with the catalogued operational characteristics, for the RWPS Torto, Santa Maria, and Bananal, respectively.

Based on the summarized data in Tables S1.1, S2.1 and S3.1 (SM), the individual pump efficiencies range from 61.2% to 81.8%, with overall motor–pump efficiencies between 58.8% and 78.6%, and power factors (cos φ) varying from 0.79 to 0.93. The corresponding hydraulic power demand per unit ranges from 30 kW (Bananal 1) to 1,387 kW (Torto 3), while total electrical power inputs reach up to 1,552 kW for the largest multi-pump arrays. These variations reflect differences in installation age, design head, and flow conditions across the three intake systems. The system incorporates check valves and protection systems against hydraulic transients to prevent energy dissipation and operational damage. These parameters support the exergy calculations described in Section 2.2.

2.1.3 Brasília WTP

The Brasília WTP began operations in 1960 using a conventional flocculation and direct filtration process. In 2007, its capacity was expanded to 2,800 L s^{-1} with the addition of flotation units, automation, and sludge management systems, which increased electricity and chemical consumption (Figure 2).

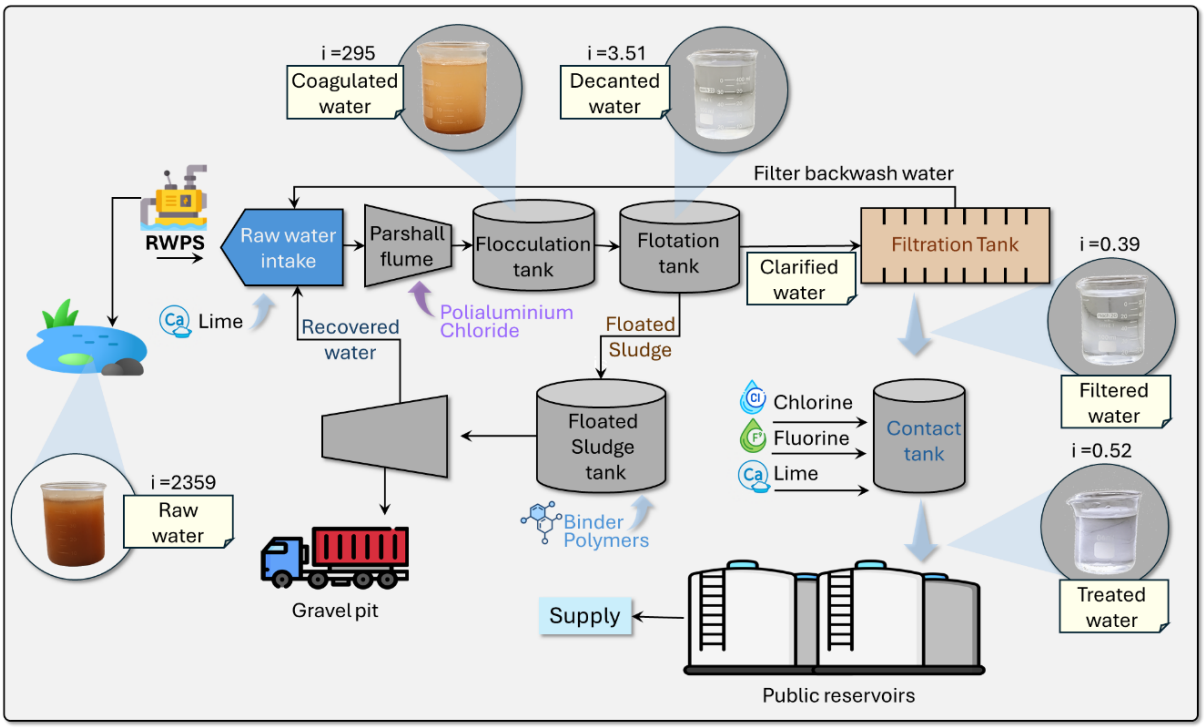

Figure 2. Flowchart of the stages of the Brasília WTP treatment process. Source: The Author, with data from CAESB (2024).

Currently, the plant treats about 2,461 L s^{-1} of raw water conveyed from the Torto and Santa Maria pipelines to the inlet tanks. The turbidity index, which varies seasonally according to the water source, determines the dosing of aluminum sulfate, ferric chloride, and quicklime (or hydrated lime) used for coagulation and pH adjustment. During flocculation and flotation, anionic and cationic organic polymers (polyelectrolytes) are added to promote particle aggregation, forming a sludge composed of sand, clay, organic matter, and residual chemicals. The sludge is centrifuged, dewatered, and transported about 40 km to a gravel pit.

The clarified water then flows through filtration tanks, where silt is periodically removed by backwashing. The backwash water is diluted with raw water (up to 5 %) and recirculated into the process, reducing water loss and preventing discharge into the stormwater system that drains to Lake Paranoá. Finally, the water passes through a contact tank, where it receives chlorine gas for disinfection, fluorosilicic acid (or sodium fluorosilicate), and lime for final pH adjustment, in compliance with ANVISA and WHO standards.

WTP consumes energy proportional to the treatment process, the operational capacity for internal water transport, compressor and blower drive, automation systems, flow control and regulation, tank and filter cleaning (backwashing), sludge removal and transportation, lighting, chemical pumping, treated water pumping, etc.

2.1.4 Transportation, storage, and distribution

The treated water is transported through pipelines, either by gravity or pumping, to storage tanks that regulate supply. It then flows through distribution networks with sufficient pressure to fill consumer reservoirs. Topographical variations and nighttime pressure increases require pressure regulation to avoid losses, achieved through pressure control valves that dissipate excess hydraulic energy and exergy. The treated WPS attached to the Brasília WTP operates with IMBIL BP pumps delivering water to reservoirs and gravity-fed networks supplying the city and neighboring administrative regions.

2.1.5 Wastewater treatment system

The wastewater treatment system in Brasília, operated by CAESB, consists of two main WWTPs: Brasília North and Brasília South (Figure 1(b)). Both employ activated sludge systems with nutrient removal and tertiary polishing, ensuring protection of Lake Paranoá. The North and South WWTPs treat 526 and 1,250 L s^{-1}, respectively, including anaerobic digestion of sludge for biogas production. Each plant includes preliminary screening and grit removal, followed by primary sedimentation. In the secondary stage, Phoredox-type reactors perform biological nitrogen and phosphorus removal via nitrification–denitrification. Advanced treatment involves coagulation with aluminum sulfate, flocculation, and flotation to remove residual solids and phosphorus (CAESB, 2024).

The resulting sludge is thickened, anaerobically digested to generate biogas, and subsequently dewatered. The dewatered sludge is transported to the centralized sludge management unit in Samambaia (15.87665° S, 48.14679° W). Although methane is produced during digestion, it is currently flared without energy recovery. The treated effluent from both plants is discharged into the northern and southern arms of Lake Paranoá by gravity or pumping. Further methodological and operational details regarding these WWTPs, including the complete exergy assessment and environmental indicators, are available in our previous publication (Franco et al., 2025).

To quantify the thermodynamic performance of the Brasília WSS, exergy analysis was applied to each subsystem described above. This approach enables a unified evaluation of mechanical, thermal, and chemical transformations across the raw water collection, pumping, treatment, distribution, and WWTP stages. By establishing control volumes and applying input–output exergy balances, it becomes possible to quantify the irreversible losses and efficiency of each operational unit.

The following section presents the formulation adopted for the exergy components and their specific relevance to the water supply subsystems.

2.2 Exergy–Water Nexus in WSS

The exergy analysis provides a thermodynamically consistent framework for evaluating the quality and degradation of energy throughout the UWC. While conventional energy balances quantify only the amount of energy consumed, exergy quantifies the useful work potential and allows identifying the irreversibilities that occur during energy transformations. This approach links energy efficiency with the physical quality of resources, offering a deeper understanding of the relationship between water, energy, and exergy (Bylka and Mróz, 2020b; Valero et al., 2009)

The boundaries considered in this study include the main stages of the Brasília urban water infrastructure: raw water abstraction, pumping, treatment, distribution, wastewater collection, and treatment. Each subsystem operates under steady-state conditions and was modeled individually through exergy balances that account for electrical, hydraulic, chemical, and biological contributions. The total exergy rate for each subsystem j is described by Equation (1).

$$\dot{X}E_{inpu,j} = \dot{X}E_{useful,j} + \dot{X}E_{losses,j} + \dot{X}E_{irrev,j} \quad (1)$$

where $\dot{X}E_{input,j}$ is the total exergy supplied to subsystem j, $\dot{X}E_{useful,j}$ is the exergy effectively converted into useful work (hydraulic or chemical), $\dot{X}E_{losses,j}$ represents recoverable exergy losses (mechanical or thermal), and $\dot{X}E_{irrev,j}$ corresponds to the irreversible destruction of exergy associated with entropy generation.

The evaluation integrates measured operational data, including flow rate, head, electrical demand, and reagent consumption, for all major facilities of the Brasília Water and Wastewater Company. The results of each subsystem balance are subsequently aggregated to form the global exergy balance of the urban water system (Section 2.2.7). This structure enables the identification of the main sources of exergy destruction, the distinction between recoverable and non-recoverable losses, and the development of consistent indicators for sustainable process optimization within the Water–Exergy–Environment framework.

2.2.1 Exergy Analysis of Water Pumping System

The exergetic performance of the motor pump assembly (MPA) in the Brasília WSS was assessed under steady-state conditions, following the second-law formulation applied to water infrastructure systems (Bylka and Mróz, 2020b). Each MPA consists of a motor–pump set that converts electrical energy into hydraulic energy to overcome the total head losses between suction and discharge. The exergy balance distinguishes four contributions: the input exergy supplied to the electric motor, the useful hydraulic exergy transmitted to the water column, the

recoverable mechanical and hydraulic losses, and the irreversibilities associated with internal thermodynamic dissipation.

The total exergy balance for each pumping unit is expressed as Equation (1), where $j = WPS$. In this analysis, $\dot{X}E_{(input,WPS)}$ is the electrical exergy rate corresponding to the measured input power P_e (Tables S1.1, S2.1, S3.1 and S6.1 (SM)) at the motor terminals, $\dot{X}E_{(useful,WPS)}$ is the hydraulic exergy effectively transmitted to the flow, $\dot{X}E_{(losses,WPS)}$ represents the recoverable hydraulic and mechanical losses, and $\dot{X}E_{(irrev.,WPS)}$ accounts for the internal destruction of exergy caused by viscous and electrical dissipation. The useful hydraulic exergy corresponds to the power delivered to the water column and is calculated as Equation (2).

$$\dot{X}E_{(useful,WPS)} = P_h = \rho\, g\, \dot{V} H_t \tag{2}$$

where ρ is the water density (1000 kg m^{-3}), g is the gravitational acceleration (9.81 m s^{-2}), $\dot{V}$ is the volumetric flow rate (m^3 s^{-1}), and H_t is the total dynamic head (m), equivalent to the measured manometric head H_m. The mechanical power transmitted through the shaft is obtained as Equation (3).

$$P_s = \frac{P_h}{\eta_b} \tag{3}$$

where η_b is the pump hydraulic efficiency (Tables S1.1, S2.1, S3.1 and S6.1 (SM)). Consequently, the recoverable exergy losses, associated with hydraulic and mechanical imperfections inside the pump, are determined by Equation (4).

$$\dot{X}E_{(losses,WPS)} = P_s - P_h = P_h(1/\eta_b - 1) \tag{4}$$

The exergy destruction term, related to the irreversibilities in the electric motor and internal conversion processes, is defined as Equation (5).

$$\dot{X}E_{(irrev.,WPS)} = P_e - P_s = P_h(1/\eta_g - 1/\eta_b) \tag{5}$$

where $\eta_g = \eta_m\, \eta_b$ is the overall efficiency of the motor–pump assembly and η_m is the motor efficiency. Finally, the exergetic efficiency (Equation (6)) of each MPA is expressed by the ratio between the useful hydraulic exergy and electrical input exergy:

$$\psi_{WPS} = \frac{\dot{X}E_{(useful,WPS)}}{\dot{X}E_{(input,WPS)}} = \frac{P_h}{P_e} = \eta_g \tag{6}$$

All exergy terms were expressed in kW for direct comparison with the electrical and hydraulic powers measured in the field. Flow and head data were converted to m^3 s^{-1} and m,

respectively, using the physical parameters of water. The closure of the exergy balance was verified by computing the residual term $|\dot{X}E_{input} - \dot{X}E_{useful} - \dot{X}E_{losses} - \dot{X}E_{irrev}|$, which remained within the acceptable numerical tolerance for each operating condition. This formulation enables distinguishing between recoverable mechanical losses and irreversible exergy destruction, providing a thermodynamically consistent representation of energy degradation in the WPS.

2.2.2 Exergy Analysis of Water Treatment Plant

The exergy balance of the Brasília WTP was established under steady-state conditions, considering the main mechanical and chemical processes involved in water clarification. Following the general formulation for exergy balance presented in Equation (1), the total input exergy supplied to the WTP ($\dot{X}E_{(input,WTP)}$) equals the sum of the useful exergy of the treated water, the recoverable exergy associated with the sludge stream, and the irreversibilities generated by internal thermodynamic processes ($\dot{X}E_{irrev,WTP}$) (Mora and De Oliveira Jr, 2006). Accordingly, the input exergy of the subsystem, Equation (7) is expressed as the sum of the mechanical and chemical contributions.

$$\dot{X}E_{input,WTP} = \dot{X}E_{me\,,WTP} + \dot{X}E_{ch,WTP} \tag{7}$$

The mechanical component $\dot{X}E_{me\,,WTP}$, represents the conversion of electrical energy into mechanical work performed by the electromechanical equipment of the treatment plant. Unlike the raw-water pumping stations, where the hydraulic exergy is determined, the internal processes of the WTP occur under nearly atmospheric conditions and do not involve significant pressure-head differences. Therefore, the mechanical exergy of the WTP was quantified directly from the total measured electrical power input of each motor-driven device (from CAESB (2024)) such as agitators, recirculation pumps, air compressors, scrapers, and auxiliary systems, as reported in Table 6.1 (SM). The sum of these electrical inputs represents the total mechanical exergy supplied to the treatment process. This approach follows the exergy formulation for non-pressurized systems, in which electrical work is fully equivalent to mechanical exergy (Szargut et al., 1988; Kotas, 1985; Valero et al., 2007).

The chemical component of the liquid phase ($\dot{X}E_{ch,WTP}$) accounts for the potential energy associated with the reagents used during coagulation, flocculation, pH adjustment, disinfection, and fluoridation. For each reagent i, the chemical exergy rate is determined by Equation (8).

$$\dot{X}E_{ch,i} = m_i\, b_{ch,i} \tag{8}$$

where m_i is the reagent mass-flow rate (g s^{-1}) and $b_{ch,i}$ is its specific chemical exergy (kJ g^{-1}). The total chemical exergy input is therefore determined by Equation (9).

$$\dot{X}E_{ch,WTP} = \sum_i \dot{m}_i b_{ch,i} \tag{9}$$

The specific exergy coefficients $b_{ch,i}$ were obtained from Szargut, Morris and Steward (1988) and correspond to the reagents employed at the Brasília WTP: polyaluminum chloride (PAC, 40 kJ g^{-1}), calcium hydroxide ($Ca(OH)_2$, 2.3 kJ g^{-1}), fluosilicic acid (H_2SiF_6, 0.52 kJ g^{-1}), chlorine gas (Cl_2, 2.46 kJ g^{-1}), and anionic polyelectrolyte (40 kJ g^{-1}). Their corresponding mass-flow rates are provided in Table 7.1 (SM), derived from CAESB (2024). The useful exergy of the subsystem corresponds to the potential energy carried by the treated water at the outlet ($\dot{X}E_{useful,WTP}$), representing the fraction of total input exergy that remains available for the distribution network.

In parallel, the chemical exergy of the solid phase (sludge) is evaluated independently as the recoverable exergy losses of the process. The corresponding rate is expressed by Equation (10).

$$\dot{X}E_{ch,sludge} = \sum_k \dot{m}_{sludge,k}\, b_{ch,k} \tag{10}$$

where $\dot{m}_{sludge,k}$ (g s^{-1}) represents the mass flow rate of compound k within the sludge and $b_{ch,k}$ (kJ g^{-1}) is its specific chemical exergy. The sludge composition reflects organic matter and metal oxides primarily derived from natural suspended solids and reagent residues; the quantitative specification used in the calculations is summarized in Tables S8.1 and S9.1 (SM) which lists concentrations, molar masses, and the standard specific chemical exergies adopted for the main constituents (CAESB (2024)). The internal exergy destruction term ($\dot{X}E_{irrev,WTP}$) represents the portion of exergy degraded by hydraulic friction, mixing, and chemical-reaction irreversibilities within the unit operations. This framework links each measurable term of Equation (1) to its thermodynamic role within the WTP, distinguishing the contributions of the liquid and solid phases and providing a coherent basis for the exergetic-efficiency evaluation presented in subsequent sections.

2.2.3 Exergy Analysis of Water Distribution

In the water distribution subsystem, exergy accounting follows Equation (1), which quantifies the depleted exergy flux ($\dot{X}E_p$) associated with treated water losses across the distribution network. These losses arise from both real and apparent components. Real losses

correspond to leakages, pipe ruptures under overpressure, particularly during nighttime operation, aging infrastructure, and malfunctioning seals, valves, or flow control devices. Apparent losses, in turn, include metering inaccuracies, unauthorized connections, and calibration or reading errors. Together, these phenomena result in significant depletion of useful energy and water resources within the Brasília WSS.

The treated water pumping system (TWPS) is responsible for conveying approximately 1,200 L s^{-1} of treated water from the WTP to the city reservoir. The station is equipped with four MPAs arranged in a (3 + 1) configuration, comprising IMBIL BP 300-340A centrifugal pumps with 380 mm impellers, coupled to WEG electric motors rated at 285 HP (212.5 kW) operating at 1,750 rpm. The system is automated by programmable logic controllers and operated through frequency inverters to regulate flow and head. Operational data, and performance and exergy balance of the TWPS are detailed in Tables S6.1, S10.1a and S10.1b (SM).

Under current operating conditions, the average flow rate is 857.97 L s^{-1}, corresponding to the "Average" condition in Table S10.1a (SM), which represents the steady-state configuration typically observed between 2020 and 2023. This station supplies urban areas surrounding Brasília and exports part of the treated water to nearby cities.

The total water loss in supply networks is calculated using the Total Loss Index (IP) and the Loss Index per Connection (IPL), defined in Equations (S1.1) and Table S11.1b (SM) according to the methodology of the National Sanitation Information System (SNIS – Sistema Nacional de Informações sobre Saneamento, 2023). The exergy depletion rate is then determined by multiplying the useful exergy rate ($\dot{X}E_u$) of the treated water by the measured loss index (IP), as shown in Equation (11).

$$\dot{X}E_P = \dot{X}E_u \times IP = 1{,}480.18 \times IP \tag{11}$$

This formulation allows translating the physical water losses of the distribution system into thermodynamic inefficiencies, representing the portion of available exergy destroyed due to uncontrolled leaks and operational deficiencies. Preventive maintenance of pressure control systems and real-time network monitoring, through macro-metering and automated valves, are key strategies to reduce such exergy depletion and enhance the overall sustainability performance of the water distribution subsystem.

2.2.4 Exergy Analysis of the Wastewater Treatment Plants

The detailed exergy characterization of the Brasília WWTPs was originally conducted by (Franco et al., 2025), who quantified the physical, chemical, and electrical exergy flows

across the main treatment units, including aeration tanks, secondary sedimentation, and sludge handling. Our previous study provided a comprehensive dataset of steady-state measurements and exergy balances that serve as the foundation for the present work. Here, these results are integrated within the broader exergy–water nexus assessment to ensure consistency and comparability with the other subsystems of the urban water cycle.

Therefore, the exergy analysis of the WWTP follows the thermodynamic formulation and results from (Franco et al., 2025) for the Brasília UWC, applying the general balance expressed in Equation (1). This approach integrates the physical, chemical, and electrical contributions of exergy to characterize the system performance and quantify internal irreversibilities throughout the treatment stages.

Under steady-state conditions, the total input exergy ($\dot{X}E_{input,WWTP}$) consists of: (i) the physical exergy of the influent wastewater ($\dot{X}E_{ph,in}$), which represents the enthalpy and pressure potential relative to the environmental reference state; (ii) the chemical exergy of dissolved and suspended pollutants ($\dot{X}E_{ch,in}$), mainly associated with organic and nutrient content; and (iii) the electrical exergy ($\dot{X}E_{el}$) consumed by aeration, pumping, and sludge-handling subsystems. The total output exergy includes the exergy effectively delivered through the treated effluent and stabilized sludge ($\dot{X}E_{useful,WWTP}$), the recoverable losses such as residual heat or unutilized biogas ($\dot{X}E_{losses,WWTP}$), and the exergy destruction due to thermodynamic irreversibilities within biological and mechanical units ($\dot{X}E_{irrev,WWTP}$). For detailed information, see data on Franco et al. (2025).

The chemical exergy of wastewater was determined based on its organic-matter load, primarily characterized by the chemical oxygen demand (COD). Following the correlation adopted by Franco et al. (2025). This formulation enables the quantification of exergy directly from routine monitoring data, ensuring compatibility with the measurements used for the Brasília WWTPs (Franco et al., 2025). All exergy flows were normalized to the environmental reference state (T_0 = 298 K; P_0 = 1 atm) to ensure comparability with other subsystems of the water supply and sanitation system.

The useful exergy corresponds to the exergy retained in the treated effluent ($\dot{X}E_{ph,out} + \dot{X}E_{ch,out}$) and, when applicable, in recovered energy carriers such as biogas or heat from sludge digestion. In systems without biogas recovery, the useful term is mainly represented by the physical exergy of the discharged effluent.

2.2.5 Exergy Balance and performance indicators

The overall exergy balance of the Brasília UWC was established by aggregating the

subsystem balances presented in Sections 2.2.1 to 2.2.4, which encompass raw-water abstraction, pumping, water treatment, distribution, and wastewater collection and treatment. Each subsystem was evaluated under steady-state conditions using measured data of flow rate, head, and electrical consumption. The global exergy balance of the integrated system is obtained by summing up the contributions of all subsystems, as expressed by Equation (12) (Kotas, 1985; Szargut, 1989).

$$\sum_j \dot{X}E_{input,j} = \sum_j \dot{X}E_{useful,j} + \sum_j \dot{X}E_{losses,j} + \sum_j \dot{X}E_{irrev,j} \quad (12)$$

To quantitatively assess the thermodynamic performance of each subsystem, three dimensionless indicators were adopted: the exergetic efficiency (ψ), the exergy destruction ratio (y_{irrev}), and the chemical-to-total input ratio (χ, for the WTP). These parameters were derived from the overall exergy balance and enable direct comparison of system performance across subsystems of the urban water supply chain. The exergetic efficiency (ψ) expresses the fraction of total exergy input converted into useful output, as defined in Equation (13) (Mora, Oliveira Jr, 2006).

$$\psi = \frac{\dot{X}E_{useful,tot}}{\dot{X}E_{input,tot}} \quad (13)$$

where $\dot{E}_{useful}$(kW) represents the useful exergy associated with the treated water and $\dot{E}_{in}$(kW) denotes the total exergy input, including electricity, chemical reagents, and fuel. This indicator quantifies the degree of thermodynamic recovery achieved by the treatment process.

The exergy destruction ratio (y_{irrev}) evaluates the share of total exergy degraded within the system due to irreversibilities associated with mechanical friction, viscous mixing, and chemical reactions, as given by Equation (14).

$$y_{irrev} = \frac{\dot{E}_{irr}}{\dot{E}_{in}} \quad (14)$$

where $\dot{E}_{irr}$(kW) corresponds to the exergy destroyed internally and $\dot{E}_{in}$is the total exergy input. High values of y_{irrev}indicate substantial thermodynamic degradation, highlighting opportunities for process optimization.

Finally, the chemical-to-total input ratio (χ) quantifies the relative contribution of chemical reagents to the total exergy input, as defined in Equation (15).

$$\chi = \frac{\dot{E}_{chem}}{\dot{E}_{in}} \tag{15}$$

where $\dot{E}_{chem}$(kW) is the chemical exergy associated with all reagents used during treatment and $\dot{E}_{in}$is the total exergy input. This parameter reflects the dominance of chemical over mechanical exergy and supports the identification of strategies to minimize reagent consumption and associated exergy losses.

To ensure consistency of the thermodynamic analysis, the integrated system was first verified for mass conservation under steady-state conditions. The global mass balance of the urban water cycle was expressed as Equation (16).

$$\dot{V}_{in} = \dot{V}_{out} \tag{16}$$

where $\dot{V}_{in}$ represents the total raw-water inflow, and $\dot{V}_{out}$ corresponds to the sum of treated effluent, distribution losses, and consumptive, defined by Equation (17).

$$\dot{V}_{out} = \dot{V}_{treated} + \dot{V}_{loss} + \dot{V}_{consumptive} \tag{17}$$

The integrated balance provides a quantitative basis for linking energy consumption, exergy degradation, and process performance across the water–wastewater continuum, supporting the development of strategies for energy recovery, optimization, and carbon-neutral operation (Bylka, Mróz, 2020b; Valero et al., 2009)

2.3 GHG Emissions Assessment

GHG emissions associated with the operation of Brasília's UWC were estimated following the GHG Protocol Corporate Accounting Standard (WRI & WBCSD, 2004) and national guidelines from the Brazilian Ministry of Science, Technology, and Innovation (MCTI, 2024).

Indirect emissions (Scope II) were calculated from electricity consumption in all subsystems using the average grid emission factor of 0.0673 kg CO_2 kWh^{-1}, representative of Brazil's 2020–2023 energy mix. Direct emissions (Scope I) were calculated considering only the diesel consumed in sludge transport trucks, with a CETESB emission factor of 2.60 kg CO_2 $L^{-}1$ and consumption of 0.94 L $h^{-}1$ (Cetesb, 2024). In water treatment processes, there is no practical production of CH_4 or CO_2.

The total hourly and annual emissions were derived by multiplying subsystem power demand by the respective emission factors, yielding both subsystem and system-wide carbon footprints. These data enable a combined thermodynamic–environmental evaluation linking

exergy destruction, energy intensity, and GHG output across the entire UWC.

3 RESULTS

The results refer to the urban water cycle of Brasília, encompassing raw water abstraction, pumping stations, water treatment, distribution, and wastewater treatment, according to the system boundaries defined in Section 2. Operational averages and design parameters used in the exergy analysis were obtained from CAESB and consolidated in Tables S1.1 to S4.1b, S6.1 to S9.1, S10.1 to S11.1b and S12.1 (SM), representing steady-state operating conditions.

3.1 Mass Flow Analysis

Figure 3 shows the Sankey diagram of the UWC of Brasilia. Quantitative mass flow assessment provides the foundation for subsequent energy and exergy analyses and validates the global mass balance established in Section 2.2.5. This verification ensures that all inflows and outflows of the UWC are conserved under steady-state conditions. The total raw water abstraction of 2.461 $m^3\ s^{-1}$, supplied by the Torto, Santa Maria, and Bananal systems, reaches the WTP without measurable volumetric losses along the pumping stages. Within WTP, the backwash water, representing up to 5% of the filtration flow, is fully recirculated to the raw water inlet, ensuring no net discharge. The treated water (2.461 $m^3\ s^{-1}$) is conveyed to the distribution network, where volumetric losses of 0.433 $m^3\ s^{-1}$ (17.6%) occur, resulting in an effective delivery of 2.028 $m^3\ s^{-1}$ to consumers. Of this amount, 1.776 $m^3\ s^{-1}$ returns to the WWTPs, while 0.252 $m^3\ s^{-1}$ corresponds to non-sewered consumptive uses such as irrigation, infiltration, leaks in collector pipes, and evaporation. The treated effluent discharged into Lake Paranoá completes the hydrological loop of the Brasília UWC.

Table S12.1 (SM) presents the validation of the mass flow data adopted for the Brasília UWC. The overall mass balance confirmed that total inflows (2.461 $m^3\ s^{-1}$) equaled the sum of treated water effluent, distribution losses, and consumptive uses (1.776 + 0.433 + 0.252 $m^3\ s^{-1}$), with a closure deviation below 0.02 %, validating the internal consistency of the dataset. The total inflow to the WTP of 2.461 $m^3\ s^{-1}$ is fully consistent with the nominal design capacity of the facility, historically rated at 2.8 $m^3\ s^{-1}$ ($\approx 240 \times 10^3\ m^3\ day^{-1}$) according to CAESB's records. This magnitude is therefore representative of a large-scale metropolitan plant and accurately reflects the operational conditions of the system. The quantified distribution losses of 0.433 $m^3\ s^{-1}$ ($\approx$ 17.6%), corresponding to 37.4 $\times\ 10^3\ m^3\ day^{-1}$, fall within the expected range for well-maintained urban networks. National averages reported by SNIS (2023) indicate overall losses of approximately 36%, while Brasília's central supply zones typically exhibit values below 20%, confirming the physical plausibility of the adopted estimate.

The effective delivered water of 2.028 $m^3\ s^{-1}$ ($175.22 \times 10^3\ m^3\ day^{-1}$) represents the volume supplied to consumers served by the Brasília WTP. Considering the metropolitan population of roughly three million inhabitants and the contribution of additional systems such as Descoberto and Pipiripau, this flow corresponds to a realistic average of about 180 L per capita per day, in agreement with official demand statistics for the Federal District. The influent to the WWTPs, equal to 1.776 $m^3\ s^{-1}$ ($153 \times 10^3\ m^3\ day^{-1}$), also matches CAESB's operational data for the North ($\approx 45 \times 10^3\ m^3\ day^{-1}$) and South ($\approx 108 \times 10^3\ m^3\ day^{-1}$) facilities, confirming the representativeness of the adopted values.

The non-sewered fraction, estimated at 0.252 $m^3\ s^{-1}$ (≈ 20% of delivered water), is consistent with findings from previous urban water studies, which report that approximately 15–25% of distributed water in semi-arid regions corresponds to non-recoverable consumptive uses such as irrigation, infiltration, and evaporation (Gleick and Palaniappan, 2010; Mitchell et al., 2001). The resulting global return efficiency of approximately 72% (1.776/2.461) indicates that nearly three-quarters of the abstracted water reenters the environment as treated effluent, reflecting the operational performance expected in fully sewered and treated urban systems. Collectively, these results confirm that the mass flow parameters used in this study are physically realistic, statistically representative, and well aligned with observed operational conditions in Brasília's water infrastructure.

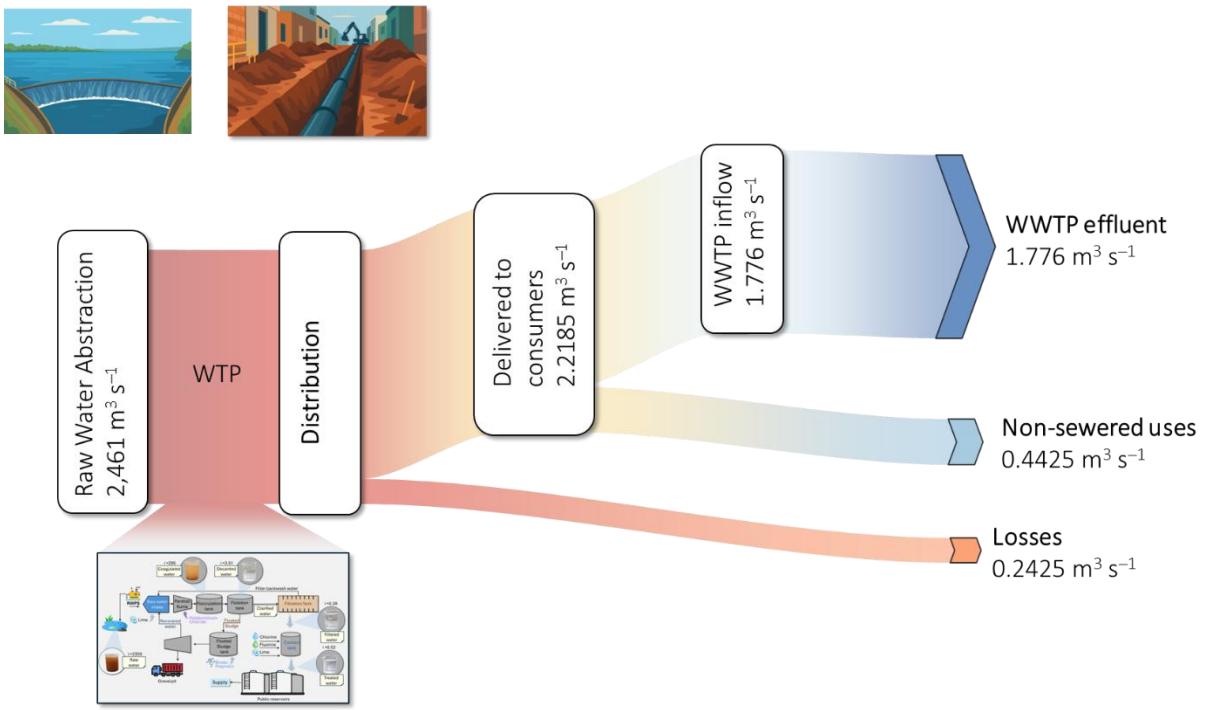

Figure 3. Sankey diagram of mass flow diagram of Brasília's UWC. Flow rates represent steady-state conditions derived from operational averages.

From a systemic perspective, the established mass balance reveals the strong

interdependence among abstraction, treatment, and recovery processes, confirming the hydraulic integration of the Brasília UWC. Based on the quantified flows, two performance indicators were derived to characterize the system's operational efficiency. The distribution loss index was determined as the ratio between volumetric losses and total abstraction flow, 0.2425/2.461=9.9%, representing the fraction of water lost within the network before reaching consumers. The return-to-environment ratio, obtained by dividing the total treated effluent by the abstraction flow, 1.776/2.461=72.1%, expresses the portion of abstracted water that is ultimately returned to the environment after treatment. These values indicate that the Brasília system performs within the range expected for modern urban networks, with distribution losses below 10 % and a high level of effluent recovery characteristic of fully sewered and treated cities. Maintaining such balanced throughput ensures the hydraulic and environmental stability of the urban water cycle and establishes a robust physical foundation for the subsequent exergy analysis, in which the energy conversion and destruction mechanisms of each subsystem are examined in detail.

3.2 Energy analysis

The distribution of electrical energy throughout the Brasília UWC reflects the strong dependence of the system on pumping operations and topographical elevation differences between abstraction and consumption areas. Electricity constitutes nearly the entire external energy input, totaling approximately 6,412 kW for the active pumping assemblies, while a minor contribution of 8.6 kW arises from diesel consumption associated with sludge transport from WTP to disposal sites. Although this contribution represents only 0.13 % of the total energy input, it was retained in the balance to ensure completeness and consistency with the system boundaries adopted for the exergy assessment.

Figure 4 summarizes the distribution of electricity consumption across the main components of the Brasília UWC. Figure 4(a) shows the energy demand of the MPAs at the Torto, Santa Maria, and Bananal subsystems. The highest consumption occurs at the Torto subsystem, where the combined operation of pumps T01, T02, and T03 accounts for approximately 49.8 % of the total electricity used for raw-water pumping. The Santa Maria subsystem, composed of pumps SM05 and SM06, contributes 35.6 %, while the Bananal subsystem (B08 + B09) accounts for the remaining 14.6 %. This distribution confirms the predominance of hydraulic energy requirements in the Torto and Santa Maria subsystems due to their larger flow rates and elevation heads.

Figure 4(b) presents the internal energy distribution within the WTP, where the recycling pumps and filter-washing operations together represent more than 60 % of the total

electricity consumption of the plant. Other processes, such as flocculation, backwashing blowers, and air-flotation compressors, account for smaller fractions, consistent with their limited mechanical load and shorter operating cycles. The internal composition of WTP's energy use highlights the predominance of mechanical operations over chemical or thermal contributions. Figure 4(c) aggregates the total electricity consumption of each subsystem, including the Brasília North (N-WWTP) and South (S-WWTP), which consume 1 164.6 kW and 1 890.2 kW, respectively (Franco et al., 2025). When integrated into the UWC balance, these units increase the total electricity demand to 10.68 MW. The raw-water pumping systems dominate the energy profile, accounting for 60.0 % of total electricity use, followed by the S-WWTP (17.7 %), N-WWTP (10.9 %), WTP (5.8 %), and TWPS (5.6 %).

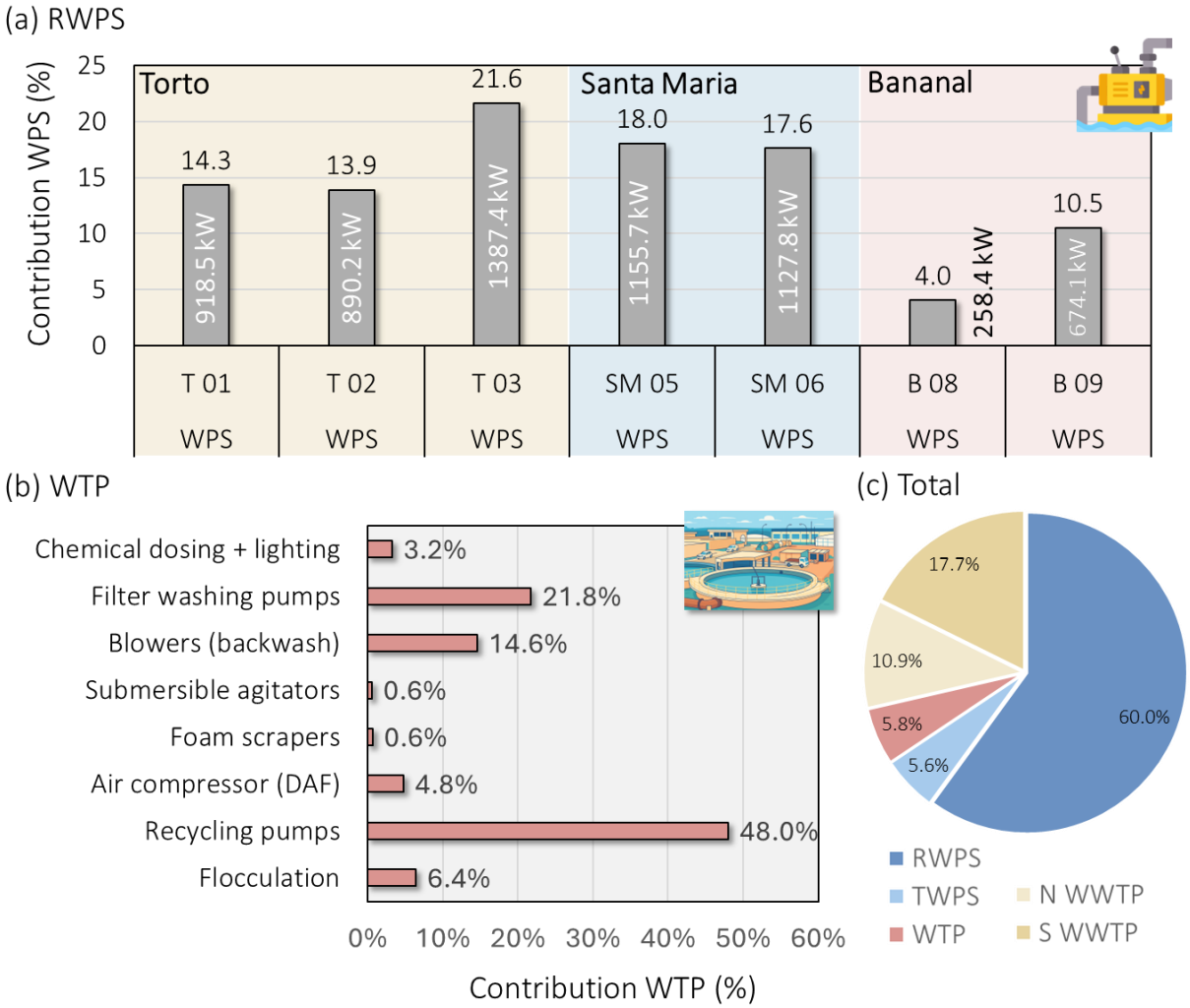

Figure 4. Energy demand distribution in the Brasília WSS. (a) Power consumption of the MPAs at the Torto (T), Santa Maria (SM), and Bananal (B) subsystems; (b) internal energy allocation among unit operations of the WTP; and (c) overall contribution of each subsystem to total electricity consumption between RWPS, WTP, TWPS, N-WWTP and S-WWTP. Values are derived from operational averages reported in Tables S4.1a, S4.1b, S6.1and S10.1a (SM) and Franco et al. (2025).

This distribution is typical of gravity-deficient supply systems, where high elevation differences require intensive hydraulic work at the abstraction stage, while wastewater treatment represents a significant share of the operational energy footprint due to aeration and recirculation processes.

Overall, the energetic characterization demonstrates that the Brasília WSS operates under a pump-dominated configuration, with energy demand strongly concentrated in the raw water pumping units. These findings provide a quantitative foundation for the subsequent exergy analysis and LCA, which evaluates the quality of energy use and identifies the main sources of irreversibility within the system.

In addition to the subsystem-specific results, the integrated energy performance of Brasília's UWC reveals key operational indicators derived directly from the measured data. The overall electricity demand of 10.68 MW, when normalized by the treated water flow rate of 2.461 $m^3\ s^{-1}$, corresponds to an energy intensity of 4.34 kWh m^{-3}. The allocation of electricity between the supply and sanitation sectors shows that about 71 % of the total energy is used for water abstraction, treatment, and distribution, while 29 % is associated with wastewater treatment. On a population basis, considering approximately 3.0 million inhabitants served by the integrated system, this corresponds to a specific power demand of 3.6 W $inhabitant^{-1}$.

Together, these indicators provide complementary insights into system efficiency and operational performance: the energy intensity (kWh m^{-3}) quantifies volumetric efficiency, the sectoral allocation (71/29) characterizes the structural distribution of energy use, and the per capita indicator (W $inhabitant^{-1}$) reflects the aggregate social energy demand required to sustain Brasília's fully integrated urban water cycle. These metrics form a consistent quantitative basis for evaluating thermodynamic performance and identifying potential efficiency improvements discussed in the subsequent exergy analysis.

3.3 Exergy Analysis

3.3.1 RWPS

Figure 5 illustrates the exergy distribution of the main RWPSs in Brasília, highlighting the relative magnitudes of losses and irreversibilities for Torto (a), Santa Maria (b), and Bananal (c). Together, these units account for the major share of the total energy demand in the UWS. In addition, the detailed exergy balance for each RWPS, including the optimized scenario with Sulzer pumps at Santa Maria, is summarized in Table S5.1 (SM). The current configuration values correspond to those illustrated in Figure 5.

The Torto RWPS, with an average electrical input of 3,196.1 kW, presented a useful

hydraulic exergy of 2,392.4 kW, corresponding to an overall exergy efficiency of approximately 74.9%. Comparing with the technical pump specifications, 582.0 kW is the hydraulic energy loss not recovered within the pumping system, due to head losses, bypass flows, and partial flow recirculation, and 221.8 kW are irreversibilities due to internal exergy destruction by mechanical friction, turbulence, and motor inefficiencies.

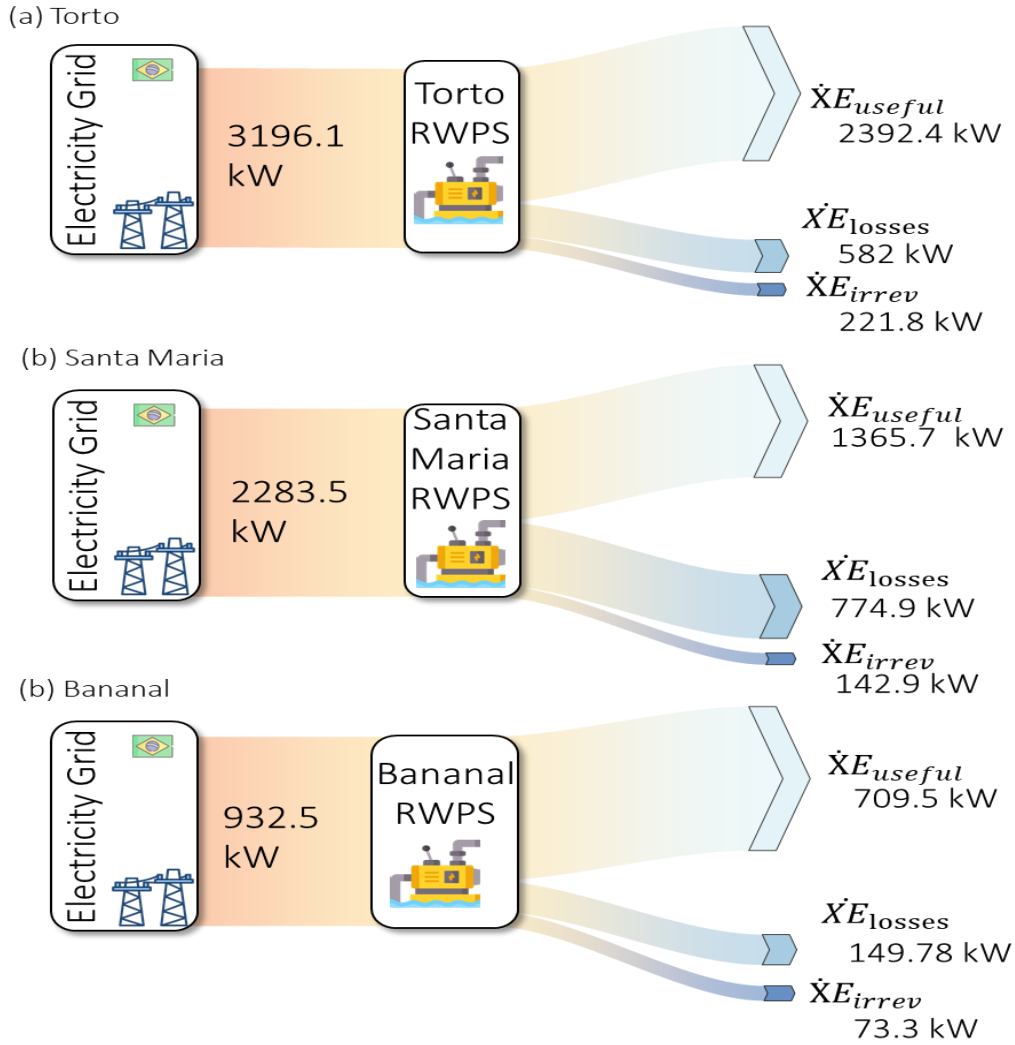

Figure 5. Exergy flow of the main RWPSs in Brasília. (a) Torto system, (b) Santa Maria system, and (c) Bananal system.

The Santa Maria RWPS exhibited a lower efficiency of 59.8%, with 2,283.5 kW of electrical exergy input and only 1,365.7 kW converted into useful hydraulic work (Table S5.1 - SM). The larger proportion of losses (774.9 kW) is attributed to aging equipment and the lower hydraulic performance of the existing Worthington pumps, which generate higher internal leakage and unproductive head. Despite this, the irreversibilities (142.9 kW) remain moderate, indicating that most inefficiencies arise from external hydraulic losses rather than electromechanical dissipation.

The Bananal subsystem, with two pumping arrays (Bananal 1 and 2), has higher exergy

efficiency, about 76.1%, with a combined electrical input of 932.5 kW (Table S5.1 - SM). The useful hydraulic exergy reached 709.5 kW, while losses and irreversibilities accounted for 149.8 kW and 73.3 kW, respectively. This behavior reflects the more recent installation of high-efficiency KSB and IMBIL brand pumps and optimized control through frequency inverters, which reduce hydraulic transients and frictional dissipation.

Comparatively, the three RWPSs demonstrate that exergy losses dominate over irreversibilities in all cases, confirming that most thermodynamic degradation in pumping operations stems from recoverable hydraulic inefficiencies rather than irreversible energy conversion. This finding suggests that system retrofits such as pump replacement, impeller redesign or pressure optimization could substantially enhance performance with relatively low capital investment. Considering the cumulative non-useful exergy across the RWPSs, including external hydraulic losses and internal irreversibilities, the total reaches about 1.95 MW, which corresponds to ≈30.3% of the total input. Of this, ≈0.44 MW (≈6.8%) is actual exergy destruction due to irreversibilities. These results indicate substantial potential for performance gains through hydraulic optimization and targeted retrofits.

3.3.2 Optimization scenario for the Santa Maria WPS

To evaluate the potential for improving exergy performance, the Santa Maria Water Pumping System (WPS) was analyzed under alternative configurations that replace the existing Worthington pumps with more efficient Sulzer or KSB models (Table 3). The objective was to estimate the recoverable exergy resulting from higher hydraulic efficiency and reduced electrical demand under identical operating conditions.

In the current configuration, the total electrical input of the three MPAs at Santa Maria is 2,283.5 kW, producing 1365.7 kW of useful hydraulic exergy and resulting in an overall exergy efficiency of 59.8%.

Replacing Worthington pumps by Sulzer SMN 402-800 units (impeller diameter 714.38 mm, η = 82.3%), the total electrical input decreases to 1,932.6 kW, while the useful exergy increases to 1,590.0 kW, yielding an efficiency of 82.3%. The corresponding recoverable exergy, accounting for reductions in both external losses and internal irreversibilities, is approximately 285 to 376 kW.

Alternatively, replacing the Worthington pumps with KSB 500-835 B models (impeller diameter 825 mm, η = 84.3%) results in slightly higher power consumption (1,058.9 kW per unit) but also higher useful exergy output (892.8 kW per unit). The efficiency rises to 84.3%, with internal exergy destruction decreasing to 77.5 kW. Although this configuration requires slightly greater electrical input, the improved hydraulic conversion compensates for the

increase, leading to similar overall exergy gains.

Table 3. Exergy balance and recoverable exergy for current and replacement pump configurations at the Santa Maria WPS.

Parameter	Worthington [a]	Sulzer [b]	KSB [b]	
Electrical input (kW)	1,367.4	966.3	1,058.9	Electrical power supplied
Useful exergy (kW)	804.1	795.0	892.9	Hydraulic exergy converted into useful pressure and flow
Exergy losses (kW)	476.9	101.4	88.5	External hydraulic losses (unrecovered flow energy)
Exergy destruction (kW)	86.4	69.9	77.5	Internal exergy destruction due to mechanical and electrical inefficiencies
Efficiency (ψ) (%)	58.8	82.3	84.3	—
Recoverable exergy (kW)	–	(285.4–375.5)	(298.3–388.4)	Potential gain in useful exergy

[a] current; [b] replacement, [c] $\dot{E}_{rec}$. Source: The Author.

Both replacement scenarios substantially enhance the thermodynamic performance of the Santa Maria WPS. The Sulzer configuration provides the largest reduction in total electricity consumption, while the KSB configuration achieves the highest exergy efficiency. On average, total non-useful exergy (losses + destruction) decreases by approximately 90% compared to the current system, indicating that modernization of the Santa Maria WPS would significantly improve the energy and exergy performance of the Brasília WSS with limited capital intervention.

3.3.3 Exergy balance of the WTP

The WTP constitutes the central thermodynamic stage of Brasília UWS chain, functioning as the interface between raw-water pumping and treated-water distribution. Its operation involves intensive mechanical and chemical processes, including coagulation, flocculation, flotation, filtration, and disinfection. The exergy balance was established according to Equation (1), distinguishing input, useful, loss, and irreversible terms presented in Tables S6.1, S7.1, S9.1, S10., S10.1b, S11.1a, and S11.1b (SM). The results are presented Figure 6 illustrates the corresponding Sankey diagram, integrating all electrical, chemical, and fuel contributions.

Figure 6.a shows the total exergy input ($\dot{X}E_{input,WTP}$) to the WTP is 1.61 MW, composed of electrical power (616.6 kW, 38.3 %), chemical reagents (862.8 kW, 53.6 %), and diesel fuel

for sludge transport (7.3 kW, 0.45 %). Also, the useful exergy ($\dot{X}E_{useful,WTP}$) associated with the treated water corresponds to 123.1 kW (7.6 %), while the exergy conveyed by the sludge ($\dot{X}E_{ch,sludge}$) accounts for 150.0 kW (9.3 %). The remaining 1.34 MW (82.9 %) represents internal irreversibilities ($\dot{X}E_{irrev,WTP}$) arising from mechanical friction, viscous mixing, and entropy generation during chemical reactions. These values result in an overall exergetic efficiency (ψ_{WTP}) of 7.6 %, confirming the dissipative character of treatment operations compared to the higher efficiencies observed for the pumping systems (59–76 %). The diagram in Figure 6.b shows the quantities of each input component.

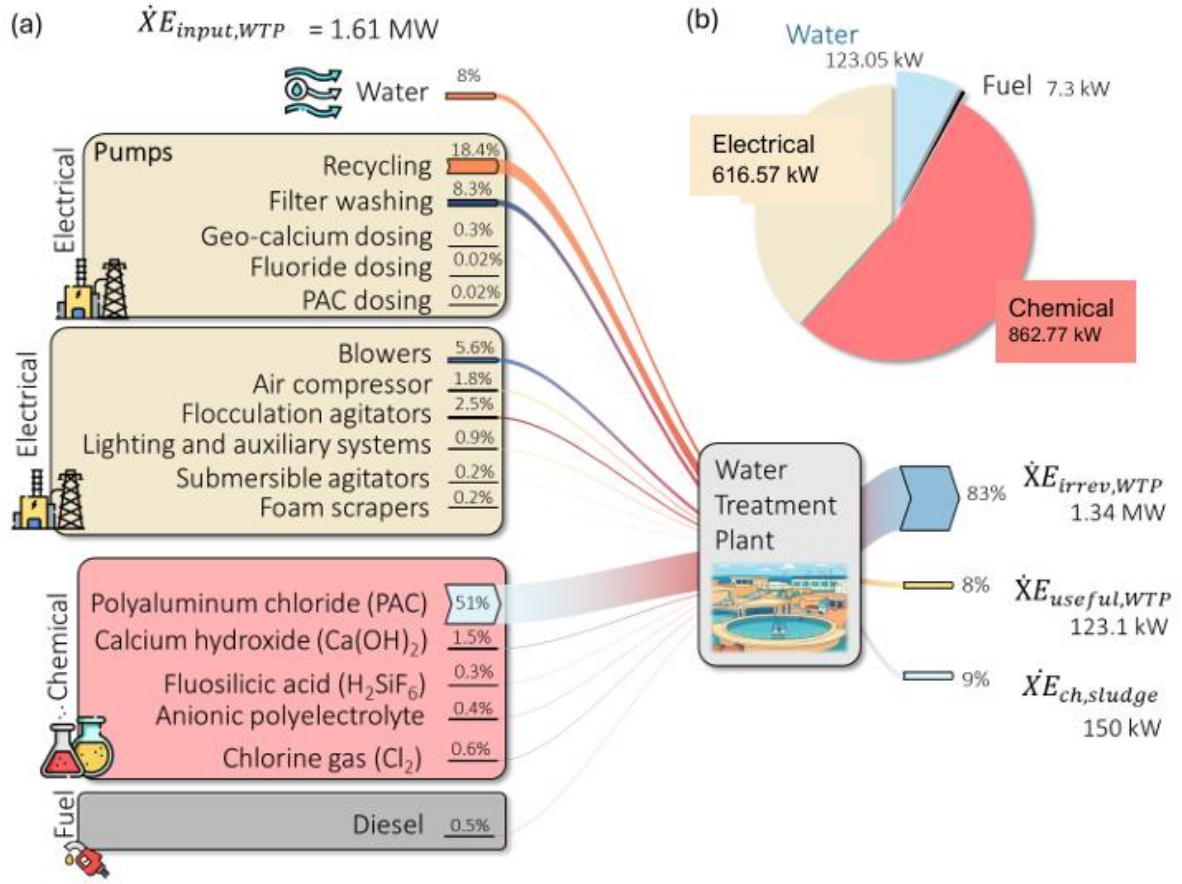

Figure 6. a. Exergy flow structure of the Brasília WTP, and b. the relative contributions of electrical, chemical, and fuel inputs to the total exergy balance.

Electrical inputs are dominated by recycling pumps, filter-washing systems, and blowers, which together account for more than 70 % of the total electrical exergy. Minor but non-negligible contributions arise from flocculation agitators (2.5 %), air compressors (1.8 %), and auxiliary lighting systems (0.9 %). On the chemical side, polyaluminum chloride (PAC) alone contributes 51 % of the total chemical exergy input, followed by calcium hydroxide (1.5 %), chlorine gas (0.6 %), fluosilicic acid (0.3 %), and anionic polyelectrolyte (0.4 %). The resulting chemical-to-total input ratio ($\chi \approx 0.54$) highlights the predominance of chemical exergy over mechanical work, emphasizing the relevance of reagent selection and dosing

optimization to minimize thermodynamic degradation

The exergy destruction ratio ($y_{irrev} \approx 0.83$) evidences the high share of internally degraded exergy, establishing a benchmark for performance improvement. From a process perspective, most exergy destruction occurs during the mixing and reaction stages, particularly in coagulation and flocculation—where entropy generation is intensified by chemical interactions and viscous dissipation. Improvement measures include automation of coagulant dosing, pressure recovery from backwash streams, and replacement of high-exergy reagents with alternatives of lower chemical potential. Collectively, these strategies could enhance ψ_{WTP} and reduce y_{irrev} leading to a more sustainable and energy-efficient operation within the urban water supply system.

3.3.4 Exergy balance of the distribution system

The treated water distribution system of Brasília comprises a network of transmission mains, reservoirs, and pumping assemblies that transfer water from the WTP to consumer zones across the Federal District. Its exergy performance was evaluated using the same formulation adopted for the previous subsystems (Equation 1), considering the electrical work of TWPS, Table S10.1a, S10.1b, and S11.1b (SM), and the hydraulic exergy depletion associated with losses in the distribution network.

TWPS employs IMBIL BP 300-340A centrifugal pumps with 380 mm impellers, arranged in a (3 + 1) configuration and driven by 285 HP (283 kW) WEG electric motors operating at 1,750 rpm, controlled by PLC and frequency inverters. Under current steady-state conditions, the average flow is 0.86 $m^3\ s^{-1}$ with a manometric head of 50 m, resulting in an average electrical exergy input ($\dot{X}E_{input}$) of 597.6 kW and useful hydraulic exergy ($\dot{X}E_{useful}$) of 422.5 kW. The external exergy losses ($\dot{X}E_p$) correspond to 33.8 kW, and the internal exergy destruction ($\dot{X}E_i$) reaches 141.3 kW, leading to a global exergy efficiency (ψ_{tp}) of 70.7 %. The corresponding mechanical indicators are motor efficiency (η_m = 95.4 %), pump hydraulic efficiency (η_b = 81.3 %), and overall electro-hydraulic efficiency (η_g = 77.6 %), with an average power factor (f_p = 0.85). These values are consistent with the performance range of large-scale water-supply pumping systems, where mechanical and electrical dissipation dominate over hydraulic losses.

Despite the relatively high efficiency of the pumping station, substantial exergy depletion occurs throughout the distribution network due to both physical and apparent losses. The average water-loss index (IP) in the Federal District between 2020 and 2022 is 34.4 %, equivalent to a mean flow loss of 2.82 $m^3\ s^{-1}$ (Table 11.1a (SM)). In Brasília alone, losses

average 17.6 %, corresponding to 242.5 L s^{-1}, with annual variation between 222.5 and 256.0 L s^{-1} (Table S11.1b (SM)). When expressed in exergetic terms, these hydraulic losses represent a depleted exergy rate ($\dot{X}E_p$) of approximately 260 kW, which corresponds to the potential energy irreversibly dissipated through leaks, unauthorized consumption, and metering inaccuracies.

The combination of mechanical inefficiencies in water treatment plants and the depletion of hydraulic exergy along the network reveals downstream degradation of the treated water's exergy flow. Although only a fraction of the water treatment plant's output is physically lost, its thermodynamic value is significant, representing approximately 43% of the useful exergy supplied by the plants. This highlights that improving distribution performance, even with small percentage reductions in losses, can save energy and exergy. For example, with preventive maintenance on distribution networks, instead of corrective maintenance as occurs today, these losses can be reduced by up to 65%, with a directly proportional impact on depleted exergy (electrical, chemical, etc.).

In summary, the Brasília distribution subsystem operates with high local pumping efficiency but experiences marked exergetic depletion throughout the network. The integration of exergy analysis with conventional loss indicators (IP and IPL) provides a comprehensive perspective of system performance, linking physical leakage control and demand-side management with the overall thermodynamic sustainability of the urban water cycle.

3.3.5 Exergy Balance of UWC

The integrated analysis of the urban water and wastewater system reveals the overall thermodynamic interactions and cumulative irreversibilities across the four main subsystems: the RWPS, the WTP, the TWPS, and the WWTP North and South, as illustrated in Figure 7.

The total exergy input from the electricity grid to the entire system reached approximately 7.0 MW, of which over 90% was associated with the water supply chain (RWPS + WTP + TWPS). The RWPS accounted for the largest single share (6.41 MW), highlighting the dominance of hydraulic conveyance energy demand in the water supply stage.

At the RWPS, an exergy efficiency of 69.7% was achieved, with 23.5% of the input exergy destroyed due to frictional and mechanical losses. The WTP exhibited comparable efficiency (69.7%), driven mainly by the energy embodied in chemical reagents (862.8 kW) and electrical inputs (616.6 kW), indicating balanced conversion between mechanical and chemical exergy inflows.

The TWPS presented the highest subsystem efficiency (70.7%), reflecting its relatively

optimized operation and smaller head losses compared to the raw water pumping stage. In contrast, the integrated WWTP subsystem exhibited the lowest exergy performance, due to the intrinsic irreversibilities of biochemical degradation and aeration processes.

When aggregated, the combined system showed an overall exergy efficiency near 69–70%, consistent across the supply chain. The principal exergy destructions were concentrated at the RWPS and WWTP, confirming these as the thermodynamic bottlenecks of the system. The total irreversibility rate in the sanitation subsystem was higher due to biological oxidation and gas emissions (CH_4 and CO_2), while the potable water chain presented mechanical and hydraulic dissipation as the main sources of degradation.

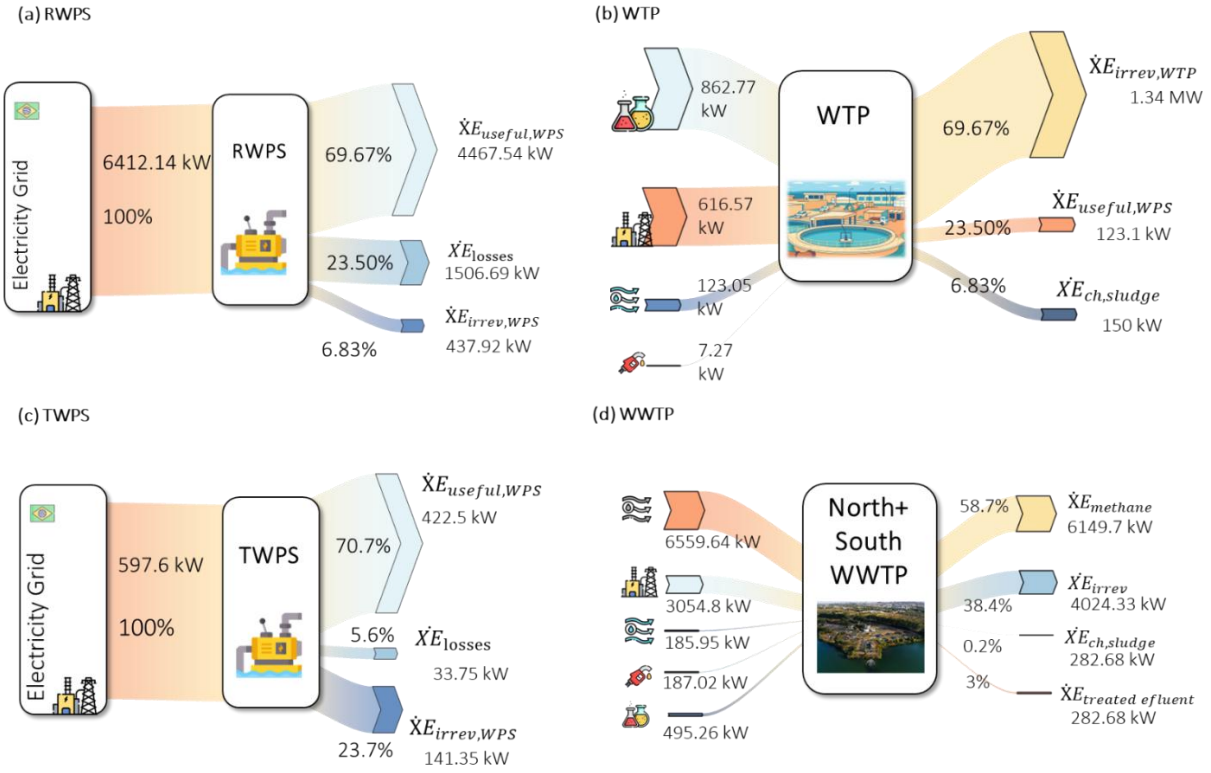

Figure 7. Exergy flow diagrams (Sankey representation) for the integrated Brasília UWC: (a) RWPS, (b) WTP, (c) TWPS, and (d) combined North and South WWTP. Adapted from (Franco et al., 2025).

The results demonstrate that improving pumping efficiency and energy recovery from sludge digestion could enhance the system-wide exergetic performance. Integrating energy valorization routes (e.g., biogas recovery, hydraulic turbines in gravity conduits) would reduce total exergy destruction and contribute to a more sustainable water–energy nexus.

3.4 GHG Emissions Analysis

The total power input to the UWC reached 10.68 MW, corresponding to an hourly emission of approximately 515 kg CO_2 h^{-1}. When converted to daily and annual scales, these values represent 12.4 t CO_2 day^{-1} and 4 520 t CO_2 $year^{-1}$, respectively. Table 4 summarizes the

contribution of each subsystem. The RWPSs dominate the carbon footprint, emitting 431 kg CO_2 h^{-1} (≈ 84 % of total emissions) due to their high electrical load.

The WTP and TWPS contribute 41.5 kg CO_2 h^{-1} and 40.2 kg CO_2 h^{-1}, respectively, whereas fuel used for sludge transportation adds only 2.5 kg CO_2 h^{-1} (< 1 %).

The overall carbon intensity of the UWC was 0.42 kg CO_2 m^{-3} of treated water, which is consistent with values reported for Brazilian metropolitan utilities operating under similar topographical conditions. The predominance of emissions associated with electricity use reflects the exergy structure of the system, where over 90 % of total input exergy originates from electrical power. Consequently, improving electromechanical efficiency directly reduces both energy demand and carbon output.

Table 4. GHG of Brasília's UWC subsystems.

Subsystem	Power demand	GHG emissions			Share
	(kW)	kg CO_2 h^{-1}	t CO_2 day^{-1}	t CO_2 $year^{-1}$	(%)
RWPS	6,412	431.5	10.36	3782	83.7
WTP	616	41.5	1	363	8
TWPS	598	40.2	0.96	352	7.8
Diesel use [a]	-	2.5	0.06	22	0.5
Total system	10,682	515.7	12.4	4520	100

[a] sludge transport; Indirect (Scope II) emissions were computed from electricity consumption using the national grid emission factor of 0.0673 kg CO_2 kWh^{-1} (MCTI 2024), while direct (Scope I) emissions correspond to diesel fuel used for sludge transport, with 2.60 kg CO_2 L^{-1} and 0.94 L h^{-1} consumption. Annualized results assume continuous operation (8,760 h $year^{-1}$). Source: The Author.

Retrofit scenarios tested for the Santa Maria RWPS indicated that replacing obsolete Worthington pumps with high-efficiency Sulzer or KSB models could reduce electricity consumption by up to 20 %, corresponding to a mitigation potential of 0.35 MW or approximately 650 t CO_2 $year^{-1}$. In the sanitation subsystem, recovering biogas from sludge digestion could displace an additional 400 t CO_2 $year^{-1}$ of grid electricity. Implementing both measures would lower total annual emissions to ≈ 3 500 t CO_2 $year^{-1}$, increasing overall exergy efficiency to above 75 %.

Integrating carbon accounting with the Water–Exergy–Environment Nexus thus enables a quantitative diagnosis of both thermodynamic and environmental performance. This coupling highlights that every kilowatt of electrical power saved through efficiency measures translates proportionally into avoided emissions, strengthening the pathway toward low-carbon, energy-resilient, and sustainable urban water management.

4. CONCLUSIONS

This study applied a comprehensive Water–Exergy–Environment Nexus to assess the thermodynamic performance of Brasília's UWC, integrating raw-water abstraction, treatment, distribution, and wastewater management into a single analytical framework. The results demonstrated that the system operates under strong hydraulic and energetic interdependence, with total electricity consumption of 10.68 MW and an average energy intensity of 4.34 kWh m^{-3}. The RWPS were identified as the most energy-demanding stage, responsible for 60% of total electricity use and exhibiting exergy efficiencies between 59.8% and 76.1%. In contrast, the WTP showed the lowest efficiency (7.6%) due to high chemical exergy inputs and internal irreversibilities associated with mixing and coagulation processes. The TWPS maintained 70.7% efficiency, while the WWTP presented higher exergy destruction caused by biological oxidation and gas emissions.

At the system level, the overall exergy efficiency of the UWC was approximately 69–70%, revealing consistent performance along the supply chain but substantial opportunities for improvement. Replacing obsolete pumps with high-efficiency models could recover up to 0.35 MW of exergy at Santa Maria station, while energy valorization of sludge biogas could enhance exergetic recovery in the sanitation subsystem.

The integrated exergy approach proved effective for diagnosing inefficiencies, quantifying irreversibilities, and identifying potential recovery pathways. By linking thermodynamic and environmental performance, this methodology supports data-driven strategies for reducing energy demand, optimizing resource use, and advancing low-carbon and sustainable urban water management in developing regions.

Acknowledgments

The authors would like to thank CAESB for cooperating with the research, Coordination for the Improvement of Higher Education Personnel (CAPES), Brazilian National Council for Scientific, and Technological Development (CNPq - process no. 305109/2023-5) for the financial support to this project, Decanato de Pesquisa e Inovação (DPI/UnB) and FAP-DF (project 469/2023).

FIRST ARTICLE REFERENCES

AGÊNCIA REGULADORA DE ÁGUAS, ENERGIA E SANEAMENTO BÁSICO DO DISTRITO FEDERAL (ADASA). **Abastecimento de água e esgotamento sanitário**. Painéis informativos. Serviço de abastecimento de água. https://www.adasa.df.gov.br/areas-de-atuacao/abastecimento-de-agua-e-esgoto. Acess 15/08/2022.

ASSOCIAÇÃO BRASILEIRA DE NORMAS TÉCNICAS (ABNT). NBR 9648: **estudos de concepção de sistemas de esgoto sanitário. Procedimento.** Rio de Janeiro, RJ, Brasil. 5 p, 1986.

_____. NBR 6400: **Bombas hidráulicas de fluxo (classe c) - ensaios de desempenho e cavitação**. Rio de Janeiro, RJ, Brasil. 26 p, 1989.

BYLKA, J.; MRÓZ, T. **Exergy evaluation of a water distribution system**. Energies 13:23 (2020).

COBO, M. J.; LÓPEZ-HERRERA, A. G.; HERRERA-VIEDMA, E.; HERRERA, F. **Scimat: a new science mapping analysis software tool. Journal of the american society for information science and technology**, v. 63, n. 8, p. 1609–1630, 2012. https://www.researchgate.net/publication/230760570_scimat_a_new_science_mapping_analysis_software_tool. Acess 02/01/2022.

COMPANHIA AMBIENTAL DO ESTADO DE SÃO PAULO (CETESB). **Emissões veiculares no Estado De São Paulo 2022.** Série relatórios/CETESB, issn 0103-4103. São Paulo, SP, Brasil. 2023. https://cetesb.sp.gov.br/veicular/relatorios-e-publicacoes/. Acess 08/12/2024.

CAESB, 2024a. COMPANHIA DE SANEAMENTO AMBIENTAL DO DISTRITO FEDERAL -**Relatório de indicadores de desempenho**. Brasilia, Distrito Federal, Brasil. https://atlas.caesb.df.gov.br/portal/apps/storymaps/stories/8d0c7820730c4be98a637c3e59522f6b. Acess 14/10/2024.

CAESB, 2024b. **Relatório de indicadores de desempenho 2023**. https://atlas.caesb.df.gov.br/portal/apps/storymaps/stories/8d0c7820730c4be98a637c3e59522f6b. Acess 14/10/2024

_____ **Sinopse do Sistema de Esgotamento Sanitário do Distrito Federal (SIESG).** 27a. Ed. 169p. Brasília, DF, Brasil. 2014b. https://atlas.caesb.df.gov.br/portal/apps/storymaps/stories/8d0c7820730c4be98a637c3e59522f6b. Acess 14/10/2022.

_____. **Estações de Tratamento de Água** CAESB. https://atlas.caesb.df.gov.br/portal/apps/storymaps/stories/8d0c7820730c4be98a637c3e59522f6b. Acess 14/10/2022.

DINCER, I.; ROSEN, M. A. **Exergy, energy, environment and sustainable development**. Elsevier. 1st ed., 454 p., 2007.

DINCER, I., ROSEN, M. A. **Exergy: energy, environment and sustainable development**. Elsevier Ltd. 2nd ed. 2013.

EPA. UNITED STATES ENVIRONMENTAL PROTECTION AGENCY. **GHG emission factors hub**. https://www.epa.gov/climateleadership/ghg-emission-factors-hub. Acess 27/04/2025.

FRANCO, V. P.; LAMAS, G. C.; FANTINI, D. G.; SIQUEIRA, M. B. B.; OLIVEIRA, S. B.; LEVY NETO, F.; CALDEIRA-PIRES, A.; SILVEIRA, E. A. **Exergy loss and optimization in brazilian urban wastewater treatment: a study of the urban water-exergy-environment nexus**. Journal of Cleaner Production, 519 (2025) 146057.

Https://doi.org/10.1016/j.jclepro.2025.146057

FUNDAÇÃO GETÚLIO VARGAS (FGV). **Programa brasileiro GHG protocol**. https://eaesp.fgv.br/centros/centro-estudos-sustentabilidade/projetos/programa-brasileiro-ghg-protocol. Acess. 29/01/2024.

GONG, M.; WALL, G. **On exergy and sustainable development – part 2: indicators and methods.** Exergy, an International Journal. Vol. 1 (4), 2001, p. 217-233.

HUANG, L. Q.; CHEN, G. Q.; ZHANG, Y.; CHEN, B. LUAN, S. J. **Exergy as a unified measure of water quality.** Communications in Nonlinear Science and Numerical Simulation, Vol. 12-5 663-672 (2007).

INTERGOVERNMENTAL PANEL ON CLIMATE CHANGE (IPCC). **2006 IPCC guidelines for national greenhouse gas inventories. Vol 5 – waste. Chapter 6 - Wastewater treatment and discharge.** IGES – Institute for Global Environmental Strategies. 2023. Kanagawa, Japan. https://www.ipcc-nggip.iges.or.jp/public/2006gl/index.html. Acess 15/12/2023.

KOTAS, T. J. **The exergy method of thermal plant analysis**. Ed. Butterworths, London, 296p, 1985.

MORAN, M. J.; SHAPIRO, N. H.; BOETTNER, D. D.; BAILEY, M. B. **Fundamentals of engineering thermodynamics**. 9th ed. John Wiley and sons. NJ, USA. 875 pp. 2018.

OLIVEIRA JR., S. **Exergy analysis and environmental impact**. Green Energy and Technology 63, 281-303 (2013).

ORTIZ, P. A. S.; FLÓREZ-ORREGO, D. A. **Exergia – conceituação e aplicação**. DEM/EPUSP/USP. 2013. https://www.academia.edu/3315176/exergia conceituação e aplicação doi_10.13140_rg.2.1.1088.8804. Acess 21/09/2023.

PEGORIN, M. C.; THEISEN, M. C. **Planejamento urbano e adaptação às mudanças climáticas: revisão de literatura no contexto de cidades resilientes**. In: xii convención sobre medio ambiente e desarollo por la integración y cooperación para la sostenibilidad. Habana, Cuba. 1-5 julio 2019. https://www.researchgate.net/publication/342703198_planejamento_urbano_e_adaptacao_as_mudancas_climaticas_revisao_de_literatura_no_contexto_de_cidades_resilientes. Acess 02/01/2022.

PERRY, R. H., & GREEN, D. W. **Perry's chemical engineers' handbook**. Ed. Mc-Graw-Hill: Knovel. 7th edition. 1997.

ROBERTS, E. **Water quality control handbook**, Mcgraw Hill, NY. 2007.

RODRÍGUEZ-MERCHAN, V.; ULLOA-ESSER, C.; BAEZA, C.; CASAS LEDÓN, Y. **Evaluation of the water–energy nexus in the treatment of urban drinking water in Chile through exergy and environmental indicators**. Journal of Cleaner Production 317: 2021.

ROSEN, M. A. **Energy crisis or exergy crisis?** Exergy an International Journal. Vol 2, 125-127. 2002.

STANEK, W.; VALERO, A.; UCHE, J.; CALVO, G. **Thermodynamic methods to evaluate resources.** Green energy and technology. Chap. 6.5, 156-165. 2017.

SZARGUT, J. **Chemical exergies of the elements.** Applied Energy, vol. 32, pp.269–286. 1988.

SZARGUT, J.; MORRIS, D.R.; STEWARD, F.R. **Exergy analysis of thermal, chemical, and metallurgical processes**. New York: Hemisphere Publishing Co, 332p. 1988.

SZARGUT, J. **Exergy method: technical and ecological applications**. Wit press co, uk. 1st ed. 161 p. 2005. Cross reference.

VALERO, A., UCHE, J., VALERO, A., MARTÍNEZ, A., ESCRIU, J. (2007). **Physical hydronomics: application of the exergy analysis to environmental costs of water bodies**. European Environment Agency.

WALL, G. **Exergy – a useful concept within resource accounting**. Institute of theoretical physics. Göteborg, Sweden, 1977. http://exergy.se/goran/thesis/paper1/paper1.html. Acess 22/11/2023.

SECOND ARTICLE: EXERGY LOSS AND OPTIMIZATION IN BRAZILIAN URBAN WASTEWATER TREATMENT: A STUDY OF THE URBAN WATER-EXERGY-ENVIRONMENT NEXUS[1]

Valtrudes Pereira Franco [a], Giulia Cruz Lamas [a], Dario Gerardo Fantini [a], Mário Benjamim Baptista de Siqueira [a], Sérgio Botelho de Oliveira [b], Flamínio Levy Neto [a], Armando Caldeira-Pires [a], Edgar A. Silveira [a*]

a. University of Brasília (UnB), Mechanical Sciences Graduate Program, Laboratory of Energy and Environment, Brasília (DF), Brazil.

b. Federal Institute of Goiás (IFG), Department of Chemistry, Goiânia (GO), Brazil.

*Corresponding author
E-mail: edgar.silveira@unb.br

ABSTRACT

This study assesses the water–exergy–environment nexus in Brasília WWTPs. Using exergy analysis, GHG quantification, and Life Cycle Assessment (LCA), it identifies inefficiencies and optimization opportunities in Brasília's North and South WWTPs, which treat 45,308.50 and 108,058.44 m^3 day^{-1} and achieve over 95% removal of chemical oxygen demand and nutrients. Exergy analysis revealed that over 97% of the total input exergy is destroyed due to unutilized methane (55–60%) and electricity consumption (28–31%). Methane was analyzed considering direct emission, flaring, and energy recovery via electricity production. LCA showed that flaring reduced emissions by ~40%, while biogas-to-electricity conversion led to further reductions of ~45%, achieving specific emissions as low as 41.95 $kgCO_2eq.year^{-1}$per population equivalent. Sludge transport, exceeding 100 m^3 day^{-1}, contributed to environmental impacts, underscoring the need for reuse alternatives such as agricultural application or biochar production. Seasonal inflow variations due to rainfall also increased energy demand and system pressure. Exergy-based indicators confirmed low environmental exergy efficiency and renewability index under current conditions. With energy recovery, the environmental exergy efficiency increased by 120.8% and 129.6%, the pollution rate decreased by 26.9% and 24.2%, and the renewability index increased by 25.4% and 35.8% for the North and South WWTPs, respectively. The results underscore exergy analysis and LCA as effective tools for diagnosing WWTP efficiency, quantifying bottlenecks, and advancing circular strategies in urban wastewater management.

KEYWORDS: Urban water cycle; Wastewater treatment plants; Exergy analysis; Life Cycle Assessment; Exergy-based indicators; Biogas recovery.

[1] Published in the Journal of Clear Production (https://doi.org/10.1016/j.jclepro.2025.146057).

INDEX SUMMARY

Nomenclature		*Symbols*	
Aluminum Sulfate	$Al_2(SO_4)_3$	Activity	a
Ammonium	NH_4	Chemical exergy of compound formation	$E_{ch,f}$
Annual mean factor	AMF	Chemical exergy related to compound concentration	$E_{ch,c}$
Biochemical oxygen demand	BOD	Destroyed exergy	E_{Dest}
Carbon	C	Dewatered sludge exergy	E_{ds}
Chemical oxygen demand	COD		
Companhia de Saneamento Ambiental do Distrito Federal	CAESB	Effluent exergy	E_{Efl}
Exergy	EXG	Environmental exergy efficiency	η_{ex}
Ferric Chloride	$FeCl_3$	Exergy	E_T
Ferrous Sulfate	$Fe_2(SO_4)_3$	Exergy of biosolid transport	E_{tr}
Greenhouse gases	GHG	Exergy of electricity consumed	E_{Elect}
Global Warming Potential	GWP	Exergy of compounds in the effluent, or final product, or useful effect	E_n
Hydrogen	H	Exergy of water used in the processes	E_w
Life cycle assessments	LCA	Exergy renewability index	λ
Lime	CaO	Gibbs free energy	ΔG_{fi}
Lower heating value	LHV	Influent exergy	E_{Ifl}
Methane	CH_4	Kinetic exergy	E_{ki}
Most Probable Number	MPN	Loss exergy	E_L
Nitrogen	N	Mechanical exergy	E_{me}
Oxygen	O2	Methane exergy in the produced biogas	E_M
Phosphoric Acid	H_3PO_4	Mole fraction	x_i
Phosphorus	P	Number of moles of elements	n_e
Raw sewage pumping station	RSPS	Pollution rate	τ_{pol}
Supplementary material	SM	Polymers and coagulants exergy	$E_{pol+coag}$
Total oxygen demand	TOD	Potential exergy	E_{po}
Wastewater treatment plants	WWTPS	Specific standard chemical exergy	E^0_{ch,n_e}
Water treatment plants	WTPS	Thermal exergy	E_{th}

1 INTRODUCTION

Global population growth, especially in urban areas, has led to soaring demand for energy, food, potable water, and natural resources, placing significant environmental strain (Huang et al., 2024). This urban expansion is closely tied to serious ecological impacts, including global warming, climate change, and freshwater scarcity, directly affecting agriculture, food production, and essential activities (Avtar et al., 2019; Bellezoni et al., 2021).

Urban sustainability depends on the efficient operation of water supply and sanitation systems, collectively called the urban water cycle (Figure 1(a)). These systems, comprising water uptake, distribution, sewage collection, and treatment, are complex and energy-intensive, requiring substantial electricity and inputs such as chemicals and fuels. Their performance directly influences water security, energy use, and environmental quality. Moreover, WWTP – key components of these systems – are significant sources of GHG emissions due to biological processes that generate carbon dioxide (CO_2), methane (CH_4), and nitrous oxide (N_2O), in addition to indirect emissions from electricity consumption (Parravicini et al., 2022; Ranieri et al., 2024b, 2023; Sharawat et al., 2021). Recent studies have addressed mitigation strategies, including energy audits, biogas recovery, and process optimization (Kłosok-Bazan et al., 2024). Despite technological progress, WWTPs in developing countries still face critical limitations, including insufficient infrastructure and investment, which hinder effective treatment and sustainability goals (Vaidya et al., 2023).

Despite widespread access to water supply systems in Brazil, significant deficits in sewage infrastructure persist, and existing treatment facilities often deliver substandard performance with notable health and environmental consequences (SNIS, 2023). Supply systems are also major energy consumers and suffer from high water losses, averaging 40.3% in 2021, resulting in wasted electricity, chemicals and other inputs used in treatment, and avoidable environmental impacts (SNIS, 2023). The supply systems consumed 13.9 TWh in the same year, equivalent to 2.55% of national electricity use (EPE, 2020). Roughly 80% of treated water eventually returns to the environment as wastewater, with variable composition influenced by domestic, industrial, and stormwater sources (ANA, 2022). Efficient management and treatment of this effluent are essential to minimizing impacts and ensuring environmental and public health protection.

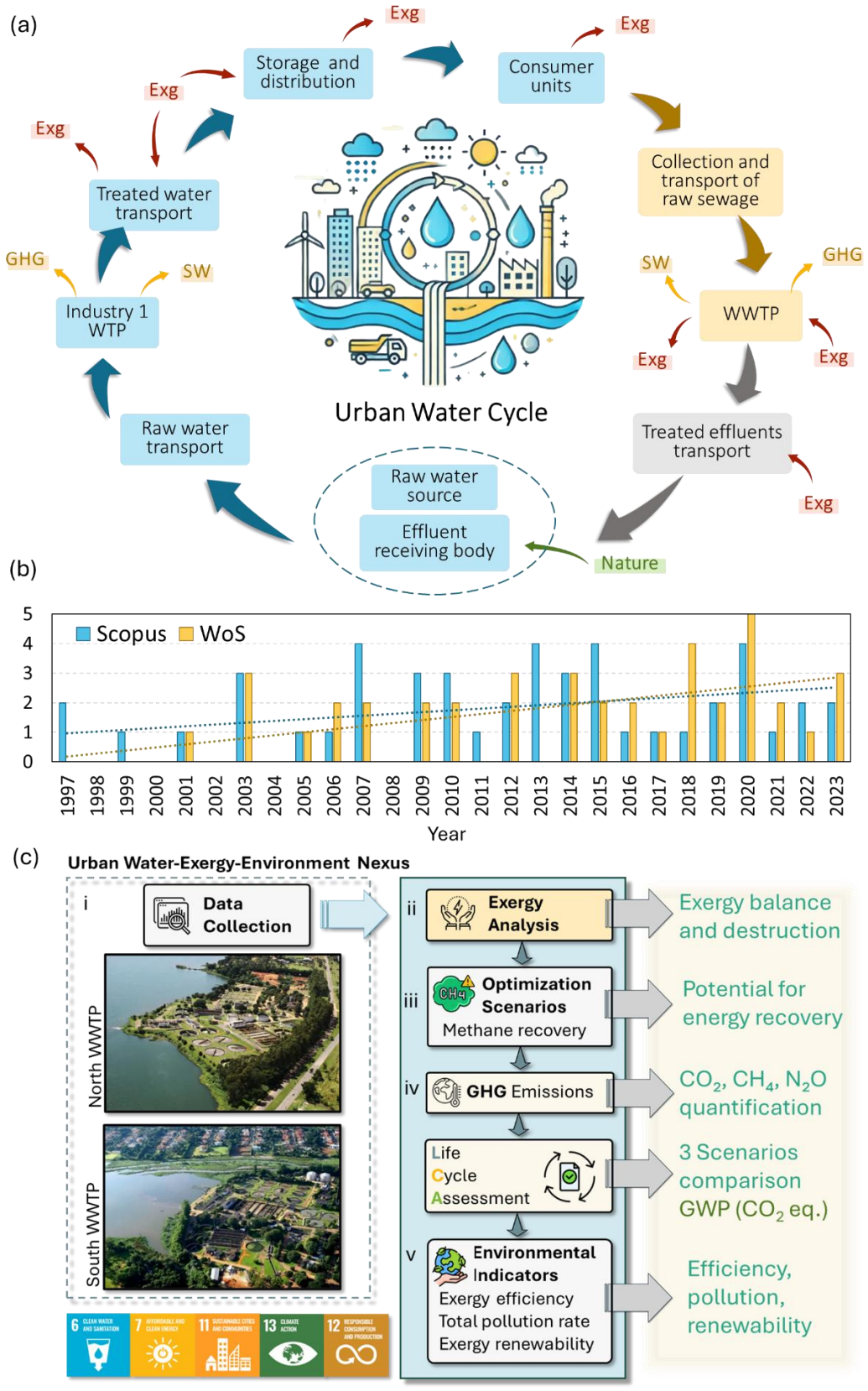

Figure 1. (a) Urban water cycle. SW – Sewage Sludge; GHG, and EXG – Exergy. (b) Evolution of publications related to the urban water-exergy nexus, based on Scopus and Web of Science databases. (c) The framework of the present analysis. LCA – Life Cycle Assessment; GWP – Global Warming Potential. Source: Adapted with images from (CAESB, 2024a).

Therefore, accurately assessing the interactions among energy, water, inputs, materials, waste, and emissions is essential for identifying resource depletions, optimizing installed capacity, and improving the overall performance of water cycle systems. Despite its importance, a comprehensive system for monitoring these relationships in urban water cycles remains scarce in the literature (Table 1), limiting the ability to mitigate freshwater insufficiency effectively, preserve water sources, and protect environmental and public health (Bellezoni et al., 2021). Advancements in these areas could provide meaningful insights into resource efficiency and sustainability improvements within the water management sector.

In this context, exergy, defined as the maximum useful work obtainable as a system reaches equilibrium with its environment, emerges as a powerful tool for evaluating the quality and efficiency of energy and material flows in urban water systems. Unlike conventional energy analysis, exergy accounts for both the quantity and the quality of resources, enabling the identification of irreversible losses and inefficiencies (Fitzsimons et al., 2016). Exergetic analysis allows for the qualification and quantification of energy and input flows, comparison between actual and ideal processes, and identification of technological, environmental, and economic improvement opportunities. This approach is suitable for assessing WWTP performance because urban water cycles function as thermodynamically open systems with intensive energy and environmental interactions.

Figure 1(b) and Table 1 highlight a few studies that have applied the exergy framework to WWTPs, especially using primary data. While prior works focused on exergetic efficiency or energy and mass balances, the present study advances by incorporating pollution rate, renewability index, environmental exergy efficiency, scenario-based GHG quantification and LCA. This combination provides a comprehensive decision-support tool not previously applied to Brazilian wastewater systems.

This study applies the Urban Water–Exergy–Environment Nexus framework to evaluate the exergetic and environmental performance of WWTPs in Brasília, Brazil (Figure 1(c)). This approach integrates detailed site-specific information, including effluent characteristics and treatment stages, which were often overlooked in previous research. By combining indicators such as exergetic efficiency, renewability index, pollution rate, GHG quantification, and Global Warming Potential (GWP), the analysis reveals systemic inefficiencies and highlights opportunities for energy recovery and resource optimization. While focused on Brasília, the context-sensitive methodology has broader applicability, offering a robust tool for sustainability assessment across diverse urban settings. The findings contribute valuable insights for improving the design, operation, and upgrading of WWTPs, advancing exergy-efficient sanitation infrastructure.

Table 1. Summary of literature on applying exergy-based analysis in water and wastewater systems.

Location / Reference	System Boundaries	Methodology	Exergy Indicators	Main Contribution
Sweden / (Hellström, 1999)	Comparison of conventional vs. source-separation systems, including nutrient transport and reuse	Exergy and nutrient flow analysis with mass balances and source-separation scenarios	Exergy consumption and nutrient flow efficiency	Pioneered application of exergy analysis to source-separation systems and nutrient recovery
Netherlands / (Wilsenach et al., 2003)	Integrated assessment of wastewater, surface water, and nutrients from source to reuse	Integration of Exergy analysis with resource recovery strategies and system redesign concepts	Exergy of organic matter, nutrients, and system integration potential	Highlighted the importance of integrated management and resource recovery for sustainability
Iran / (Khosravi et al., 2013)	Urban WWTP includes individual treatment units and network optimization	Exergy analysis applied to unit-level performance with a focus on environmental degradation	Environmental Exergy Efficiency and Total Pollution Rate	Introduced a dual-index optimization framework and applied it to real WWTP
Ireland / (Fitzsimons et al., 2016)	Two Irish WWTPs with similar technologies but varying influent qualities	Benchmarking using exergetic efficiency and destruction to identify improvement areas	Exergy destruction and exergetic efficiency	Demonstrated use of exergy benchmarking as a comparative tool for WWTP performance
Poland / (Bylka and Mróz, 2020)	Water intake, treatment, and distribution system in Poznań, including pumping and pressure management	Exergy modeling for mechanical/potential exergy in distribution networks	Mechanical and potential exergy	Developed a modeling tool for visualizing and optimizing exergy use in urban water systems
Iran / (Malboosi et al., 2021)	South Tehran WWTP and six others: includes screening, grit chamber, primary/secondary clarifiers, aerobic and anaerobic reactors, dewatering, and heat	Comprehensive exergy analysis across all treatment units using mass and energy balances, including comparison among seven WWTPs	Functional and universal exergy efficiency; exergy destruction by unit; exergy of sludge, biogas, effluent	Demonstrated that over 90% of exergy destruction occurs in aerobic reactors due to chemical transformation; proposed optimized energy recovery via biogas; introduced

	exchange; accounts for sludge, biogas, and effluent flows			Grossman diagram for system-wide exergy visualization
Brazil / This Study	North and South WWTPs in Brasília; includes influent, treatment, methane flaring, sludge transport, and seasonal flow variation	Exergy analysis, GHG quantification, Life Cycle Assessment focusing on GWP, optimization scenario for methane recovery, environmental indicators benchmarking	η_{exergy}; λ (renewability index); total pollution rate; exergy destruction	Integrated exergy analysis, LCA, and GHG quantification using operational data to assess WWTP performance under biogas valorization scenarios, showing that methane recovery and sludge reuse can triple efficiency, reduce pollution by 60%, and support circular and climate mitigation strategies

η_{exergy} – environmental exergy efficiency; λ – exergy renewability index; TPR (total pollution rate); EEE (environmental exergy efficiency); CH_4; WWTP; UASB (upflow anaerobic sludge blanket reactor); CEPT (chemically enhanced primary treatment); GHG emissions (CO_2, CH_4, N_2O); GWP (Global Warming Potential).

2 METHODOLOGY

This research employs a quantitative and diagnostic approach to evaluate the performance of two large-scale municipal WWTPs in Brasília, Brazil – namely, the North and South WWTPs. The methodology is structured into six main steps (Figure 1(c)): i. System definition and data collection (Section 2.1), ii. Exergy analysis (Section 2.2), iii. Biogas recovery potential (Section 2.3), iv. Life cycle assessment focusing on Global Warming Potential (carbon footprint) (Section 2.4), and v. Environmental performance indicators (Section 2.5).

2.1 Sanitation Systems in Brasília: Structure and Operation

In this section, the boundaries of each WWTP are defined from influent entry to final sludge transportation. Operational and design data are described and quantified, including flow rates, energy consumption, methane production, and sludge volumes.

The sanitation infrastructure in Brasília, illustrated in Figure 2, is managed by the CAESB – Environmental Sanitation Company of the Federal District (CAESB, 2024a). It comprises a collection network that channels wastewater from treated water consumers to WWTP North (15°44′38.26″S, 47°52′41.89″W) and WWTP South (15°50′32.90″S, 47°54′35.01″W) (Figure 2(a)), whose treatment process flow diagrams are shown in Figures 2(b) and (c), respectively. WWTP South serves the central and southern regions, while WWTP North covers the northern areas.

These WWTPs utilize secondary treatment processes, including activated sludge and biological treatment technologies, achieving high pollutant removal efficiencies. Both facilities discharge treated effluent into the respective northern and southern arms of Lake *Paranoá* (Figure 2(a)), either by gravity or through pumping.

Since their operation began in 1962, these WWTPs have implemented secondary treatment with activated sludge and biological treatment technologies. Expanded in 1995, Brasília South now handles up to 1,500 L s^{-1}, while WWTP North was upgraded to manage 920 L s^{-1}. Both operate with the tertiary treatment system, dewatered lime and high efficiency, with the treated flow at WWTP South currently at 1,250 L s^{-1} (85% of capacity) and WWTP North at 526 L s^{-1} (57.2% of capacity), with additional storage for peak periods (CAESB, 2024a).

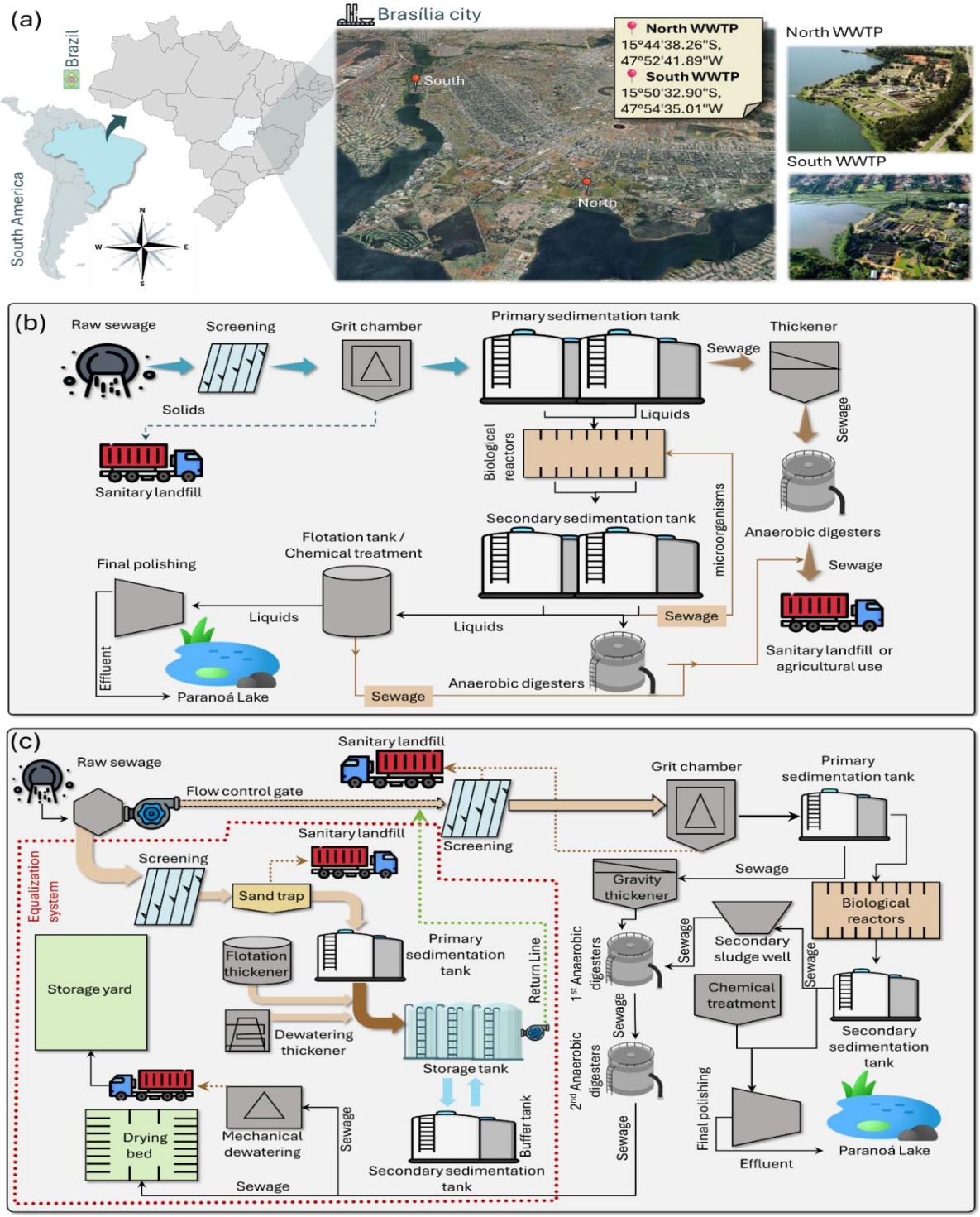

Figure 2. (a) Aerial view of the wastewater treatment infrastructure in Brasília, indicating the locations of the North and South WWTPs. (b) Process flow diagram of the South WWTP, illustrating primary, secondary, and tertiary treatment stages; (c) Process flow diagram of the North WWTP, with similar treatment configurations adapted to local hydraulic conditions. Source: adapted from (CAESB, 2024a).

2.1.1 Treatment Process Overview

Initial treatment in both plants begins with coarse screening and grit removal, where debris is collected and transported to a sludge management facility. Primary treatment follows in sedimentation containers to separate solids and sludge, which is further processed in secondary treatment. Aerobic, anaerobic, and facultative microorganisms reduce organic matter, while nitrogen and a high phosphorus level are removed through nitrification and denitrification (luxury uptake). Biological treatment uses activated sludge to remove phosphorus and nitrogen in three-stage Phoredox reactors, where a portion of the microbial biomass is recirculated to support the process. Advanced treatment, or final polishing, involves coagulation with aluminum sulfate, flocculation, and flotation to remove remaining phosphorus and solids.

The resulting chemical sludge is integrated with other process sludge in anaerobic digesters to generate biogas and nutrient-rich sludge, later dewatered and transported to the sludge management unit (SMU), coordinates 15°52′35.94″S, 48°08′48.44″W, in *Samambaia*, administrative region of the Federal District. This rigorous treatment framework in Brasília's WWTPs enhances environmental sustainability and supports effective resource recovery.

2.1.2 Data Quality and Statistics

The description of the datasets used in this study, including their respective sources and quality classification, is provided in Table 1.2 (SM). Data were primarily obtained from operational records and technical reports of the water utility (CAESB, 2024b), with primary data collected in situ and secondary data derived from internal literature or monitoring reports.

A statistical comparison of measured parameters was conducted to evaluate operational differences between the two WWTPs analyzed in this study. Monthly series data for influent and effluent characteristics, chemical consumption, energy use, and sludge production were collected for both the North and South WWTPs from 2020 to 2023. For each parameter, descriptive statistics were calculated (mean and standard deviation), and a non-parametric Mann-Whitney U test was applied to assess significant differences between the two independent samples, given the non-normality of some datasets and their unequal sample sizes (Franchitti et al., 2024; Mann and Whitney, 1947). The statistical significance level was set at $p < 0.05$. All analyses were performed using Python (v3.11), with data visualization and hypothesis testing conducted via the SciPy and Matplotlib libraries.

2.2 Exergy Analysis

This section calculates the exergy associated with all material and energy flows based on the second law of thermodynamics. The formulation includes the chemical, physical, and thermal exergy of water, wastewater, chemical reagents, electricity, and biogas. Metrics such as exergy destruction and the renewability index were derived to characterize system performance.

2.2.1 Exergy Balance and Definitions

In steady-state wastewater treatment processes, the total exergy is determined by the difference, or balance, between the influent and effluent exergies within the control volumes surrounding the treatment plants, as shown in Eq. (1) (Hellström, 1999; Malboosi et al., 2021).

This measure represents the amount of exergy required to restore wastewater to a composition as close to its original water state relative to a reference environment, thereby completing the urban water cycle.

$$E_T = \left(E_{Ifl} - E_{Efl}\right) = \left[E_{th} + E_{me} + E_{ch,f} + E_{ch,c} + E_{ki} + E_{po}\right]_{Efl}^{Ifl} \quad (1)$$

In Eq. (1), (E_T) represents the total exergy (kW) given by the difference between E_{Ifl}, the influent exergy to the plant (kW), and E_{Efl}, the effluent exergy (kW). E_{th} represents the thermal exergy (kW), E_{me} the mechanical exergy (kW), $E_{ch,f}$ the chemical exergy of formation in compounds of influent and effluent wastewater or effluent sludge (kW), $E_{ch,c}$ the chemical exergy of concentration in compounds of influent and effluent wastewater or effluent sludge (kW), the E_{ki} the kinetic exergy (kW) and E_{po} the potential exergy (kW) (Hellström, 1999; Malboosi et al., 2021).

WWTPs generally have minimal variation in wastewater temperature, the geometric level at entry and exit, and flow velocity (the hydraulic retention time in the WWTPs ranges from 12 to 18h at wastewater temperatures of 19 to 26 ºC) (CAESB, 2024a). As a result, thermal (E_{th}), potential (E_{po}), and kinetic (E_{ki}) exergies are insignificant and can be disregarded in Eq. (1). Thus, the influent exergy consists of the chemical and concentration exergies of wastewater compounds, operational resources such as electricity and process water for plant operation, and residual product transport. The exergies related to labor and plant infrastructure were not considered. The mechanical exergy (E_{me}) refers mainly to the electricity consumed by high-pressure compressors

for aeration in treatment processes. E_{me} contribution is accounted for in the total electricity consumed in WWTPs (Hellström, 1999; Malboosi et al., 2021).

Effluent exergy includes the residual chemical and concentration exergies in the treated wastewater, dewatered sludge, nutrients in the dewatered sludge, and the potentially useful methane gas generated. Polymers and coagulants are inputs for the deactivation of sludge entering and exiting the control volume, and their exergy is accounted for in the exergy renewability indicator discussed later (Section 2.5).

2.2.2 Physicochemical Estimation of Wastewater and Sludge Exergy

The physicochemical terms for organic influent, effluent, and dewatered sludge compounds are determined by Eq. (2), using estimative processes adapted for wastewater based on Stanek et al. (2017).

$$E_{ch,f} + E_{ch,c} = \left[\sum_i y_i \left(\Delta G_{fi} + \sum_e n_e E^0_{ch,n_e}\right)_i\right]_p + RT_0 \sum_i x_i \ln\left(\frac{a_i}{a_0}\right) \quad (2)$$

where y_i represents the moles of the substance i divided by the total mass of the solution; ΔG_{fi}, Gibbs free energy (J); n_e, the number of moles of elements (e) forming a compound (i); E^0_{ch,n_e}, specific standard chemical exergy (kJ g^{-1}) of organic matter; x_i, mole fraction; and a, activity; R, universal gas constant (8.31 J mol^{-1} K^{-1}); T_0, Standard ambient temperature (298.15 K). The subscript 0 denotes the properties of reference water (Stanek et al., 2017).

The terms in Eq. (2) are determined using operational data measured (primary data) at the treatment plants. However, some considerations must be made before applying the analysis: i) wastewater is a fluid with a pollutant load, and the chemical exergy of its pollutants causes harm to aquatic environments (Das et al., 2024; Huang et al., 2007); ii) it is composed of approximately 99.9% water and 0.1% dissolved and suspended substances that can be removed through proper treatment (Koul et al., 2022); iii) wastewater is considered as the substance $C_{10}H_{18}O_3N$, with a molecular weight of 200.2548 g mol^{-1} (Owen, 1982; Stanek et al., 2017); iv) total nitrogen is assumed to be in the form of ammonium (NH_4), with a molecular weight of 18.040 g mol^{-1}.

2.2.3 Chemical Exergy of Compounds and Concentration of Organic Matter

Determining the total chemical exergy of wastewater presents significant challenges due to the complexity and high cost of identifying and quantifying the standard chemical exergy of

pollutants. To overcome this difficulty, (Hellström and Kärrman, 1997) theoretically divided the wastewater flow into specific segments and calculated the standard chemical exergy of each segment through practical simplifications, with results that, according to the author, did not differ from actual values. This method is also adopted in this study.

The calculation of the chemical exergy using Eq. (2) precedes the determination of the chemical exergy of organic matter (E^0_{ch,n_e}) of pollutants in the influent wastewater, effluent, and dewatered sludge. Since pollutant composition is not typically measured in WWTPs, the determination is performed using boundary solutions, as presented by (Fitzsimons et al., 2016; Hellström and Kärrman, 1997; Khosravi et al., 2013; Malboosi et al., 2021; Mora Bejarano, 2009; Tai and Matsushige, 1986).

Tai and Matsushige were the first to determine the standard chemical exergy of organic matter in wastewater (E^0_{ch,n_e}) using calculation methods, relating it to the total oxygen demand (TOD) (Tai and Matsushige, 1986). The authors considered 138 organic substances without identifying contaminants if wastewater consists only of carbon, hydrogen, and oxygen. Khosravi et al. revised the method and found that 24 of the 138 substances are short-chain compounds or do not contain nitrogen, typical of wastewater pollutants (Khosravi et al., 2013). Assuming that all organic matter is converted into carbon dioxide, water, and nitric acid, the authors correlated the standard chemical exergy to the TOD of the remaining 114 compounds, obtaining Eq. (3) with the linear regression (R^2=0.9923) (Khosravi et al., 2013).

$$E^0_{ch,n_e}\ (\text{J L}^{-1}) = 13.7\ (\text{kJ g}^{-1})\ \text{TOD}\ (\text{mg L}^{-1}) - 116 \quad (3)$$

The standard chemical exergy of compounds is obtained from the literature (Szargut, 1989). The TOD is determined through chemical analyses of the compounds, a practice uncommon in WWTPs, thus requiring the use of the simplified boundary solution TOD≈COD (chemical oxygen demand) proposed by (Alley, 2007). Although less precise, this simplification is acceptable since exergy analysis aims to evaluate WWTP components rather than develop designs that require higher accuracy (Khosravi et al., 2013).

Determining the chemical exergy of dewatered sludge requires knowledge of the chemical composition of the residues, which is as challenging to identify as that of raw wastewater.

However, according to (Hellström and Kärrman, 1997):

i) the organic matter in sludge consists of a composition of cell fibers and cellulose with sufficient nitrogen concentration, making it relatively easy to determine the chemical exergy of sludge, as most of it is related to organic matter;

ii) ii) over 80% of the nitrogen present in wastewater and less than 10% in sludge is ammoniacal nitrogen, making it unnecessary to calculate the number of fibers and cellulose cells to determine the chemical exergy of organic matter and nutrients in the sludge;

iii) iii) all phosphorus is precipitated through the addition of coagulants such as lime (Ca_2^+) and aluminum sulfate (Al_3^+), and the nitrogen in organic compounds is filamentous.

Thus, dewatered sludge can be represented by the compound C_5H_7NO (molecular weight: 97.11558 g mol^{-1}), and its chemical exergy can be calculated using Eq. (3).

The detailed calculations of the chemical exergies ($E_{ch,f}$) and concentration exergies ($E_{ch,c}$) of the compounds in the influent and effluent liquid wastewater and the dewatered sludge from the North and South WWTPs are presented in Table S2.2 (SM) and Table S3.2 (SM).

The standard chemical exergies of the nutrients and coagulants used, the metals present in wastewater and dewatered sludge, and the exergy of the methane produced are also calculated based on (Rivero and Garfias, 2006; Szargut, 1989). According to (Metcalf et al., 2002), in activated sludge systems, phosphorus and nitrogen are the two main nutrients responsible for cell growth, present as phosphate ions (HPO_4^{2-}) and ammonium (NH_4^+), respectively. Potassium, on the other hand, has a negligible concentration in wastewater.

These considerations simplify the calculation of the chemical exergy of nutrients using the standard chemical exergies. In WWTPs treating industrial wastewater, the iron content is generally high, and its chemical exergy is significant, making the exergy contributions of other metals negligible. In Brasília, however, wastewater is predominantly domestic, with insignificant metal concentrations, except for iron, which is included in the analysis. Table 2 summarizes the key compositional parameters of the treated wastewater from both plants.

Table 2. Chemical compounds present in the treatment processes at the North and South WWTPs and their standard chemical exergy (E^0_{ch,n_e}).

Chemical compound	E^0_{ch,n_e}(kJ g^{-1}) [b]	Chemical compound	E^0_{ch,n_e}(kJ g^{-1}) [b]
Inorganics [a]		Organics [a]	
Lime (CaO)	2.3	Methane (CH_4)	51.8
Ferric Chloride ($FeCl_3$)	1.4	Polymers	40.0
Phosphorus (P)	28.1	*Metals*	
Aluminum Sulfate ($Al_2(SO_4)_3$)	1.0	Iron (Fe)	6.7
Ferrous Sulfate ($Fe_2(SO_4)_3$)	0.9	*Nitrogenous*	
Phosphoric Acid (H_3PO_4) (HPO_4^{2-})–1.1		Ammonium (NH_4^+)	21.8

[a] Monthly daily averages compounds; [b] standard tables by (Szargut, 1989). Source: Adapted data from (CAESB, 2024a).

2.2.4 Exergy Destruction

Exergy destruction represents the irreversible loss of useful energy within the system due to inefficiencies, internal entropy generation, or dissipation into unusable forms. In wastewater treatment plants, such losses are primarily associated with biological degradation, chemical reactions, heat dissipation, and the incomplete utilization of energy-rich byproducts such as methane, dewatered sludge, and residual chemical compounds, which could otherwise contribute to the useful exergy output.

To quantify this loss, the exergy destruction (E_{Dest}) was calculated by subtracting the sum of useful and recoverable exergy outputs from the total exergy inputs to the system, as defined in Eq. (4) (Hellström, 1999; Horrigan, 2016; Malboosi et al., 2021).

$$E_T = E_{Dest} = \left[(E_{ch,f} + E_{ch,c}) + E_{Elect} + E_w + E_{tr}\right]_{Ifl} - \left[E_n + E_{ds} + E_{pol+coag} + E_M\right]_{Efl} \quad (4)$$

Here, E_{Dest} represent the exergy destroyed (kW); E_{Elect}, the exergy of electricity consumed (kW); E_w, the exergy of water used in the processes (kW); E_{tr}, the exergy of biosolid transport (kW); E_n, the exergy of chemical compounds ($E_{ch,f} + E_{ch,c}$) in the effluent wastewater (kW); E_{ds}, chemical exergy of dewatered sludge or waste exergy (kW); $E_{pol+coag}$, exergy of polymers and

coagulants (kW), and E_M, the methane exergy in the produced biogas (kW) (Hellström, 1999; Horrigan, 2016).

The exergy of the electricity consumed (E_{Elect}) refers to that used in high-pressure air compressors for aeration, internal transfer pumping, lighting, etc., and is included in the total measured consumption of the WWTPs. The exergy of the water (E_w) used in the treatment processes refers to the exergy of the water consumed in cleaning and diluting chemical products, measured by water meters at the stations. These terms account for material and energy flows that either exit the system or are consumed during treatment. Notably, E_M is currently not recovered in the plants studied and is included to reflect potential optimization. $E_{pol+coag}$ corresponds to the chemical energy embodied in reagents that are not reutilized.

By calculating E_{Dest}, it is possible to identify the main inefficiencies and irreversibilities in the treatment process, supporting the development of strategies for energy recovery, emissions reduction, and overall process optimization.

2.3 Biogas Recovery Potential

Methane produced during anaerobic digestion in the studied WWTPs flares without energy recovery. A hypothetical recovery scenario was developed to evaluate its energy potential in which the biogas is purified and used to power an internal combustion engine coupled to a generator.

The chemical exergy of methane was estimated based on its average lower heating value (LHV_{CH_4}) of 10.85 kWh m^{-3}, which is representative of purified methane typically obtained from biogas upgrading (Jordão, 2007; Vilardi et al., 2020). An overall conversion efficiency (η) of 20% was assumed for the combined system (engine + generator), in line with small-scale applications in decentralized energy recovery systems (Jordão, 2007; L.C. S. Lobato, 2011).

The daily volume of methane produced (Q_{CH_4}) was estimated using the methodology proposed by the IPCC (2006) and adapted by Lobato (2011) which relates methane generation to chemical oxygen demand (COD) removal (detailed in the SM through Eqs. (S1–S4)). The average COD removal efficiencies from 2020 to 2023 were 95.19% and 95.53% for the North and South WWTPs, respectively. According to Lobato (2011), high COD removal enhances methane generation by reducing dissolution losses, gas-phase emissions, and sulfate interference. The useful exergy output from methane recovery was calculated using Eq. (5) (Nourin et al., 2021).

$$E_{CH_4,recovery} = Q_{CH_4}.LHV_{CH_4}.\eta \quad (5)$$

This estimation supports the construction of a methane-to-energy recovery scenario, contributing to the improvement of process efficiency and to reduces GHG emissions associated with flaring (the pollution potential of methane is approximately 80 to 86 times greater than that of CO2 within a 20-year period and 28 to 34 times greater within a 100-year period, according to (IPCC, 2013).

2.4 Life Cycle Assessment - GHG in WWTPs

2.4.1 Goal and Scope

LCA was carried out using Sphera's LCA for Experts software (v.10.9.0.20, old GaBi), adopting a cradle-to-grave approach. GHG emissions were characterized using the IPCC AR6 methodology (100-year time horizon), including biogenic carbon. The assessment contemplated a carbon footprint analysis, focusing on the GWP impact category. All background data were obtained from the integrated databases of Sphera LCA for Experts, supplemented by Ecoinvent database (v.3.11). The system boundaries comprise the influent raw sewage (or raw wastewater), chemical products and electricity used in its treatment and diesel oil for trucks used in sludge transport, resulting in three main outputs: sludge, effluent treated wastewater (or sewage), and biogas. The system configuration is illustrated in Figure 3 and further detailed in Figure S1.2 (SM), which presents the technological model developed within the Sphera software.

Influent transport for sludge was modeled using the Euro VI 32-ton truck available in the software's transport library. This vehicle type was selected due to its alignment with current European emission standards and its suitability for representing heavy-duty transport in municipal waste collection systems. Its inclusion allows for a realistic estimate of transport-related emissions, particularly relevant for centralized treatment scenarios. The trucks were assumed to consume 5.2 L of diesel per kilometer traveled, with total operational distances of 29.69 km for WWTP-N and 45.40 km for WWTP-S. CO_2 emissions from diesel combustion were disregarded because reliable measurements were not available.

Three scenarios were analyzed. In the first (Sc1), all biogas generated during the treatment process are directly emitted to the atmosphere, without energy recovery. In the second scenario (Sc2), the biogas is entirely combusted in a flare system, mitigating methane emissions.

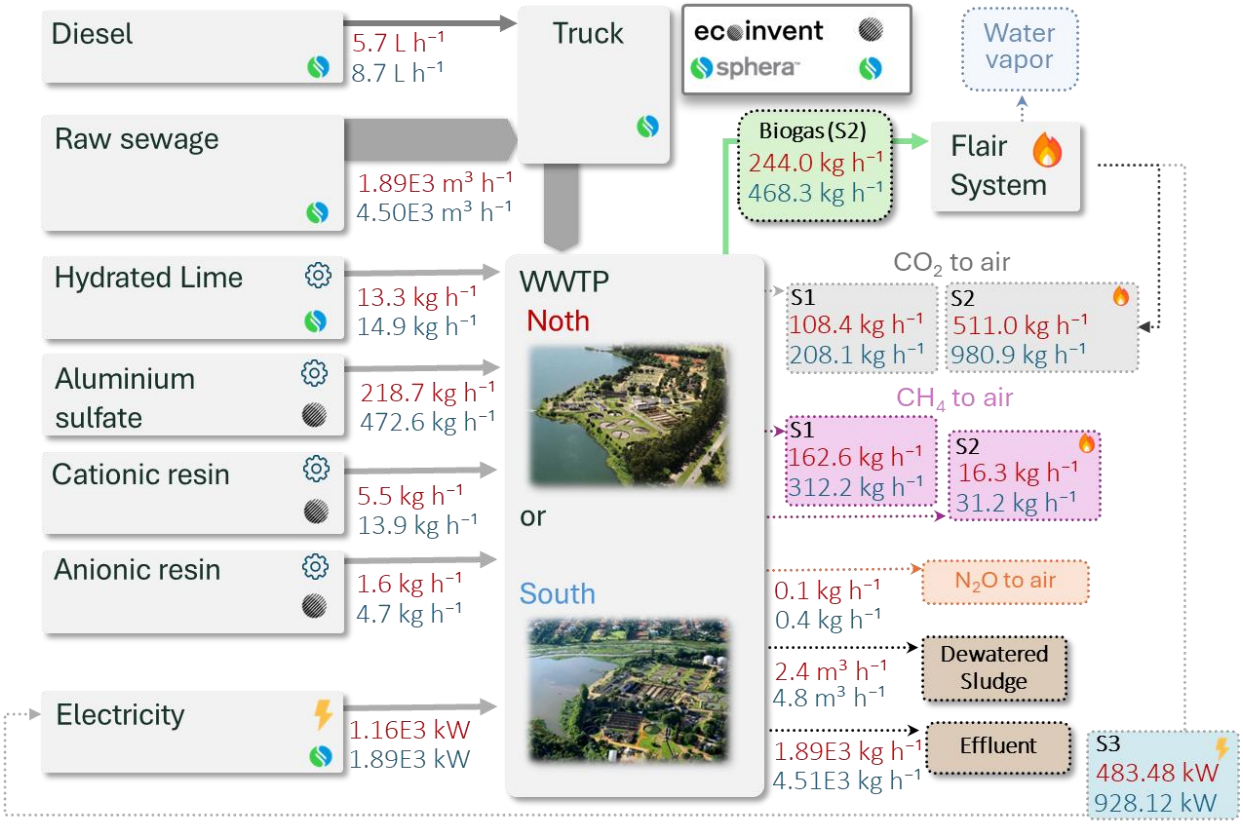

Figure 3. System boundaries for the LCA (carbon footprint) of WWTPs, including diesel oil for sludge transport, effluent treated sewage, and biogas handling under three scenarios: Scenario (Sc1) – without flaring, (Sc2) – with flaring, and (Sc3) – energy recovery (biogas directed to a combined heat-and-power unit).

For this scenario, fugitive emissions were considered as 10% of the total biogas produced, comprising 5% of methane remaining in the residual gas phase and 5% lost through leaks and condensate purges, as reported by Possetti et al. (2021), and aligned with the 5% estimate used by Ranieri et al. (2024b) to represent typical leakage during handling and combustion processes in wastewater treatment plants.

The third scenario (Sc3) introduces energy recovery, with the biogas directed to a combined heat-and-power unit that, assuming a 20% conversion efficiency, generates electricity for plant operations and heat for the digesters, thereby enhancing emissions reduction and improving the system's energy self-sufficiency.

The energy recovery potential was estimated based on the lower heating value (LHV) of biomethane, as detailed in the SM.

2.4.2 Life Cycle Inventory

In alignment with international protocols, particularly the GHG Protocol, GHG emissions from wastewater treatment systems are categorized into three scopes: Scope I (Direct emissions): Emissions directly resulting from processes under the control of the operator, such as biological treatment and on-site fuel combustion; Scope II (Indirect emissions): Emissions associated with purchased electricity, heat, or cooling; Scope III (Other indirect emissions): Emissions upstream or downstream of the value chain, including sludge transport and infrastructure (IPCC, 2006; WRI and WBCSD, 2004).

In WWTPs, indirect emissions are primarily associated with producing electricity consumed by the treatment processes. Meanwhile, direct emissions arise primarily from the biological processes of nitrification, denitrification, and anaerobic digestion. These reactions include water vapor, methane (CH_4), nitrous oxide (N_2O), and carbon dioxide (CO_2), as summarized in Table S4.2 (SM).

CO_2 emissions result from aerobic and anaerobic fermentation reactions, methane combustion, and the use of fossil fuels to transport sludge and other byproducts. Emissions associated with electricity consumption were estimated considering the Brazilian energy mix in Sphera LCA software.

CH_4 emissions stem from anaerobic degradation of organic matter and are calculated based on biogas volumes, methane content, and flaring practices. Although CH_4 is commonly flared, reducing its warming potential, its volume and concentration are typically measured only for research purposes or energy generation prospects, and the data for the assessed WWTPs were not available. Therefore, its emissions were estimated using mathematical models such as the one proposed by Chernicharo (2016), detailed by Equations S1.2 - S3.2 (SM).

N_2O emissions result from the breakdown of nitrogenous compounds, such as nitrates and proteins, during the aeration phase. N_2O is an intermediate product in both nitrification and denitrification processes, and its formation is influenced by operational parameters such as pH, temperature, and the concentrations of dissolved oxygen and nitrites (N_2O^-). Highlighted the limited number of studies on N_2O emissions in Brazilian WWTPs, although interest in this topic has been growing (Daudt, 2019; Daudt et al., 2019). Emission rates can vary significantly depending on the treatment technology, operational conditions, pollutant load, altitude, and local

climate. Consequently, reliable assessments of the environmental impact and mitigation strategies for N_2O remain limited.

The most national studies still apply the methodology established by the (IPCC, 2006), particularly Eq. (6), which estimates N_2O emissions in kg year^{-1} using commonly measured influent and effluent nitrogen concentrations, with adjustments for plant-specific conditions (Ribeiro, 2017; Ribeiro et al., 2018).

$$E_{N_2O\,emission} = P \,.\, \mathrm{GU_{WWTP}} \,.\, \mathrm{FD_{ic}} \,.\, \mathrm{FE_{WWTP}} \quad (6)$$

Here, P stands for the population corresponding to the wastewater treatment plant, GU_{WWTP} denotes the plant utilization rate in percentage, while $\mathrm{FD_{ic}}$ refers to the industrial and commercial discharge factor, which is commonly assumed to be 1.25. Finally, $\mathrm{FE_{WWTP}}$ is the specific emission factor to the WWTP, expressed in grams of N_2O per capita per year.

Based on a weighted average from several Brazilian studies, the emission factor was corrected to 7.81 g N_2O per capita per year for the characteristics of WWTPs in Brasília - such as treatment type, scale, altitude (~1,100 m), mild climate, and predominantly domestic sewage composition with high nitrogen removal efficiency (Daudt, 2019; Daudt et al., 2019). The resulting corrected emission factor led to the simplified Eq. (7) being adopted in this study. This approach ensures a more accurate estimation of N_2O emissions under local operating conditions.

$$E_{N_2O\,emission} = P \,.\, \mathrm{GU_{WWTP}} \,.\, (\,1.25) \,.\, (\,7.81) \quad (7)$$

Figure 3 illustrates the energy and mass flows, and Table S5.2 (SM) presents the LCI tabulated values used for the assessment, structured by treatment station and scenario. All flows are expressed per hour of operation. Inventory inputs and outputs include influent transport, energy and reagent consumption, sludge and effluent generation, and biogas emissions or flaring. Biogas composition was considered 60% CH_4 and 40% CO_2 by volume.

2.5 Exergy-Based Environmental Indicators

In this section, environmental metrics such as environmental exergy efficiency and the exergy renewability index were calculated and compared between both WWTPs to assess resource depletion and sustainability.

As thermodynamic conversion processes, the energy, operational, and environmental performance of WWTPs can be evaluated and compared through exergy efficiency and environmental indicators. In thermodynamic systems, there are distinct formulations for determining the exergy efficiency of processes, depending on the objective of the determination and the defined control volume, generally expressed as the ratio between the exergy of the desired product and the exergy introduced.

Mora Bejarano and Oliveira (2006) and Khosravi et al. (2013), based on the work of (Makarytchev, 1998), used environmental exergy efficiency (η_{ex}) and the pollution rate (τ_{pol}) as evaluation criteria for WWTPs. They concluded that exergy analysis is a coherent approach aligned with technological options that prioritize environmental sustainability and is useful for quantifying and optimizing the environmental performance of both process units and entire WWTPs (Khosravi et al., 2013). The similarity between the technologies and treatment processes studied by these authors and those of the North and South WWTPs supports applying and evaluating those criteria to these plants.

Environmental exergy efficiency (η_{ex}) calculated by Eq. (8) (Khosravi et al., 2013) is the ratio between the exergy of the final product (kW) or exergy of nutrients in the wastewater effluent (E_n) and the total exergy (kW) of natural resources and inputs consumed in the treatment processes (inputs).

$$\eta_{ex} = \frac{E_n}{\left(E_{ch,f} + E_{ch,c} + E_{Elect} + E_w + E_{tr}\right)_{Ifl}} \tag{8}$$

Increasing exergy efficiency reduces resource consumption, minimizes waste and emissions, and consequently decreases environmental impact while improving the environmental performance of processes at the treatment plants. It serves as an indicator of the theoretical potential for process improvements. However, excessive electricity usage and other inputs, as well as the failure to utilize methane for electricity generation and sludge for agricultural purposes, contribute to reduced efficiency.

Meanwhile, the total pollution rate (τ_{pol}), given by Eq. (9) (Khosravi et al., 2013), is the ratio between destroyed exergy (kW), including waste and emissions, and the exergy (kW) of the final product (E_n), or the useful effect of the process.

$$\tau_{pol} = \frac{E_{Dest} + (E_{ds} + E_M)}{E_n} \quad (9)$$

In addition to these indicators, Kotas (1985) introduced the exergy renewability index (λ) to wastewater treatment systems, given by Eq. (10), also explored by Fitzsimons et al. (2016) and Mora Bejarano (2009). This index is defined as the ratio between the exergy (kW) of the final product in the wastewater treatment system or useful effect (E_n), and the sum of exergies (kW) of non-renewable resources used in the wastewater treatment system ($E_{Elect} + E_{tr}$), the chemical exergy of formation and composition of the influent sewage $\left(E_{ch,f} + E_{ch,c}\right)_{afl}$, the exergy of the water used in processes (E_w), sludge deactivation exergy ($E_{pol+coag}$), methane exergy in produced biogas (E_M) or emissions exergy, and waste exergy (E_{ds}). Polymers and coagulants are added to facilitate and increase the sedimentation rate of suspended solids in the sludge, so their chemical exergy is accounted for as deactivation exergy.

$$\lambda = \frac{E_n}{(E_{Elect} + E_{tr} + \left(E_{ch,f} + E_{ch,c}\right)_{afl} + E_w - E_{pol+coag} - E_{ds} - E_M)} \quad (10)$$

According to Hellström; Kärrman (1997), the renewability index addresses a limitation of exergy analysis, which does not account for whether exergy sources are renewable. The index quantifies the system's capacity to restore the environment to its pre-process conditions. However, it is essential to define the size and compatibility of the control volume appropriate for the analysis, as it influences the value of λ. If the control volume is excessively large, it encompasses more energy conversion processes, reducing the index value due to increased irreversibility and the contribution of non-renewable inputs to the process, especially when comparing different wastewater treatment processes.

In most real cases, $\lambda < 1$, indicating that the treatment system operates in an environmentally unfavorable manner, as it does not restore the initial conditions of the processes, meaning there is no useful utilization of the exergy generated in the WWTPs. If $\lambda = 1$, the renewable exergy surpasses the non-renewable exergy, and the treatment occurs in an environmentally balanced manner. If $\lambda > 1$, the system generates renewable exergy exceeding the non-renewable demand, and the surplus can be used to restore the environment to its pre-process conditions.

3 RESULTS AND DISCUSSION

3.1 Assessment of the North and South WWTPs

Due to its larger collection area, the flow rate of influent wastewater at the South WWTP (108,058.44 m^3 day^{-1}) is significantly higher than that of the North WWTP (45,308.50 m^3 day^{-1}).

However, during the rainy season in Brasília, flows increase significantly due to rainwater infiltration into the sewage collection networks, overloading the WWTPs, increasing energy consumption and input, and reducing treatment efficiency. Figure 4 shows the average flows of influent wastewater from each plant from 2020 to 2023 and the average monthly rainfall index over the last 30 years in Brasília (INMET, 2024).

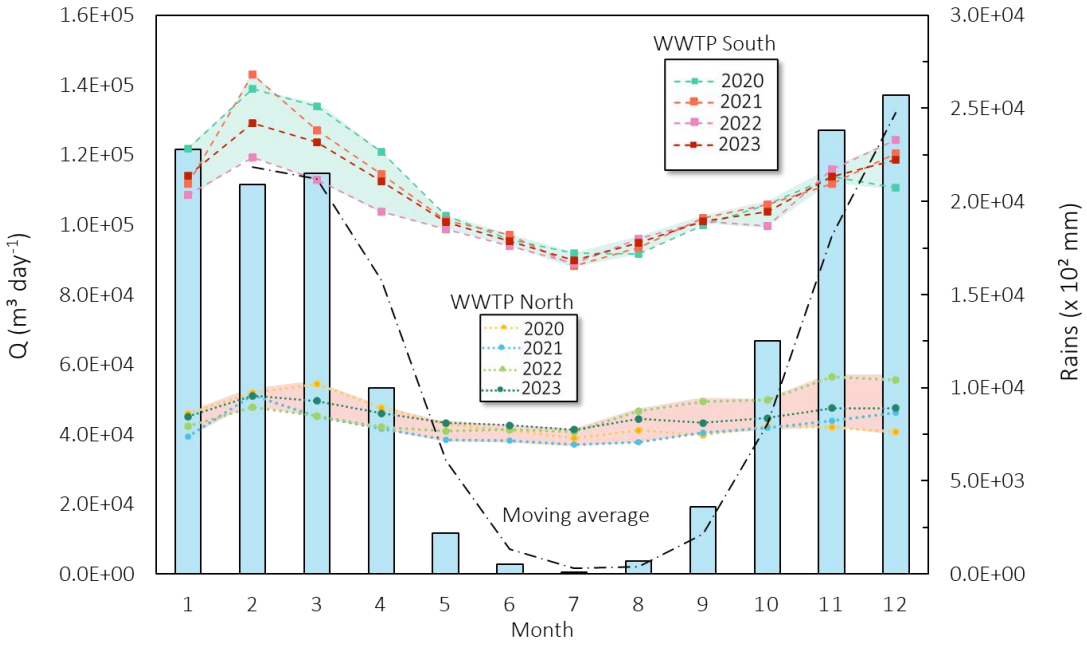

Figure 4. Daily influent wastewater flow at the North and South WWTPs over 12 months and the average rainfall index for Brasília ($\times 10^2$ mm).

Table 3 presents the measurement data from the plants used in the exergy calculations (CAESB, 2024b). Although polymers and coagulants used for sludge deactivation are introduced as inputs, they are accounted for alongside waste and emissions when calculating the indicators. In addition, Table 6.2 (SM), and Figures S1.2-S4.2 (SM) present a statistical comparison between the North and South WWTPs based on the mean values and standard deviations of 18 operational and performance parameters. The results highlight significant differences ($p < 0.05$) across most indicators, particularly in influent flow rates, energy consumption, and chemical usage.

Table 3. Operational and performance data of wastewater treatment processes used in the exergy analysis, including influent/effluent concentrations, removed compounds, and removal efficiencies at the North and South WWTPs.

Measured data	North WWTP		South WWTP	
	Average	SD [d]	Average	SD [d]
Inputs and outputs [a]				
Influent wastewater flow (m^3 day^{-1})	45,308.50	2903.87	108,058.44	12326.62
Power (kWh day^{-1})	27,950.06	1389.25	45,364.49	2505.74
Process water (m^3 day^{-1}) [c]	108.41	-	212.91	-
Polyanionic (kg day^{-1})	37.98	4.95	112.22	17.33
Polycationic (kg day^{-1})	132.57	12.90	333.56	26.87
Aluminum sulfate (kg day^{-1})	5,248.70	612.01	11,341.40	985.75
Hydrated lime (kg day^{-1})	318.44	49.44	358.42	78.27
Dewatered sludge (m^3 day^{-1})	58.73	4.59	116.13	11.53
Removed compounds and removal rates [a]				
Total Nitrogen Influent (mg L^{-1})	65.12	3.71	64.35	7.61
Total Nitrogen Effluent (mg L^{-1})	8.02	1.85	7.78	1.06
Removal Rate (%)	87.69	-	87.92	-
Phosphorus Influent (mg L^{-1})	7.04	0.51	6.66	0.98
Phosphorus Effluent (mg L^{-1})	0.33	0.07	0.23	0.06
Removal Rate (%)	95.29	-	96.59	-
Suspended Solids Influent (mg L^{-1})	307.32	31.45	221.84	23.01
Suspended Solids Effluent (mg L^{-1})	6.30	0.62	4.47	0.8
Removal Rate (%)	97.95	-	97.99	-
COD Influent (mg L^{-1})	656.00	43.31	533.45	80.3
COD Effluent (mg L^{-1})	31.50	3.02	23.46	2.93
Removal Rate (%)	95.20	-	95.60	-
BOD Influent (mg L^{-1})	350.06	33.39	332.32	46.33
BOD Effluent (mg L^{-1})	6.16	1.43	7.62	1.64
Removal Rate (%)	98.24	-	97.71	-
E. coli Influent (MPN 100mL) [b]	1.57E+07	7.62E+06	1.07E+07	2.39E+06

E. coli Effluent (MPN 100mL)	1.05E+05	3.76E+04	5.11E+04	3.37E+04
Removal Rate (%)	99.33	-	99.52	-

[a] Monthly daily average over twelve months during 2020-2023. [b] MPN – Most Probable Number per 100 mL. [c.] The monthly average reported by the treatment plant. [d] SD – Standard deviation. Source: With data from (CAESB, 2024a).

The South WWTP, which serves a broader catchment area, consistently exhibited higher values for energy demand (1,378,526.37 ± 111,759.38 kWh day^{-1} vs. 849,284.27 ± 36,926.69 kWh day^{-1}), sludge production, and chemical inputs, including aluminum sulfate and polymeric coagulants. Despite these scale differences, both plants achieved similarly high removal efficiencies due to their similar technologies for COD, BOD, total nitrogen, phosphorus, suspended solids, and *E. coli*, with no statistically significant discrepancies in effluent quality metrics. These findings suggest that while the operational loads and resource requirements scale proportionally with plant capacity, treatment effectiveness remains consistently high in both systems.

Electricity consumption accounted for a substantial portion of total exergy input: 27,950.05 kWh day^{-1} at North WWTP and 45,364.49 kWh day^{-1} at South WWTP. Dewatered sludge volumes were also notably higher at the South WWTP, at 116.13 m^3 day^{-1} compared to 58.73 m^3 day^{-1} at the North WWTP, further contributing to operational energy demands.

The high electricity consumption in treatment processes and the daily transport of dewatered sludge account for the reduced exergy efficiency and the high residual pollution rate of plants. In the first case, this demand is intrinsic to the high pollutant removal efficiency of the treatment process (around 98%). In the second case, it is due to the distance between the WWTPs and the disposal site, as well as the high moisture content of the sludge (approximately 97%).

Recent international studies reinforce the importance of evaluating precipitation impacts on wastewater treatment systems under the lens of climate change. Reznik et al., (2020), through an econometric analysis of 163 WWTPs across China, demonstrated that average annual and intra-annual precipitation variability significantly influence operational and maintenance costs. Their results indicate that plants exposed to greater rainfall variability tend to experience increased treatment costs due to process instabilities and overloading events, especially when stormwater is combined with sewage flow. Similarly, Ranieri et al. (2024a) assessed seven major WWTPs in Apulia, Southern Italy, and found a direct correlation between rainfall intensity and electrical consumption. For instance, in the Lecce plant, energy consumption rose from 0.36 to 0.51 kWh m^{-}

^{3} as rainfall intensity increased from 0.8 mm min^{-1} to 2.9 mm min^{-1}. The study also noted a reduction in BOD removal efficiency under high precipitation conditions, likely due to dilution and hydraulic overloads (Ranieri et al., 2024a). These findings corroborate the behavior observed in Brasília, where increased rainfall leads to higher influent volumes and potential performance drops, especially in activated sludge systems designed for average flow conditions.

3.2 Exergy of Treatment Processes

3.2.1 Chemical Exergy of Wastewater Compounds

The chemical exergy of compounds in the influent and effluent wastewater, as well as in the dewatered sludge ($E_{ch,f} + E_{ch,c}$), was estimated based on COD, nitrogen, phosphorus, and iron concentrations. These four components were selected due to their relevance to organic and nutrient loads, while other constituents presented negligible contributions to total exergy. The values were calculated using Eq. (3), based on data presented in Tables 2 and 3, following the methodology detailed in the SM. Results are summarized in Table 4.

The chemical exergy of the influent was considerably higher than that of the effluent in both facilities, reflecting effective removal of exergy-carrying compounds. In both WWTPs, COD was the dominant contributor, accounting for approximately 87% of the total chemical exergy in the influent. Nitrogen contributed around 13% in the North and 17% in the South WWTPs, while phosphorus and iron together accounted for less than 1%.

The effluent retained only 3.9% and 4.1% of the original chemical exergy in the North and South WWTPs, respectively, confirming high removal efficiency. Notably, nitrogen remained the primary residual contributor in the effluent, reflecting the challenges of complete nitrogen removal in biological systems.

These values align with those reported by Khosravi et al., (2013), who estimated a total chemical exergy input of approximately 3.3 MW for a comparable urban wastewater treatment plant.

In our study, the North WWTP exhibited an influent chemical exergy load of 2.48 MW, while the South WWTP reached 4.57 MW, reflecting differences in treatment capacity and organic load.

Table 4. Total chemical exergy of organic matter ($E_{ch,f} + E_{ch,c}$) for the main compounds in the mixture at the North and South WWTPs.

Compounds in the mixture [a]	North WWTP	South WWTP
Influent Wastewater Exergy (kW)		
COD	2,165.86	3,762.66
Nitrogen	315.24	810.04
Phosphorus	0.33	0.77
Iron	0.06	0.10
($E_{ch,f} + E_{ch,c}$) Influent	2,481.49	4,573.57
Effluent Wastewater Exergy (kW)		
COD	42.14	53.46
Nitrogen	53.67	133.36
Phosphorus	0.01	0.01
Iron	0.01	0.02
($E_{ch,f} + E_{ch,c}$) Effluent	95.83	186.85
Dewatered Sludge Exergy (kW)		
COD	9.98	14.99
Nitrogen	0.11	0.31
Phosphorus	0.02	0.02
Iron	0.00	0.00
($E_{ch,f} + E_{ch,c}$) Sludge	10.11	15.32

[a] Monthly daily average.

3.2.2 Exergy of Operational Resources and Generated Byproducts

Table 5 presents the results of the exergy calculations for operational resources used and generated byproducts, considering the quantities consumed, produced, and the standard chemical exergy (E^0_{ch,n_e}) values from the general tables of Szargut (1989). The standard chemical exergy of regular S-500 diesel fuel is determined based on the chemical composition $C_{14.09}H_{24.78}$ proposed by Jannatkhah et al. (2020).

Methane production, while significant (55.69% and 60.35% of total exergy at the North and South WWTPs, respectively) was not utilized for energy recovery, representing a major untapped

resource. The difference between the exergy of the sludge discharged from the two WWTPs results from the different composition of the influent wastewater.

Table 5. Exergy of consumed inputs and generated byproducts (outputs) at the North and South WWTPs.

	North WWTP			South WWTP		
	E^0_{ch,n_e} (kJ g^{-1})	Quantity (g s^{-1})	Exergy (kW)	E^0_{ch,n_e} (kJ g^{-1})	Quantity (g s^{-1})	Exergy (kW)
Inputs [a]						
Process water	0.05	1,254.80	62.74	0.05	2,464.20	123.21
Diesel	45.43	1.62	73.60	45.43	2.50	113.58
Electricity	-	-	1,164.59	-	-	1,890.19
Byproduct (outputs) [a]						
Dewatered sludge	14.42	0.70	10.10	11.04	1.448	15.99
CH_4 produced	51.8	40.66	2,106.19	51.8	78.06	4,043.51
Polymers [b]	40.00	1.97	78.80	40.00	5.16	206.40
Hidrated lime [c]	2.30	3.69	8.49	2.30	4.15	9.55
Aluminum sulfate [c]	1.00	60.75	60.75	1.00	131.27	131.27

[a] Monthly daily average. [b] Anionic and cationic polymers. [c] Coagulants.

3.2.3 Exergy Balance

Table 6 presents the detailed exergy balance for the North and South WWTPs, calculated based on Eq. (2). The analysis integrates data on influent composition, operational inputs, outputs, and waste streams from Tables 2 to 5. Complementary Sankey diagrams in Fig. 5(a) and (b) visually illustrate the distribution of exergy flows within each facility.

A predominant feature of both systems is the significant exergy irreversibility. Exergy losses and destruction accounted for 97.47% of total input exergy at North WWTP and 97.21% at South WWTP, underscoring the inherent inefficiencies in conventional activated sludge processes. Such high degrees of irreversibility are consistent with previous findings for biological treatment systems, where biochemical reactions and energy-intensive operations contribute substantially to exergy dissipation (Przydatek, 2024).

Methane accounted for 55.68% and 60.35% of total exergy at the North and South WWTPs. However, the actual operational setup flares this methane, resulting in substantial exergy losses and environmental emissions. Electricity usage was the second largest contributor to exergy input (30.79% and 28.21% at the North and South WWTPs, respectively). This highlights the need for energy-efficient technologies in aeration and pumping systems, reinforcing observations by Ghimire et al. (2021), who associated these units with substantial operational and environmental burdens.

Table 6. Exergy balance (kW) of the North and South WWTPs. Percentages are relative to influent exergy.

Components Exergy (kW)	Symbols	Plants			
		North WWTP	(%)	South WWTP	(%)
Influent Wastewater	$(E_{ch,f} + E_{ch,c})$	2,481.5	65.6	4,573.6	68.3
Electricity	$E_{Elect.}$	1,164.6	30.8	1,890.2	28.2
Sludge Transport	E_{tr}	73.4	1.9	113.6	1.7
Process water	E_{water}	62.7	1.7	123.2	1.8
(1) Total Influent Exergy (inputs)		3,782.3	100,0	6,700.6	100,0
Effluent Wastewater	E_n	95.8	2.5	186.8	2.8
(2) Total Effluent Exergy (output)		95.8	2.5	186.8	2.8
Methane (CH_4)	E_M	2,106.2	55.7	4,043.5	60.4
Dewatered Sludge	E_{ds}	10.1	0.3	16.0	0.2
Polymers and Coagulants	$E_{pol+coag}$	148.0	3.9	347.2	5.2
(3) Lost Exergy (waste + emissions)		2,264.3	59.9	4,406.7	65.8
(4) Destroyed + Lost Exergy (1) – (2)		3,686.4	97.5	6,513.7	97.2
(5) Destroyed Exergy (1) – (2)– (3)	E_{Dest}	1,422.1	37.6	2,107.0	31.4

Finally, the contribution of chemical additives (polymers and coagulants) and sludge transport to the exergy balance, although relatively small (approximately 5% combined), should not be overlooked. Although these percentages may seem minor, they impose significant environmental and economic costs due to the sludge's high moisture content and transport distances (B. Muzaffar et al., 2022; Delre et al., 2019). Exploring local reuse strategies, such as

utilizing sludge for agricultural applications or producing biochar (Chagas et al., 2024; Cruz et al., 2024; Menezes et al., 2022), could mitigate these impacts and contribute to circular economy principles (Jiang et al., 2020; Lazić et al., 2020).

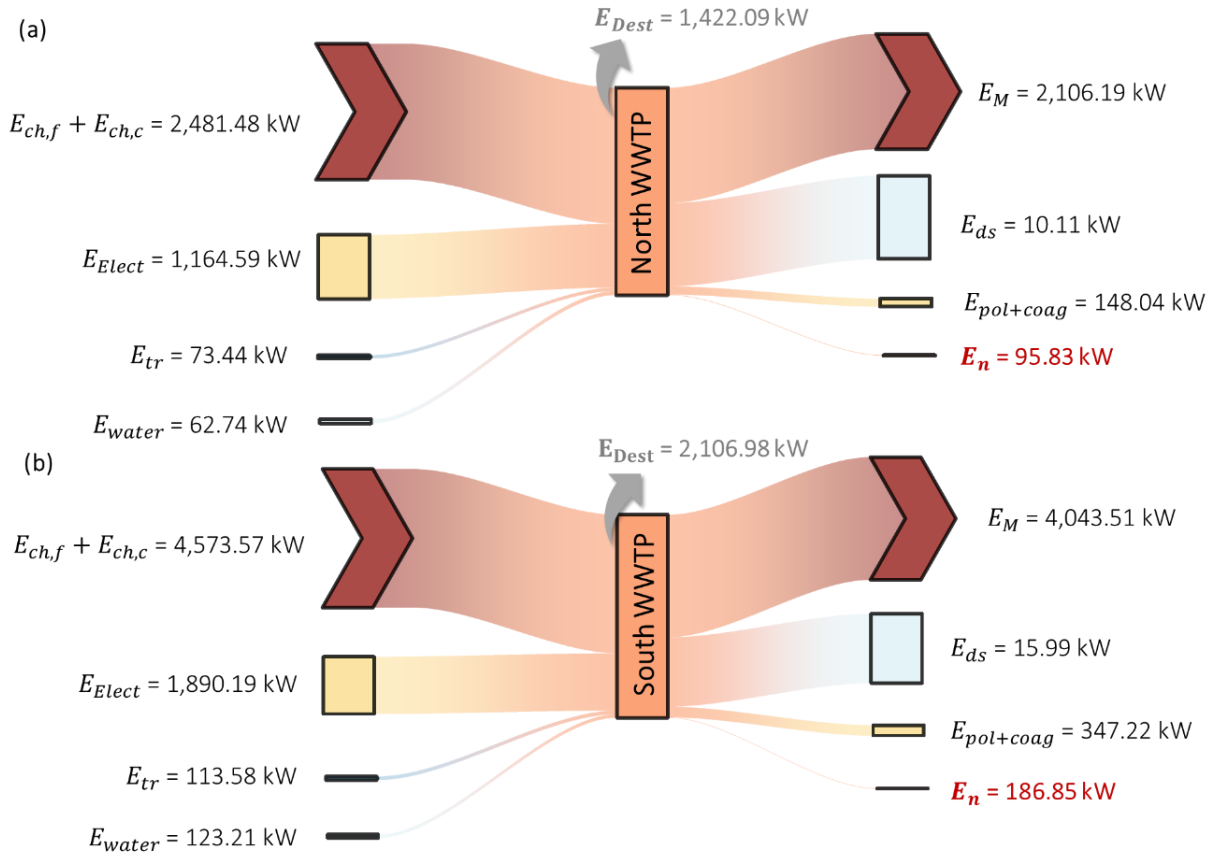

Figure 5. Sankey exergy flow diagrams for wastewater treatment plants considering the exergy balances (kW) for (a) the North WWTP and (b) the South WWTP.

3.3 Potential Useful Exergy of Produced Methane

Table 7 presents the estimated methane volumes produced in the WWTPs and the corresponding energy recovery potential under a hypothetical electricity generation scenario. On average, the North and South WWTPs produced 5,347.2 and 10,264.9 m^3 day^{-1} of methane, equivalent to 2,417.4 and 4,640.6 kWh day^{-1} of chemical energy content, respectively. Considering a conversion efficiency of 20%, the potential electrical energy that could be recovered reaches 483.5 kWh day^{-1} in the North plant and 928.1 kWh day^{-1} in the South plant.

These values correspond to only 1.73% and 2.05% of the total consumption, respectively, compared to the current electricity demand. This indicates that while biogas recovery has limited

capacity to meet overall plant demands, it could still contribute to operational efficiency and emissions reducing, especially if redirected for thermal uses such as sludge drying with direct flaring.

Table 7. The percentage of electrical energy potentially produced with CH_4 at the North and South WWTPs.

Plants		North WWTP	South WWTP
Q_{CH_4}	(m^3 day^{-1})	5,347.20	10,264.90
LHV	(kWh m^{-3})	10.85	10.85
CH_4 Energy	(kWh day^{-1})	1,322.50	2,538.80
(A) Actual Energy production [a]	(kWh day^{-1})	483.48	928.12
(B) Energy consumption in WWTPs	(kWh day^{-1})	27,950.06	45,364.49
(A)/(B) [b]	(%)	1.73	2.05

[a] Potential energy generation with 20% efficiency. [b] Ratio of energy generation to energy consumption.

Figure 6 provides a detailed monthly profile of methane production and associated exergy from 2020 to 2023. Figure 6(a) shows that the South WWTP consistently produced higher volumes of methane across all months, with peaks above 12,000 m^3 $month^{-1}$ observed in the dry season (August and December). North WWTP shows more stability, with monthly production between 4,600 and 5,800 m^3. These differences are attributed to the higher treatment capacity of the South plant and possibly to variations in organic load.

Figure 6(b) shows the corresponding chemical exergy of the produced methane. The South WWTP reached values near 4,900 kWh $month^{-1}$ by the end of the year, while the North WWTP remained below 2,300 kWh $month^{-1}$. These results reinforce the potential of the South plant to serve as a decentralized source of energy, even at partial recovery. These findings highlight the relevance of integrating biogas recovery strategies and refining emission estimates as part of broader sustainability goals in urban wastewater treatment, discussed next.

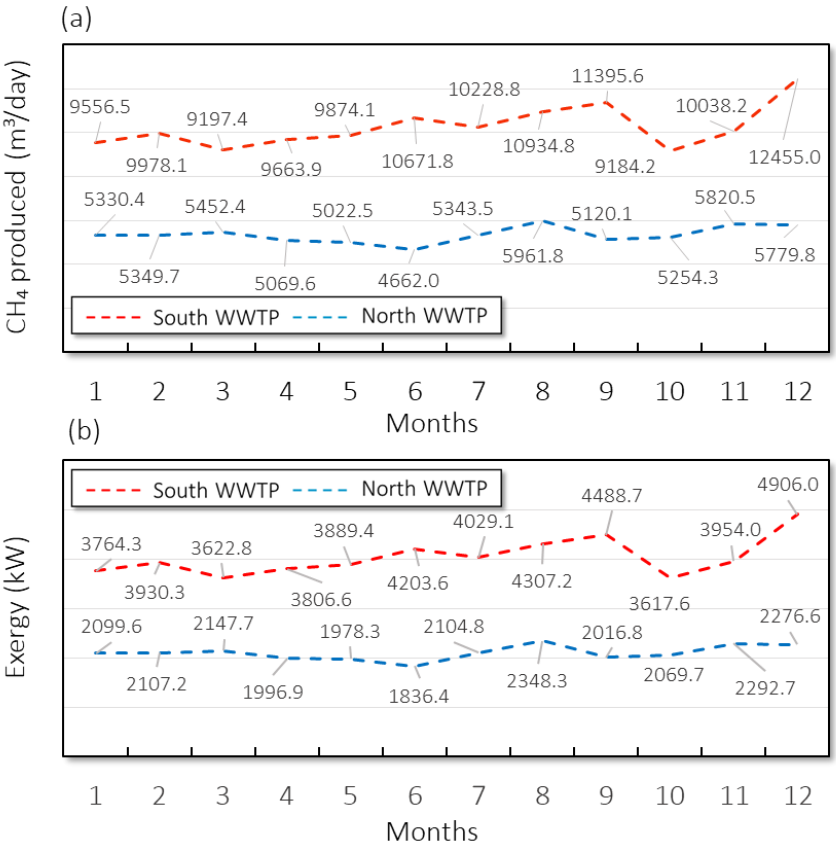

Figure 6. (a) Methane production at the WWTPs and (b) exergy associated with the produced methane, based on 12-month averages from 2020 to 2023. Source: Adapted data from (CAESB, 2024a).

3.4 Life Cycle Assessment - Carbon Footprint

The climate impact of WWTPs was assessed through the quantification of GHG emissions using the IPCC AR6 methodology. The analysis included both fossil and biogenic carbon flows and considered direct and indirect emissions within the defined system boundaries. Results are expressed as total emissions ($kgCO_2eq.$), avoided emissions from biogas flaring, and specific emissions per equivalent inhabitant ($kgCO_2eq.PE^{-1}year^{-1}$), where PE denotes the population served.

Table 8 presents the GWP results for both wastewater treatment plants, considering the three scenarios: (Sc1) uncontrolled atmospheric emission (baseline), (Sc2) flaring, and (Sc3) energy recovery through electricity production. Considering Scenario Sc1, North WWTP reported emissions reaching 1,757.59 kg $CO_2eq.$, while in South WWTP, they amounted to 3,344.98 kg CO_2eq. In contrast, the adoption of biogas flaring (Sc2) reduced emissions to 1,062.28 kg CO_2eq.

and 2,010.23 kg CO_2eq., respectively, avoiding emissions, relative to Sc1, of 695.31 kg CO_2eq. for WWTP-N and 1,334.75 kg CO_2eq. for WWTP-S, representing relative reductions of 39.56% and 39.90%. Further mitigation was observed in the energy recovery scenario (Sc3), where emissions were reduced to 971.12 kg CO_2eq. in WWTP-N and 1,835.23 kg CO_2eq. in WWTP-S. Compared to the baseline (Sc1), these values correspond to avoided emissions of 786.47 kg CO_2eq. (44.75%) and 1,509.74 kg CO_2eq. (45.13%), respectively. The results highlight the substantial climate benefit of adopting biogas flaring as a mitigation strategy in WWTP, as also indicated by the literature (Parravicini et al., 2022; Ranieri et al., 2024b, 2023; Sharawat et al., 2021; Singh et al., 2020).

Table 8. Climate change impact results for North and South WWTPs under three biogas management scenarios (Sc1, Sc2 and Sc3).

	North WWTP			South WWTP		
Indicator	Sc1	Sc2	Sc3	Sc1	Sc2	Sc3
Population served (PE)	144,763	144,763	144,763	383,205	383,205	383,205
Total GHG emissions (kgCO_2eq.)	1,757.59	1,062.28	971.12	3,344.98	2,010.23	1,835.23
Avoided emissions (kgCO_2eq.)	–	695.31	786.47	–	1,334.75	1,509.74
Relative reduction (%)	–	39.56%	44.75%	–	39.90%	45.13%
Emissions per PE (kgCO_2eq.PE^{-1} $year^{-1}$)	106.36	64.28	58.77	76.47	45.95	41.95

Sc1 – without biogas flaring; Sc2 – with biogas flaring; Sc3 – with energy recovery.

When normalized by the population served, the emission in the baseline scenario were 106.36 and 76.47 for North and South WWTP. Obtained results lower than those reported by Ranieri et al., (2023), who quantified 134.6 kg CO_2eq.PE^{-1} $year^{-1}$ in anaerobic treatment systems without gas recovery.

In Scenario (Sc2), emissions dropped to 64.28 and 45.95 kg CO_2eq.PE^{-1} $year^{-1}$ for WWTP-N and WWTP-S, respectively. These values align with literature benchmarks. For instance, Ranieri et al. (2024b) assessing a WWTPs in southern Italy's reported emissions of 83 kg CO_2eq. $PE^{-1}year^{-1}$ under baseline configurations, which dropped to 62 kg CO_2eq. PE^{-1} $year^{-1}$ considering flaring. In the energy recovery scenario (Sc3), specific emissions were reduced by 44.75% in WWTP-N and

45.13% in WWTP-S compared to the baseline (Sc1), reaching 58.77 and 41.95 kg CO2eq. PE^{-1} $year^{-1}$, respectively.

These values fall below the emission ranges reported by Patel et al. (2025), who observed 43–53% reductions in climate impacts from bio methanation systems, depending on the electricity source.

Overall, the results reinforce the importance of biogas management strategies for reducing the climate impact of wastewater treatment. Implementing flaring, although not the most energy-efficient use of biogas, presents a low-cost and effective solution for GHG mitigation when energy recovery is not feasible.

3.5 Exergy Indicators and Destroyed Exergy

Table 9 shows the calculated results for environmental exergy efficiency (η_{ex}), pollution rate (τ_{pol}), and renewability index (λ) considering the conditions without methane utilization and with methane utilization through energy recovery.

Table 9. Exergy indicators with and without theoretical methane utilization at the plants.

Plants	Without CH_4 use			With CH_4 use		
	η_{ex}	τ_{pol}	λ	η_{ex}	τ_{pol}	λ
North WWTP	0.024	36.92	0.063	0.053	26.98	0.079
South WWTP	0.027	33.00	0.081	0.062	25.01	0.110

The indicators obtained in this study are proportionally consistent with the literature. For example, the exergetic efficiency of the North and South WWTPs without methane valorization (η_{ex} of 0.024 and 0.027, respectively) are in close agreement with those reported for the *Barueri* WWTP (0.021–0.024) by Mora Bejarano, Oliveira (2006). The improvement in exergy efficiency (η_{ex}) observed under methane recovery (from 0.024 to 0.053 at the North WWTP and from 0.027 to 0.062 at the South WWTP, representing increases of 120.8% and 129.6%, respectively) is lower than the reported by Khosravi et al. (2013), who observed a 192% increase in exergetic efficiency (from 0.0614 to 0.179), following process optimization in a municipal WWTP.

Pollution rates (τ_{pol}) obtained under baseline conditions (36.9 and 33.0) also align well with the $\tau_{pol} \approx 34.2$ reported for the Barueri plant (Mora Bejarano and Oliveira, 2006). These similarities are attributed to analogous treatment technologies (activated sludge with high organic

and nutrient removal) and similar flow conditions. Applying energy recovery from methane, the pollution rate decreased to 26.98 and 25.01 for North and South WWTPs, respectively, reflecting reductions of 26.9% and 24.2%, and enhanced sustainability with biogas utilization. If the sludge is also used for agricultural purposes, efficiencies would increase even further, and the pollution rate would reduce and could be eliminated.

The renewability index values ($\lambda = 0.063$ for the North WWTP and 0.081 for the South WWTP) indicate that both plants still operate in an environmentally unfavorable manner due to the limited utilization of recoverable exergy in methane and sludge. Under methane recovery, these values increase to 0.079 and 0.110, respectively, representing relative improvements of 25.4% and 35.8%. This enhancement reflects progress toward more sustainable system configurations by promoting the partial recovery of energy that would otherwise be lost. These values are slightly higher than the $\lambda = 0.048$ reported for *Barueri* by Mora Bejarano and Oliveira (2006), likely due to specific operational conditions and possibly narrower system boundaries in the present analysis. Under methane recovery, the values increase to 0.079 (North WWTP) and 0.110 (South WWTP). These findings confirm the importance of methane valorization, as reported by Erguvan and MacPhee (2021) and Ghimire et al. (2021), particularly in enhancing resource circularity and reducing fossil energy reliance.

Table 10 presents the values of destroyed exergy in the treatment processes under baseline conditions (without methane recovery), the additional destroyed exergy when methane is valorized, and the amount of exergy that becomes recoverable in this scenario.

Under baseline conditions, the destroyed exergy accounted for 1,422.09 kW at the North WWTP (representing 37.60% of the total influent exergy) and 2,106.98 kW at the South WWTP (31.44%). These values reflect the high energy demand for pollutant removal and the losses associated with sludge and untreated methane.

Table 10. Destroyed exergy without and with methane utilization and recoverable destroyed exergy.

Plants	Destroyed Exergy (E_{Dest})				Recoverable Exergy (2) - (1)	
	Without CH_4 use (1)		With CH_4 use (2)			
	(kW)	(%) [a]	(kW)	(%) [a]	(kW)	(%) [a]
North	1,422.09	37.60	2,575.53	68.10	1153.44	30.50
South	2,106.98	31.44	5,003.80	74.68	2896.82	43.23

[a] Percentage is relative to the influent exergy at the plants.

When methane recovery is incorporated into the system, destroyed exergy increases to 2,575.53 kW at the North WWTP and to 5,003.80 kW at the South WWTP. Although these values appear higher, they include the transformation of biogas into usable energy, which shifts a portion of previously lost energy into the recoverable domain. Consequently, 1,153.44 kW (30.50% of influent exergy) becomes recoverable at the North WWTP, and 2,896.82 kW (43.23% of influent exergy) at the South WWTP.

This shift highlights the significant contribution of methane valorization to exergy recovery. While the total destroyed exergy appears numerically higher, this results from including the recovery pathway and its transformation losses. The net effect is a substantial gain in usable exergy and an improvement in overall system efficiency. The South WWTP, with its larger influent volume and methane production, presents a greater absolute recovery potential, demonstrating the relevance of scale for energy integration strategies. These findings emphasize the importance of converting high-exergy components such as methane into useful energy forms, thereby reducing resource degradation, and improving environmental performance.

4 LIMITATIONS AND PROSPECTS

One limitation is the reliance on operational data from the North and South WWTPs in Brasília, which, while representative of urban systems in similar regions, may not fully reflect the diversity of treatment technologies and operational contexts globally. The findings are particularly relevant to activated sludge systems but may require adaptation for other treatment configurations.

Additionally, the study focused on steady-state exergy analysis, capturing system performance under current operating conditions. Dynamic factors, such as variations in influent composition, pollutant loads, or operational changes over time, were not explored but could

significantly influence exergy balances and efficiency. Economic and logistical considerations of proposed interventions, such as methane-to-energy systems or sludge reuse strategies, were not quantitatively assessed, leaving gaps in understanding their feasibility and scalability.

Future research should expand the scope by integrating dynamic modeling to capture temporal variations in treatment performance and emissions (Deutsch et al., 2022). Exploring the economic viability of methane recovery systems and innovative sludge reuse approaches across diverse geographical and technological contexts will further enhance the practical applicability of the findings. These efforts can contribute to advancing sustainable wastewater management practices globally, enhancing the role of treatment systems in climate change mitigation and resource recovery, and supporting the transition toward more resilient and sustainable urban infrastructure.

5 CONCLUSIONS

This study demonstrates the relevance of exergy analysis combined with GHG quantification, LCA and sustainability indexes as an integrated framework for identifying inefficiencies and supporting improvements in wastewater treatment. The North and South WWTPs in Brasília achieved high pollutant removal efficiencies (>95%), yet exhibited exergy destruction rates of 97.47% and 97.21%, respectively. Electricity consumption accounted for 30.79% and 28.21% of total exergy input, reinforcing the need for energy-efficient technologies. Methane flaring represented a major source of exergy loss, with methane accounting for 55.68% and 60.35% of input exergy.

Under energy recovery scenarios, exergy efficiency increased by 120.8% at North WWTP and 129.6% at South WWTP. The pollution rate dropped by 26.9% and 24.2%, while the renewability index improved by 25.4% and 35.8%, respectively. Although sludge transport contributed less than 2% of exergy input, daily volumes exceeded 100 m^3, imposing significant environmental and logistic costs. Local reuse alternatives, such as agricultural application or biochar production, offer promising mitigation routes.

From the LCA perspective, total GHG emissions were reduced by 39.56% (North) and 39.90% (South) through flaring, and by 44.75% and 45.13% with biogas-to-electricity conversion. Emission intensities reached as low as 58.77 and 41.95 kg CO_2eq. PE^{-1} $year^{-1}$, aligned to benchmarks reported in literature. Overall, the findings highlight the role of integrated exergy–

LCA approaches in supporting climate mitigation, circular economy strategies, and the transition toward more sustainable wastewater infrastructure.

ACKNOWLEDGMENTS

The authors would like to thank CAESB for cooperating with the research, Coordination for the Improvement of Higher Education Personnel (CAPES), Brazilian National Council for Scientific and Technological Development (CNPq - process no. 305109/2023-5) for the financial support to this project, Decanato de Pesquisa e Inovação (DPI/UnB) and FAP DF (project 469/2023).

SECOND ARTICLE REFERENCES

ALLEY, E.R., 2007. **Water quality control handbook**. McGraw-Hill.

ANA, 2022. Agência Nacional de Águas – **Relatório da conjuntura de recursos hídricos do Brasil: Qualidade e Quantidade da Água** [WWW Document]. URL https://relatorio-conjuntura-ana-2021.webflow.io/capitulos/quanti-quali (accessed 5.5.25).

AVTAR, R., TRIPATHI, S., AGGARWAL, A.K., KUMAR, P., 2019. **Population-urbanization-energy nexus: A review**. Resources. https://doi.org/10.3390/resources8030136

B. MUZAFFAR, W.M., AZNAH, A., HALIM, H., 2022. **Energy Efficiency and Nutrient Removal Performance: Comparison Between Several Types of Activated Sludge Process**. IOP Conf Ser Earth Environ Sci. https://doi.org/10.1088/1755-1315/1091/1/012056

BELLEZONI, R.A., MENG, F., HE, P., SETO, K.C., 2021. **Understanding and conceptualizing how urban green and blue infrastructure affects the food, water, and energy nexus: A synthesis of the literature**. J Clean Prod 289. https://doi.org/10.1016/j.jclepro.2021.125825

BYLKA, J., MRÓZ, T., 2020. **Exergy evaluation of a water distribution system**. Energies (Basel) 13. https://doi.org/10.3390/en13236221

CAESB, 2024a. COMPANHIA DE SANEAMENTO AMBIENTAL DO DISTRITO FEDERAL -**Relatório de indicadores de desempenho**. Brasilia, Distrito Federal, Brasil.

CAESB, 2024b. **Relatório de indicadores de desempenho 2023**.

CHERNICHARO, C.A.L., 2016. **Reatores anaeróbios: princípios do tratamento biológico de águas residuárias**. 3rd ed. Editora UFMG, Belo Horizonte, Minas Gerais, Brasil.

DAS, S., PARIDA, V.K., TIWARY, C.S., GUPTA, A.K., CHOWDHURY, S., 2024. **Emerging Contaminants in the Aquatic Environment: Fate, Occurrence, Impacts, and Toxicity**. pp. 1–32. https://doi.org/10.1021/bk-2024-1475.ch001

DAUDT, G.C., 2019. **Emissões de N2O e de CO2 por um reator em bateladas sequenciais com lodo granular aeróbio no tratamento de esgoto sanitário**. Florianópolis, SC, Brasil.

DAUDT, G.C., XAVIER, J.A., MEOTTI, B., GUIMARÃES, L.B., DA COSTA1, R.H.R., 2019. **Researching new ways to reduce N2O emission from a granular sludge sequencing batch reactor treating domestic wastewater under subtropical climate conditions**. Brazilian Journal of Chemical Engineering 36, 209–220. https://doi.org/10.1590/0104-6632.20190361s20170566

DELRE, A., HOEVE, M. TEN, SCHEUTZ, C., 2019. **Site-Specific Carbon Footprints of Scandinavian Wastewater Treatment Plants, Using the Life Cycle Assessment Approach**. J Clean Prod. https://doi.org/10.1016/j.jclepro.2018.11.200

DEUTSCH, L., LAMAS, G.C., PEREIRA, T.S., SILVEIRA, E.A., CALDEIRA-PIRES, A., 2022. **Life cycle and risk assessment of vinasse storage dams: A Brazilian sugar-energy refinery analysis**. Sustainable Futures 4, 100083. https://doi.org/10.1016/j.sftr.2022.100083

EPE, 2020. EMPRESA DE PESQUISA ENERGÉTICA - **Balanço Energético Nacional 2020**. [WWW Document]. URL https://www.epe.gov.br/sites-pt/publicacoes-dados-abertos/publicacoes/PublicacoesArquivos/publicacao-479/topico-528/BEN2020_sp.pdf (accessed 5.5.25).

ERGUVAN, M., MACPHEE, D., 2021. **Can a Wastewater Treatment Plant Power Itself? Results From a Novel Biokinetic-Thermodynamic Analysis.** J — Multidisciplinary Scientific Journal. https://doi.org/10.3390/j4040045

FITZSIMONS, L., HORRIGAN, M., MCNAMARA, G., DOHERTY, E., PHELAN, T., CORCORAN, B., DELAURÉ, Y., CLIFFORD, E., 2016. **Assessing the thermodynamic performance of Irish municipal wastewater treatment plants using exergy analysis: A potential benchmarking approach**. J Clean Prod 131, 387–398. https://doi.org/10.1016/j.jclepro.2016.05.016

FRANCHITTI, E., PEDULLÀ, M., MADSEN, A.M., TRAVERSI, D., 2024. **Effect of anaerobic digestion on pathogens and antimicrobial resistance in the sewage sludge.** Environ Int 191. https://doi.org/10.1016/j.envint.2024.108998

GHIMIRE, U., SARPONG, G., GUDE, V.G., 2021. **Transitioning Wastewater Treatment Plants Toward Circular Economy and Energy Sustainability**. ACS Omega. https://doi.org/10.1021/acsomega.0c05827

HELLSTRÖM, D., 1999. **Exergy Analysis: A Comparison of Source Separation Systems and Conventional Treatment Systems**. Water Environment Research 71, 1354–1363. https://doi.org/10.2175/106143096X122302

HELLSTRÖM, D., KÄRRMAN, E., 1997. **Exergy analysis and nutrient flows of various sewerage systems.** Water Science and Technology 35, 135–144. https://doi.org/10.1016/S0273-1223(97)00191-1

HORRIGAN, M., 2016. **The Use of Exergy Analysis to Benchmark the Resource Efficiency of Municipal Waste Water Treatment Plants in Ireland**. Dublin.

HUANG, L., LI, H., LI, Y., 2024. **Greenhouse gas accounting methodologies for wastewater treatment plants: A review**. J Clean Prod. https://doi.org/10.1016/j.jclepro.2024.141424

HUANG, L.Q., CHEN, G.Q., ZHANG, Y., CHEN, B., LUAN, S.J., 2007. **Exergy as a unified measure of water quality.** Commun Nonlinear Sci Numer Simul 12, 663–672. https://doi.org/10.1016/j.cnsns.2005.04.009

INMET, 2024. INSTITUTO NACIONAL DE METEOROLOGIA. **Dados históricos anuais – Precipitação 2024** [WWW Document]. URL https://portal.inmet.gov.br/dadoshistoricos (accessed 5.12.25).

IPCC, 2006. 2006 IPCC **Guidelines for National Greenhouse Gas Inventories. Volume 5: Waste**. Hayama, Japan.

IPCC, 2013. **Anthropogenic and Natural Radiative Forcing.** In: Climate Change 2013: The Physical Science Basis. Contribution of Working Group I to the Fifth Assessment Report of the Intergovernmental Panel on Climate Change [Stocker, T.F., D. Qin, G.-K. Plattner, M. Tignor, S.K. Allen, J. Boschung, A. Nauels, Y. Xia, V. Bex and P.M. Midgley (eds.)]. Cambridge University Press, Cambridge, United Kingdom and New York, NY, USA https://www.ipcc.ch/site/assets/uploads/2018/02/WG1AR5_Chapter08_FINAL.pdf. WG1AR5_Chapter08_FINAL.pdf. Acess. 12.11.2025.

JANNATKHAH, J., NAJAFI, B., GHAEBI, H., 2020. **Energy and exergy analysis of combined ORC – ERC system for biodiesel-fed diesel engine waste heat recovery**. Energy Convers Manag 209. https://doi.org/10.1016/j.enconman.2020.112658

JIANG, H., HUA, M., ZHANG, J., CHENG, P., YE, Z., HUANG, M., JIN, Q., 2020**. Sustainability Efficiency Assessment of Wastewater Treatment Plants in China: A Data Envelopment Analysis Based on Cluster Benchmarking**. J Clean Prod. https://doi.org/10.1016/j.jclepro.2019.118729

JORDÃO, E.P., 2007. **Reatores Anaeróbios.** Engenharia Sanitaria e Ambiental 12, 239–239. https://doi.org/10.1590/S1413-41522007000300001

KHOSRAVI, S., PANJESHAHI, M.H., ATAEI, A., 2013. **Application of exergy analysis for quantification and optimisation of the environmental performance in wastewater treatment plants**. International Journal of Exergy 12, 119. https://doi.org/10.1504/IJEX.2013.052552

KŁOSOK-BAZAN, I., RAK, A., BOGUNIEWICZ-ZABŁOCKA, J., KUCZUK, A., CAPODAGLIO, A.G., 2024. **Evaluating Energy Efficiency Parameters of Municipal Wastewater Treatment Plants in Terms of Management Strategies and Carbon Footprint Reduction: Insights from Three Polish Facilities**. Energies (Basel) 17. https://doi.org/10.3390/en17225745

KOTAS, T.J., 1985. **The Exergy Method of Thermal Plant Analysis**. Butterworths, London.

KOUL, B., YADAV, D., SINGH, S., KUMAR, M., SONG, M., 2022. **Insights into the Domestic Wastewater Treatment (DWWT) Regimes: A Review**. Water (Switzerland). https://doi.org/10.3390/w14213542

LAZIĆ, A., A, H., NEWMAN, J.F., BARESEL, C., 2020. **Sustainable SBR Treatment: Treatment Efficiency, Energy, Carbon Footprint**. International Journal of Water and Wastewater Treatment. https://doi.org/10.16966/2381-5299.162

LOBATO, L. C. S. **Aproveitamento energético de biogás gerado em reatores UASB tratando esgoto doméstico** (PhD). UFMG, Belo Horizonte. 2011.

LOUREIRO, D., SILVA, C., CARDOSO, M. A., MAMADE, A., ALEGRE, H., ROSA, M. J., 2020. **The Development of a Framework for Assessing the Energy Efficiency in Urban Water Systems and Its Demonstration in the Portuguese Water Sector**. Water (Basel). https://doi.org/10.3390/w12010134

MAKARYTCHEV, S. V, 1998. **Environmental impact analysis of ACFB-based gas and power cogeneration**. Energy 23, 711–717.

MALBOOSI, S., HASHEMIAN, S. M. CHAHARTAGHI, M., 2021. **Exergy analysis in the processes of municipal wastewater treatment plants.** Energy Sources, Part A: Recovery, Utilization, and Environmental Effects 47, 9759–9781. https://doi.org/10.1080/15567036.2021.1956646

MANN, H. B., WHITNEY, D. R. **On a Test of Whether one of Two Random Variables is Stochastically Larger than the Other**. The Annals of Mathematical Statistics 18, 50–60. 1947. https://doi.org/10.1214/aoms/1177730491

MENEZES, L.N.B., SILVEIRA, E.A., MAZZONI, J.V.S., EVARISTO, R.B.W., RODRIGUES, J.S., LAMAS, G.C., SUAREZ, P.A.Z., GHESTI, G.F. 2022.**Alternative valuation pathways for**

primary, secondary, and tertiary sewage sludge: biochar and bio-oil production for sustainable energy. Biomass Convers Biorefin. https://doi.org/10.1007/s13399-022-02543-9

METCALF, E.I., TCHOBANOGLOUS, G., BURTON, F.L., STENSEL H.D. 2002. **Wastewater engineering: treatment and reuse.**

MORA BEJARANO, C.H. 2009. **Avaliação exergoecológica de processos de tratamento de esgoto**. USP, São Paulo.

MORA BEJARANO, C.H., OLIVEIRA, J. 2006. **Environmental exergy analysis of wastewater treatment plants**. Engenharia Termica 5.

NOURIN, F.N., ABBAS, A.I., QANDIL, M.D., AMANO, R.S., 2021. **Analytical study to use the excess digester gas of wastewater treatment plants**. Journal of Energy Resources Technology, Transactions of the ASME 143. https://doi.org/10.1115/1.4047603

OWEN, W.F., 1982. **Energy in wastewater treatment.** Prentice-Hall, Inc., Englewood Cliffs, NJ.

PARRAVICINI, V., NIELSEN, P.H., THORNBERG, D., PISTOCCHI, A., 2022. **Evaluation of greenhouse gas emissions from the European urban wastewater sector, and options for their reduction**. Science of the Total Environment 838. https://doi.org/10.1016/j.scitotenv.2022.156322

PATEL, G.H., HORTTANAINEN, M., KOKKO, M., YÖRÜKLÜ, H.C., HAVUKAINEN, J., 2025. **Environmental performance of biomethanation based on life cycle assessment**. Energy 320, 135244. https://doi.org/10.1016/j.energy.2025.135244

PRZYDATEK, G., 2024. **Environmental and Energy Efficiency of a Selected Municipal Wastewater Treatment Plant – A Case Study**. Engineering Research Express. https://doi.org/10.1088/2631-8695/ad6232

RANIERI, E., D'ONGHIA, G., LOPOPOLO, L., GIKAS, P., RANIERI, F., GIKA, E., SPAGNOLO, V., HERRERA, J.A., RANIERI, A.C., 2024a. **Influence of climate change on wastewater treatment plants performances and energy costs in Apulia, south Italy**. Chemosphere 350. https://doi.org/10.1016/j.chemosphere.2023.141087

RANIERI, E., D'ONGHIA, G., LOPOPOLO, L., GIKAS, P., RANIERI, F., GIKA, E., SPAGNOLO, V., RANIERI, A.C., 2023. **Evaluation of greenhouse gas emissions from aerobic and anaerobic wastewater treatment plants in Southeast of Italy**. J Environ Manage 337. https://doi.org/10.1016/j.jenvman.2023.117767

RANIERI, E., D'ONGHIA, G., RANIERI, F., LOPOPOLO, L., GREGORIO, S., RANIERI, A.C., 2024b. **Compensatory measures to reduce GHGs in wastewater treatment plants in Southern Italy**. Journal of Water Process Engineering 60. https://doi.org/10.1016/j.jwpe.2024.105128

REZNIK, A., JIANG, Y., DINAR, A., 2020. **The impacts of climate change on wastewater treatment costs: Evidence from the wastewater sector in china**. Water (Switzerland) 12. https://doi.org/10.3390/w12113272

RIBEIRO, R. P. 2017. **Emissões de Óxido Nitroso em diferentes condições operacionais de sistema** (PhD). Universidade Federal Fluminense, Niterói, RJ.

RIBEIRO, R.P., KLIGERMAN, D.C., MELLO, W.Z. DE, SILVA, D.D.P., CORREIA, R.D.F., OLIVEIRA, J.L. DA M., 2018. **Effects of different operating conditions on total nitrogen removal routes and nitrous oxide emissions in a lab-scale activated sludge system**. Ambiente

e Agua - An Interdisciplinary Journal of Applied Science 13, 1. https://doi.org/10.4136/ambi-agua.2174

RIVERO, R., GARFIAS, M., 2006. **Standard chemical exergy of elements updated.** Energy 31, 3310–3326. https://doi.org/10.1016/j.energy.2006.03.020

SHARAWAT, I., DAHIYA, R., DAHIYA, R.P., 2021. **Analysis of a wastewater treatment plant for energy consumption and greenhouse gas emissions**. International Journal of Environmental Science and Technology 18, 871–884. https://doi.org/10.1007/s13762-020-02893-9

SINGH, A.D., UPADHYAY, A., SHRIVASTAVA, S., VIVEKANAND, V., 2020. **Life-cycle assessment of sewage sludge-based large-scale biogas plant. Bioresour** Technol 309. https://doi.org/10.1016/j.biortech.2020.123373

SNIS, 2023. SISTEMA NACIONAL DE INFORMAÇÕES SOBRE SANEAMENTO - **Diagnóstico Anual de Água e Esgoto 2022** [WWW Document]. URL https://www.gov.br/cidades/pt-br/acesso-a-informacao/acoes-e-programas/saneamento/snis (accessed 5.5.25).

STANEK, W., VALERO, ALICIA, VALERO, ANTONIO, UCHE, J., CALVO, G., 2017. **Thermodynamic Methods to Evaluate Resource**s. pp. 131–165. https://doi.org/10.1007/978-3-319-48649-9_6

SZARGUT, J., 1989. **Chemical Exergies of the Elements**, Applied Energy.

TAI, S., MATSUSHIGE, K., 1986. **Chemical exergy of organic matter in wastewater**. International Journal of Environmental Studies 27, 301–315. https://doi.org/10.1080/00207238608710299

VAIDYA, R., VERMA, K., KUMAR, M., HOYSALL, C., RAO, L., 2023. **Assessing wastewater management challenges in developing countries: a case study of India, current status and future scope**. Environ Dev Sustain 26, 19369–19396. https://doi.org/10.1007/s10668-023-03540-2

VILARDI, G., BASSANO, C., DEIANA, P., VERDONE, N., 2020. **Exergy and energy analysis of three biogas upgrading processes.** Energy Convers Manag 224. https://doi.org/10.1016/j.enconman.2020.113323

WILSENACH, J.A., MAURER, M., LARSEN, T.A., VAN LOOSDRECHT, M.C.M., 2003**. From waste treatment to integrated resource management.**

WRI, WBCSD, 2004. **The Greenhouse Gas Protocol: A Corporate Accounting and Reporting Standard** (Revised Edition). Washington.

SUPPLEMENTARY MATERIAL

SM1 - FIRST ARTICLE

1 Resume

This Supplementary Material provides the full descriptive context and the complete tabular data that support the analyses reported in the manuscript “Towards Sustainable Urban Water Management: A Thermodynamic–Environmental Nexus Approach”. Each subsection explains data measurement, how the operating conditions relate to the system topology, and how the values should be interpreted inside the study boundaries.

2 Methodology

2.1 Raw water pumping stations (RWPS) characterization

2.1.1 Torto RWPS

The Torto RWPS RWPS (blue indicator – 4 in Figure 1(b), 15°46′37.769"S and 47°54′23.721"W) is one of the three main abstraction subsystems that supply raw water to the Brasília WTP. It is located along the Torto stream and operates four MPAs, identified as 01(A+B), 02(A+B), 03(A+B), and 04(A+B). Each MPA is installed in a (3+1) configuration, in which two units operate simultaneously under normal conditions while one remains on standby to ensure redundancy and continuous service. Each MPA itself is composed of two identical centrifugal pumps connected in series, designated as stages A and B. Both pumps are mounted on a common shaft and driven by a high-power electric motor equipped with a soft starter to minimize mechanical stress and electrical current peaks during start-up.

MPAs 01 and 02 are equipped with Allis-Chalmers model 213-909-507/18×16/SF centrifugal pumps, while MPAs 03 and 04 operate with Worthington model 12-LN-26/BX 24888 pumps. All units are designed for continuous operation under high head conditions and are connected to the main Torto and Santa Maria (will be seen in the next item) raw water pipelines with a nominal diameter of 1,000 mm.

Under normal conditions, suction is provided directly from the Torto intake channel. However, during specific hydraulic situations such as overpressure in the Santa Maria pipeline, MPAs 01 and 02 operate under bypass mode, indicated with an asterisk in Table S1.1.

Table S1.1. Measured and catalogued operational characteristics of the Main Pumping Stations at the Torto raw Water Pumping Systems (WPS).

WPS	Torto							
Manufacturer	Allis Chalmers					Worthington		
MPA	01 (A+B)	02 (A+B)	01 (A+B)*	02 (A+B)*	Catalogs inform.	03 (A+B)	04 (A+B)	Catalogs inform.
$\dot{\boldsymbol{Q}}$ (L s^{-1})	726.1	655.8	726.1	655.8	-	730.1	708.6	763.1
$\boldsymbol{H_m}$ (m)	141.4	140.3	101.4	100.3	-	143.2	143.3	143.0
$\boldsymbol{P_h}$ (kW)	1,006.9	902.4	722.0	645.0	-	1,025.3	995.7	1,070.2
$\boldsymbol{P_e}$ (kW)	1,281.0	1,245.1	918.5	890.2	-	1,387.4	1,336.4	1,341.0
$\boldsymbol{P_x}$ (kW)	1,230.9	1,196.7	882.7	855.5	-	1,333.3	1,284.7	1,289.4
I (A)*	373.0	348.0	373.0	348.0	392.0	3890	393.0	395.0
$\boldsymbol{\eta_m}$ (%)	96.1	96.1	96.1	96.1	96.1	96.1	96.1	96.1
$\boldsymbol{\eta_b}$ (%)	81.8	75.4	81.8	75.4	84.0	76.9	77.5	83.0
$\boldsymbol{\eta_g}$(%)	78.6	72.5	78.6	72.5	80.7	73.9	74.5	79.8
$\boldsymbol{f_p}$	0.90	0.93	0.90	0.93	-	0.88	0.86	-

Symbology: $\dot{Q}$ – flow; H_m – manometric head; P_h – hidraulic power; P_e –electric power; P_x – axe power; I – measured current; η_m – electric motor efficiency; η_b – pump efficiency; η_g – motor pump efficiency; f_P – power factor. The (2+1) configuration ensures operational redundancy and allows alternating duty cycles, preventing excessive wear of individual units. Each MPA consists of two pumps (A and B) connected in series on a single shaft and powered by a common high-capacity motor with a soft starter. Bypass operation (*) corresponds to suction assisted by the Santa Maria discharge line, reducing total dynamic head and power demand. Catalog data are included only for comparison and are excluded from inventory calculations. Source: Source: With data from (CAESB, 2024a).

In this configuration, the suction side of the Torto WPS receives pre-pressurized water from the Santa Maria discharge line. This reduces the required suction head and leads to a significant reduction in electrical power consumption, with an average decrease of approximately 20 to 25 percent compared to normal operation.

Measurements included suction and discharge pressures, flow rate, current, voltage, and power factor. Performance testing followed the Brazilian Standard NBR 6400 (ABNT, 1989) for hydraulic flow pumps. The resulting data are summarized in Table S1.1, which also includes catalog values provided by CAESB (2024) for reference.

2.1.2 Santa Maria RWPS

The Santa Maria RWPS is located on the Santa Maria stream and represents one of the main raw water abstraction units of the Brasília WSS. It operates in an integrated manner with the Torto and Bananal systems, discharging water through a 1,000 mm diameter pipeline that converges toward the Brasília WTP.

The system consists of three MPAs, identified as 05(A+B), 06(A+B), and 07(A+B). Each MPA is arranged in a (2+1) configuration, in which two units operate simultaneously under normal conditions while one remains on standby to guarantee operational continuity. Each MPA contains two identical pumps connected in series (stages A and B) mounted on a single shaft and driven by a high-power electric motor equipped with a soft starter to reduce transients during start-up.

All MPAs at Santa Maria is assembled with Worthington centrifugal pumps, model 12-LN-26/BX 24888, which are designed for medium-head operation with relatively high flow rates. The system presents uniform flow and head conditions across the three MPAs, though slight variations are observed due to the different commissioning years of each installation. Over time, minor differences in motor efficiency and hydraulic performance have been recorded, mainly related to aging and the need for reactive power compensation.

The performance parameters summarized in Table S2.1 were measured according to the Brazilian Standard NBR 6400 (ABNT, 1989), which specifies the procedures for hydraulic performance and cavitation testing of centrifugal pumps. Measurements were performed by CAESB and include suction and discharge pressures, flow rate, current, voltage, and power factor. The data reflects steady-state conditions under nominal flow rates and are consistent with the

equipment catalog information provided by the manufacturer. MPAs with Sulzer pumps, which can replace the current ones, are also being assembled in parallel.

Table S2.1. Measured and catalogued operational characteristics of the Main Pumping Stations at Santa Maria WPS, with actual (Worthington) and possible substitution (Sulzer) pump.

WPS	Santa Maria						
Pump brand	Worthington				Sulzer		
MPA	05 (A+B)	06 (A+B)	07 (A+B)	Catalog informs.	05 (A+B)	06 (A+B)	07 (A+B)
$\dot{\boldsymbol{Q}}$ (L s^{-1})	702.2	681.3	784.6	785.9	725.00	725.00	725.00
$\boldsymbol{H_m}$ (m)	101.2	100.1	104.5	101.8	112.00	112.00	112.00
$\boldsymbol{P_h}$ (kW)	696.9	668.8	804.1	784.6	795.00	795.00	795.00
$\boldsymbol{P_e}$ (kW)	1,155.7	1,127.8	1,367.4	1,284.1	966.32	966.32	966.32
$\boldsymbol{P_x}$ (kW)	1,111.5	1,083.9	1,313.8	1,234.0	928.63	928.63	928.63
I (A)*	320.0	306.0	358.0	399.0	297.6	297.6	297.6
$\boldsymbol{\eta_m}$ (%)	96.1	96.1	96.1	96.1	96.10	96.10	96.10
$\boldsymbol{\eta_b}$ (%)	62.7	61.7	61.2	63.6	85.61	85.61	85.61
$\boldsymbol{\eta_g}$(%)	60.3	59.3	58.8	61.1	82.27	82.27	82.27
$\boldsymbol{f_p}$	0.91	0.91	0.92	-	0.92	0.92	0.92

Symbology: $\dot{Q}$ – flow; H_m – manometric head; P_h – hidraulic power; P_e –electric power; P_x – axe power; I – measured current; η_m – electric motor efficiency; η_b – pump efficiency; η_g – motor pump efficiency; f_P – power factor. Source: With data CAESB (2024a).

2.1.3 Bananal 1 and Bananal 2 RWPS

The Bananal RWPS, called Bananal 1 and Bananal 2, operate in parallel and are responsible for supplying additional water from the Bananal stream to the Santa Maria pipeline. Both systems are critical components of the raw water abstraction infrastructure that feeds the Brasília WTP, complementing the flows provided by the Torto and Santa Maria systems.

Each subsystem operates with three MPAs installed in a (2+1) configuration, meaning that two assemblies operate simultaneously while one remains on standby for redundancy and reliability. Within each MPA, the pumps are driven by individual high-efficiency electric motors with soft starters to minimize current peaks and mechanical stress during start-up.

Bananal 1 RWPS is assembled with KSB vertical submersible pumps, model KRTK 300-400/506XG-S, each with an impeller diameter of 321 mm. These units operate under low head and high flow conditions, supplying water from shallow levels to the main suction chamber that leads toward the Santa Maria line. The system allows operation in three possible configurations: a single pump (1), two pumps in parallel (1+2), or three pumps in parallel (1+2+3). Flexibility in operation

ensures adaptability to seasonal variations in flow and water level.

Bananal 2 RWPS operates under significantly higher head conditions and is assembled with IMBIL horizontal centrifugal pumps, model BP 250-700 C, with an impeller diameter of 633 mm. These pumps inject water directly into the Santa Maria pipeline, with discharge heads ranging from 152 to 160 m. Like as Bananal 1, the station can operate with one, two, or three pumps in parallel, according to demand for raw water transfer to the treatment plant.

Performance tests were conducted according to the Brazilian Standard NBR 6400 (ABNT, 1989), including measurements of pressure, flow, electrical current, voltage, and power factor. The data presented in Table S3.1 represent measured averages for 2022–2023 under normal operating conditions.

Table S3.1. Measured and catalog pump characteristics of Bananal 1 and 2 WPS.

WPS	Bananal 1		Bananal 2	
Pump brand	KSB		Imbil	
MPA	08	Catalog inform	09	Catalog inform
$\dot{\boldsymbol{Q}}$ (L s^{-1})	440.5	750.0	440.8	750.0
$\boldsymbol{H_m}$ (mca)	8.0	11.7	153.5	160.2
$\boldsymbol{P_h}$ (kW)	35.4	88.2	674.1	1,178.3
$\boldsymbol{P_e}$ (kW)	49.0	128.6	883.5	1,552.9
$\boldsymbol{P_x}$ (kW)	44.9	117.7	846.8	1,487.7
I (A)*	72.0	96.0	102.0	102.0
$\boldsymbol{\eta_m}$ (%)	91.5	91.5	95.8	95.8
$\boldsymbol{\eta_b}$ (%)	78.9	74.9	79.6	79.2
$\boldsymbol{\eta_g}$ (%)	72.2	68.5	76.3	75.9
$\boldsymbol{f_p}$	0.79	0.79	0.84	0.84

Symbology: $\dot{Q}$ – flow; H_m – manometric head; P_h – hidraulic power; P_e –electric power; P_x – axe power; I – measured current; η_m – electric motor efficiency; η_b – pump efficiency; η_g – motor pump efficiency; f_P – power factor. *Averages between 2022 and 2023 CAESB (2024a). KSB pump model KRTK 300-400/506XG-S, impeller diameter 321 mm; Imbil pump model BP 250-700 C, impeller diameter 633 mm. Source: The Author with data CAESB (2024a)). Each Bananal subsystem operates in a (2+1) configuration with three pumps installed in parallel to meet variable flow demands. Bananal 1 is designed for low head and high flow transfer using submersible KSB pumps, while Bananal 2 handles high head injection using horizontal Imbil pumps. The combination (1+2) indicates the number of active pumps operating in parallel. Both systems discharge into the Santa Maria pipeline, allowing combined pumping operation during peak water demand periods.

Those RWPS represent the highest electricity consumption in the WSS, with demand directly proportional to the required flow rate and pumping head. To ensure operational safety and prevent damage to pipelines and pumps, the system incorporates check valves, flow block valves, suction devices, and protection systems against hydraulic transients (energy/exergy dissipators).

2.1.4 Inventory and resume of energy demand of RWPS.

The power consumption of the RWPS corresponds to the energy required to overcome static head and hydraulic losses along the pipelines that connect the abstraction units to the treatment plant. Variations among systems are due to differences in manometric head, discharge length, and flow rate.

The Torto RWPS presents the highest demand due to its elevated pumping head and four high-capacity MPAs operating continuously. Two operational configurations are considered for the Torto system: (i) the normal configuration, in which MPAs 01(A+B) to 04(A+B) operate under standard suction from the Torto intake, and (ii) the bypass configuration, where MPAs 01(A+B) and 02(A+B) are replaced by their bypass equivalents (01(A+B)* and 02(A+B)*), operating under reduced suction head by hydraulic assistance from the Santa Maria discharge line.

The Santa Maria and Bananal systems operate under normal conditions and use only measured operational data. Bananal 1 operates at low head and high flow with submersible KSB pumps, whereas Bananal 2 operates at high head using horizontal IMBIL brand pumps connected directly to the Santa Maria pipeline.

This configuration represents an alternative operational mode that is occasionally adopted during high-demand or maintenance periods. The subtotal “Torto (normal)” corresponds to the continuous operation of MPAs 01–04 under standard suction conditions from the Torto intake. The subtotal “Torto (bypass substitution)” represents an alternative scenario in which MPAs 01 and 02 are replaced by their bypass equivalents, while MPAs 03 and 04 remain under normal conditions. Catalog and current average values were excluded from the inventory, as they serve only as reference data for equipment specification and are not representative of actual field operation. Electrical power values correspond to average steady-state measurements under full-load conditions, recorded by CAESB during 2022–2023.

Table S4.1a shows the consolidated electrical power inventory for all raw water pumping subsystems, highlighting the two operational configurations of the Torto RWPS (normal and bypass substitution) and the measured power demand of each MPA obtained from CAESB (2024a). The subtotals for Santa Maria, Bananal 1, and Bananal 2 RWPSs correspond exclusively to measured operation and reflect the total power delivered by the motor–pump assemblies during nominal discharge. Table S4.1b summarizes the energy balance in the RWPs.

Table S4.1a. Inventory of power of installed RWPS Torto, Santa Maria and Bananal 1 and 2.

RWPS	MPA or block	Electrical power (kW)	Description
Torto	01 (A+B)	1,281	Allis-Chalmers model 213-909-507/18×16/SF
Torto	02 (A+B)	1,245.1	Allis-Chalmers model 213-909-507/18×16/SF
Torto	03 (A+B)	1,387.4	Worthington model 12-LN-26/BX 24888
Torto	04 (A+B)	1,336.4	Worthington model 12-LN-26/BX 24888
Torto	Subtotal – normal	5,249.9	
Torto	01 (A+B) *	918.5	Reduced suction head (Santa Maria-assisted)
Torto	02 (A+B) *	890.2	Reduced suction head (Santa Maria-assisted)
Torto	03 (A+B)	1,387.4	Worthington model 12-LN-26/BX 24888
Torto	04 (A+B)	1,336.4	Worthington model 12-LN-26/BX 24888
Torto	Subtotal – bypass	4,532.5	Substitutes 01–02 by their bypass equivalents
Santa Maria	05 (A+B)	1,155.7	Worthington model 12-LN-26/BX 24888
Santa Maria	06 (A+B)	1,127.8	Worthington model 12-LN-26/BX 24888
Santa Maria	07 (A+B)	1,367.4	Worthington model 12-LN-26/BX 24888
Santa Maria	Subtotal – St Maria	3,650.9	
Bananal 1	08 (1), 08 (1+2), 08 (1+2+3)	258.4	KSB submersible pumps (low head)
Bananal 2	09 (1), 09 (1+2), 09 (1+2+3)	3,162.8	IMBIL horizontal pumps (high head)

The symbol (*) identifies bypass operation, in which the suction head of the Torto pumping units 01(A+B) and 02(A+B) is reduced due to hydraulic pressurization from Santa Maria discharge line.

Table S4.1b. Summary of effective electrical power balance RWPS.

System	MPA or block	Electrical power (kW)	Description
Torto	01 (A+B)*	918.5	Reduced suction head (Santa Maria-assisted)
Torto	02 (A+B)*	890.2	Reduced suction head (Santa Maria-assisted)
Torto	03 (A+B)	1387.4	Worthington model 12-LN-26/BX 24888
Torto	Subtotal Torto	4532.5	Substitutes 01–02 by their bypass equivalents
Santa Maria	05 (A+B)	1155.7	Worthington model 12-LN-26/BX 24888
Santa Maria	06 (A+B)	1127.8	Worthington model 12-LN-26/BX 24888
Santa Maria	Subtotal St Maria	6816	
Bananal 1 WPS	08	49	KSB submersible pumps (low head)
Bananal 2 WPS	09	883	Imbil horizontal pumps (high head)
Bananal	Subtotal Bananal	932	

The symbol (*) identifies bypass operation, in which the suction head of the Torto pumping units 01(A+B) and 02(A+B) is reduced due to hydraulic pressurization from the Santa Maria discharge line.

2.2 Exergy analysis of RWPS

Table S5.1 Exergy balance in the gross WPS with the current MPS with bypass water at Torto RWPS and replacement of the MPS pumps at Santa Maria RWPS with Sulzer brand pumps.

RWPS	Torto	Santa Maria		Bananal 1	Bananal 2	Total (kW)	
	Current	Current	Subst	Current	Current	Current	Subst
$\dot{X}E_{input,RWPS}$ (kW)	3,196.1	2,283.5	1,932.6	49.0	883.5	6,412.1	6,061.2
$\dot{X}E_{useful,RWPS}$ (kW)	2,392.4	1,365.7	1,590.0	35.4	674.1	4,467.6	4,691.9
$\dot{X}E_{losses,RWPS}$ (kW)	582.0	774.9	202.7	6.18	143.6	1,506.7	934.5
$\dot{X}E_{irrev.,RWPS}$ (kW)	221.8	142.9	139.9	7.5	65.8	438.0	435.0

3.3 Inventory of energy demand and exergy balance of Brasília WTP

2.3.1 Electrical consumption at the Brasília WTP

WTP represents the final and most energy-intensive stage of the urban water system. It includes several unit processes—flocculation, flotation, filtration, chemical dosing, and sludge handling—each of which involves electromechanical equipment powered by medium- and low-voltage systems, as the Table S6.1 shows. All devices are automatically controlled through variable frequency drives and soft starters to ensure stable operation and energy efficiency.

The electrical power values correspond to average operational measurements obtained during steady-state operation at nominal flow conditions. The equipment list includes only process-related devices directly involved in water treatment and auxiliary operations. Administrative buildings, workshops, and external infrastructure were excluded from the inventory. Each power value represents the effective motor input power, including transmission losses and the rated efficiency of the drive systems. The total electrical demand (616.6 kW) corresponds to the sum of all measured equipment loads and represents approximately 5 % of the total energy consumption of the Brasília water supply system under normal operation. All motors are controlled through variable frequency drives (VFDs) and soft starters, which reduce starting currents and improve power factor stability across the treatment stages. The data were compiled from CAESB's operational logs and verified with field measurements collected between 2022 and 2023, forming the basis for the exergy and LCA modeling in Sections 2.3 and 2.4 of the main text.

Table S6.1. Electrical power inventory of the Brasília WTP.

Equipment	Nr. of units	Unit power (kW)	Total power (kW)	Remarks
Flocculation agitators	18	2.2	39.6	Paddle-type mechanical agitators with variable speed
Recycling pumps	8	37	296	Recirculation of treated water for flotation and backwash
Air compressor	1	29.4	29.4	Used for the dissolved air flotation (DAF) unit
Foam scrapers	16	0.25	4	Mechanical surface skimmers at flotation tanks
Submersible agitators	2	1.7	3.4	Mixing of clarified water
Blowers	2	45	90	Backwashing of filter media
Filter washing pumps	3	44.7	134.1	Water supply for rapid filter cleaning
Fluoride dosing pumps	2	0.18	0.36	Fluorosilicic acid dosing system
PAC dosing pumps	2	0.18	0.36	Polyaluminum chloride dosing system
Geo-calcium dosing pumps (1)	1	1.1	1.1	Calcium hydroxide dosing system
Geo-calcium dosing pumps (2)	5	0.75	3.75	Additional dosing units for lime slurry
Lighting and auxiliary systems	1	14.5	14.5	Indoor and outdoor lighting, monitoring, and control
Total internal WTP demand			616.6	Total electrical load of WTP

The inventory presented in Table S6.1 lists each equipment type, the number of installed units, and the corresponding power demand CAESB (2024). These data are derived from CAESB's operational records and field measurements conducted during 2022–2023. The total internal power demand of the WTP amounts to 616.6 kW, which represents approximately 5.0 percent of the total electricity consumption of the Brasília water supply system under normal operation.

2.3.2 Chemical inputs for the Brasília WTP

The chemical inventory summarizes the reagents employed at the Brasília WTP and quantifies their respective standard chemical exergies. These inputs correspond to the materials used during flocculation, pH correction, fluoridation, disinfection, and sludge conditioning processes. The inventory is essential for evaluating the exergo environmental performance of the system, as chemical exergy accounts for the embedded energy potential associated with each reagent's molecular composition and

production pathway. The chemical composition and specific exergy coefficients were obtained from the database of Szargut, Morris, and Steward (1988), as recommended for exergy analyses of chemical processes. Flow rates and consumption values were derived from CAESB's operational data (2024a) and represent the average steady-state operation of the plant.

Each reagent plays a specific role in maintaining water quality and treatment efficiency. Polyaluminum chloride (PAC) is used as the main coagulant to promote particle agglomeration during the flocculation stage. Calcium hydroxide ($Ca(OH)_2$) serves as an alkalizing agent, regulating the pH and optimizing the coagulation reaction. Fluosilicic acid (H_2SiF_6) is applied for fluoridation, ensuring compliance with public health requirements for fluoride concentration. Chlorine gas (Cl_2) is used as a disinfectant to eliminate pathogenic microorganisms before water distribution. Finally, an anionic polyelectrolyte is added in small quantities as a coagulation aid, improving the formation and settling of flocs.

The exergy content of each chemical was determined by multiplying its mass flow rate by its specific chemical exergy, expressed in kilojoules per gram. Table S7.1 show detailed inventory, including the mass flow rates, exergy coefficients, and total exergy contributions of each substance.

Table S7.1. Chemical inputs used in the Brasília WTP and their standard chemical exergy.

Chemical input	Function or process stage	Mass flow ($g\ s^{-1}$)	Specific exergy ($kJ\ g^{-1}$)	Total exergy (kW)	Remarks
Polyaluminum chloride (PAC)	Coagulant dosing during flocculation	20.45	40	817.92	Main coagulant; responsible for turbidity removal and solids aggregation
Calcium hydroxide ($Ca(OH)_2$)	pH correction and alkalization	10.8	2.3	24.84	Alkalizing agent that enhances coagulant efficiency and precipitation reactions
Fluosilicic acid (H_2SiF_6)	Fluoridation	8.87	0.52	4.61	Provides fluoride for dental health control; low exergy contribution
Chlorine gas (Cl_2)	Disinfection	3.82	2.46	9.39	Primary disinfectant ensuring microbiological safety of treated water
Anionic polyelectrolyte	Coagulation aid	0.15	40	6.16	High exergy value despite small dosage; improves floc structure
Total				862.9	Sum of all chemical exergy contributions

Specific exergy values were obtained from the reference database of Szargut, Morris, and Steward (1988). Mass flow rates were derived from CAESB's operational records and represent steady-state average conditions during 2022–2023.

2.3.3 Dewatered sludge of Brasilia WTP

Table S8.1- Characteristics of the dewatered sludge from the Brasília WTP

WTP Flow rate ($L\ s^{-1}$)	Sludge production ($g\ s^{-1}$)	COD ($mg\ L^{-1}$)	Sludge density ($g\ cm^{-3}$)	MW ($mg\ mol^{-1}$)	MW ($mol\ L^{-1}$)	Polychloride used ($g\ s^{-1}$)	Polychloride MW (g mol)	Density of polychloride, aluminum, and iron ($g\ cm^{-3}$)
2,461	76.09	132.5	1,030	97,120	0.0137	3.68	101.96	3.99

MW – molecular weight.

Table S9.1 - Exergy of the main compounds of the sludge from the Brasília WTP.

Compound	Influent	xi	E^0_{ch,n_e}*	$\sum_i(\mu_i - \mu_{0,i})\,x_i$ (1)	RT_0	(a_i)	$ln(a_i)$	$RT_0\sum x_i\,ln(a_i)$ (2)	(1) + (2)	Specific chemical exergy	Exergy of the compound	
	($mol\ L^{-1}$)	($mol\ mol^{-1}$)	($kJ\ mol^{-1}$)	(kJ/mol^{-1})				($kJ\ mol^{-1}$)	($kJ\ mol^{-1}$)	($kJ\ L^{-1}$)	(kW)	Total %
COD	0.0137	0.02214	1,322.06	29.2721	2.478	0.0137	-4.2926	-0.2356	29.0366	0.3969	0.029	0.4
Aluminum	0.489	0.79157	210.46	166.5916	2.478	0.489	-0.7161	-1.4049	165.1868	80.7215	5.963	90.7
Iron	0.115	0.18628	374.16	69.7003	2.478	0.115	-2.1628	-0.9986	68.7018	7.9007	0.58	8.9
Total	0.617	1.00000	1,906.67	265.5641				-2.6390	262.9251	89.0191	6.576	100.0

2.4 Exergy Analysis of Water Distribution (TWPS and Losses)

Table 10.1a shows the operational data and exergy balance of the TWPS, Table 10.1b, as mentioned in the item 3.3.4.

Table S10.1a. Operational data and performance of the TWPS.

MPA	1	1+2	1+2+3	Average
Pump	IMBIL brand, model BP 300-340A, 380 mm rotor			
$\dot{Q}$ (L s^{-1})	402.5	786.8	1,198.3	857.97
H_m (mca)	50.7	53.6	55.3	50.21
P_h (kW)	200.1	413.6	649.8	422.5
P_e (kW)	283.4	582.1	919.2	597.6
P_x (kW)	246.5	506.2	799.3	519.6
I (A)*	103.5	103.5	103.5	103.5
η_m (%)	94.8	95.1	95.4	95.4
η_b (%)	81.2	81.7	81.3	81.3
η_g (%)	77.0	77.7	77.6	77.6
f_p	0.85	0.85	0.85	0.85

Source: The Author with data CAESB (2024).

Table S10.1b. Exergy balance and performance of the TWPS.

MPS	1	1+2	1+2+3	Current media
Pump	IMBIL brand, model BP 300-340A, 380 mm rotor			
$\dot{X}E_{input,RWPS}$ (kW)	283.4	582.1	919.2	597.6
$\dot{X}E_{useful,RWPS}$ (kW)	200.1	413.6	649.8	422.5
$\dot{X}E_{losses,RWPS}$ (kW)	28.3	53.9	86.4	33.75
$\dot{X}E_{irrev.,RWPS}$ (kW)	55.0	114.7	183.0	141.35
ε (%)	70.6	71.0	70.7	70.7
$\dot{E}_p/\dot{E}_a$ (%)	10.0	9.3	9.4	5.6

During water distribution, significant exergy and treated water depletion occur due to real losses caused by leaks, ruptures in over-pressurized networks, especially during nighttime operation, aging infrastructure, defective seals, and malfunctioning valves and flow control devices. Additionally, periodic discharges from public pipelines and reservoirs contribute to such losses. Preventive maintenance of pressure control systems and network monitoring can mitigate these effects, employing hydraulic energy dissipation valves (macro-metering) to regulate pressure and flow.

Apparent losses also occur at consumer connections (micro-metering), including inaccuracies in water meters, unauthorized connections, meter reading errors, and calibration issues. The total water loss in supply systems can be quantified using the total loss index (IP, in

%) and the loss index per connection (IPL, in L Con^{-1} day), according to the methodology adopted by the National Sanitation Information System (SNIS, 2023):

$$IP\ (\%) = ((AG006 + AG018 - AG010 - AG024) / (AG006 + AG018 - AG024))\ x\ 100 \quad \text{(S1)}$$

$$IPL = ((AG006 + AG018 - AG010 - AG024)\ x\ 10^3) / (AG002\ x\ 10^3) / 365 \quad \text{(S2)}$$

where:

- $AG002$: number of active water connections;
- $AG006$: annual volume of water produced (10^3 m^3 year^{-1});
- $AG010$: annual volume of water consumed (10^3 m^3 year^{-1});
- $AG018$: annual volume of imported treated water (10^3 m^3 year^{-1}; zero if no imports occur);
- $AG024$: annual volume of service water (10^3 m^3 year^{-1}).

Although some level of total loss (TL) is inherent to any supply system, minimizing it is essential to conserve natural water resources, reduce operational and capital expenditures, and enhance both exergy efficiency and environmental performance.

Tables S11.1a and 11.1b summarize the water loss in Federal District and Brasília, with respective exergy lost in period 2020-2022

Table S11.1a Water losses indexes in Federal District.

Year	AG002	AG006	AG010	AG024	IP	IPL	Losses
	(Connections)	10^3 (m^3 y^{-1})	10^3 (m^3 y^{-1})	10^3 (m^3 y^{-1})	(%)	(L conn^{-1} day)	(L s^{-1})
2022	715810	258311	161766	13917,95	33,81	316,25	2807,76
2021	706376	254016	156271	13334,01	35,07	327,39	2864,18
2020	694171	251705	156275	13580,92	34,37	323,04	2781,54
Average	705452	254677	158104	13611	34,42	322,23	2817,83

Table S11.1b Water losses in Brasilia and the relative exergy loss.

Year	AG002	AG006	AG010	AG024	IP	IPL	Loss	$\dot{X}E_{loss}$
	(conn.)	10^3(m^3 y^{-1})	10^3(m^3 y^{-1})	10^3(m^3 y^{-1})	(%)	(L conn^{-1} day)	(L s^{-1})	(kW)
2022	80.626	41761,64	32540,92	1552,7	19,07	260,56	256,05	282,27
2021	79.008	42752,58	33740,46	1549,3	18,11	258,79	248,95	268,06
2020	78.372	44604,09	36399,61	1520,7	15,51	233,65	222,47	229,58
Average	79.335	43.039	34.227	1.541	17,56	251,00	242,49	259,97

Table S12.1. Consistency of mass flow values for the Brasília UWC.

Stage	Flow [a]	Equivalent [b]	Evaluation
Abstraction	2.461	212.6	Consistent with the nominal capacity of the Brasília WTP
Distribution losses	0.2425	21	Typical range of real and apparent losses in urban networks
Delivered to consumers	2.2185	191.7	Coherent with the water demand of the served population
WWTP inflow	1.776	153.4	In line with CAESB's operational data for Brasília North and South WWTPs
Non-sewered uses	0.4425	38.3	Compatible with evapotranspiration and infiltration in the local climate
WWTP effluent	1.776	153.4	Consistent with reported effluent discharge to Lake Paranoá

[a] (m^3/s) [b] ($\times 10^3$ m^3 day^{-1})

2.5 Submersible pump (with electric motor) selection for RWPS EAB.RBN.001

Dados de funcionamento			
Vazão pretendido	250,000 l/s	Vazão Nominal	250,000 l/s
Altura manométrica pretendida	11,71 m	Altura total calculada	11,71 m
		Rendimento	74,9 %
Fluido bombeado	Água Água limpa Não contendo substâncias químicas e mecânicas que afetem os materiais	Potência absorvida	51,49 HP
		Velocidade de rotação da bomba	1184 rpm
		Potência máxima no diâm. nominal	52,14 HP
Temperatura ambiente	20,0 °C	Altura de Shuttoff	17,55 m
Temperatura do Fluido	20,0 °C	Projeto	Sistema simples 1 x 100 %
Densidade do fluído	998 kg/m³		
Viscosidade do fluído	1,00 mm²/s	Teste de performance	Sim
Projeto			
Projeto	Monobloco submersível	Código de material	SIC/SIC/NBR
Tipo de instalação	Vertical	Tipo de rotor	Rotor multicanal de fluxo radial (K)
Flange de sucção de acordo com (DN1)	Não usinado	Anel Desg. do Corpo	Anel Desg. do Corpo
Flange de recalque da bomba conforme (DN2)	EN 1092-2 / DN 300 / PN 10	Diâmetro do rotor	321,0 mm
		Dimensão da passagem livre	100,0 mm
Vedação	2 Selos mecânicos tipo Tandem, com reservatório de óleo	Sentido de rotação do motor	Sentido Horário
		Cor	Azul ultramarino (RAL5002) azul-KSB
Fabricante	KSB		
Tipo	MG		
Motor, acessórios			
Tipo de motor	Motor elétrico	Enrolamento do motor	380 V
Modelo (fabricante)	KSB	Número de pólos	6
Tipo de construção do motor	Motor sub. KSB	Modo de partida	Partida direta
Letra do código NEMA	F	Modo de ligação	Delta
Freqüência	60 Hz	Método de refrigeração do motor	Resfriamento da superfície
Tensão Nominal	380 V	Versão do motor	X
Potência Nominal P2	65,00 HP	Projeto do cabo	Mangueira de borracha
Reserva disponível	26,24 %	Entrada do cabo	Selado ao longo de todo o comprimento
Corrente nominal	103,0 A	Cabo de alimentação	AWG 5-4
Taxa da corrente de partida	5,3	Número de cabos de alimentação	2
Classe de isolamento	F conforme IEC 34-1	Cabo de controle	AWG 15-12
Proteção do motor	IP68	Número de cabos de controle	1
Cos phi a carga 4/4	0,79	Sensor de umidade	Com
Rendimento do motor a carga 4/4	91,5 %	Comprimento do cabo	15,00 m
Fator de serviço do motor	1,15		
Sensor de temperatura	Interruptor bimetálico/PTC		

Figure S1.1. Submersible pump systems from RWPS EAB.RBN.001. KSB brand pumps, model KRKT 300-400/506XG-S, arrangement (2+1), direct start.

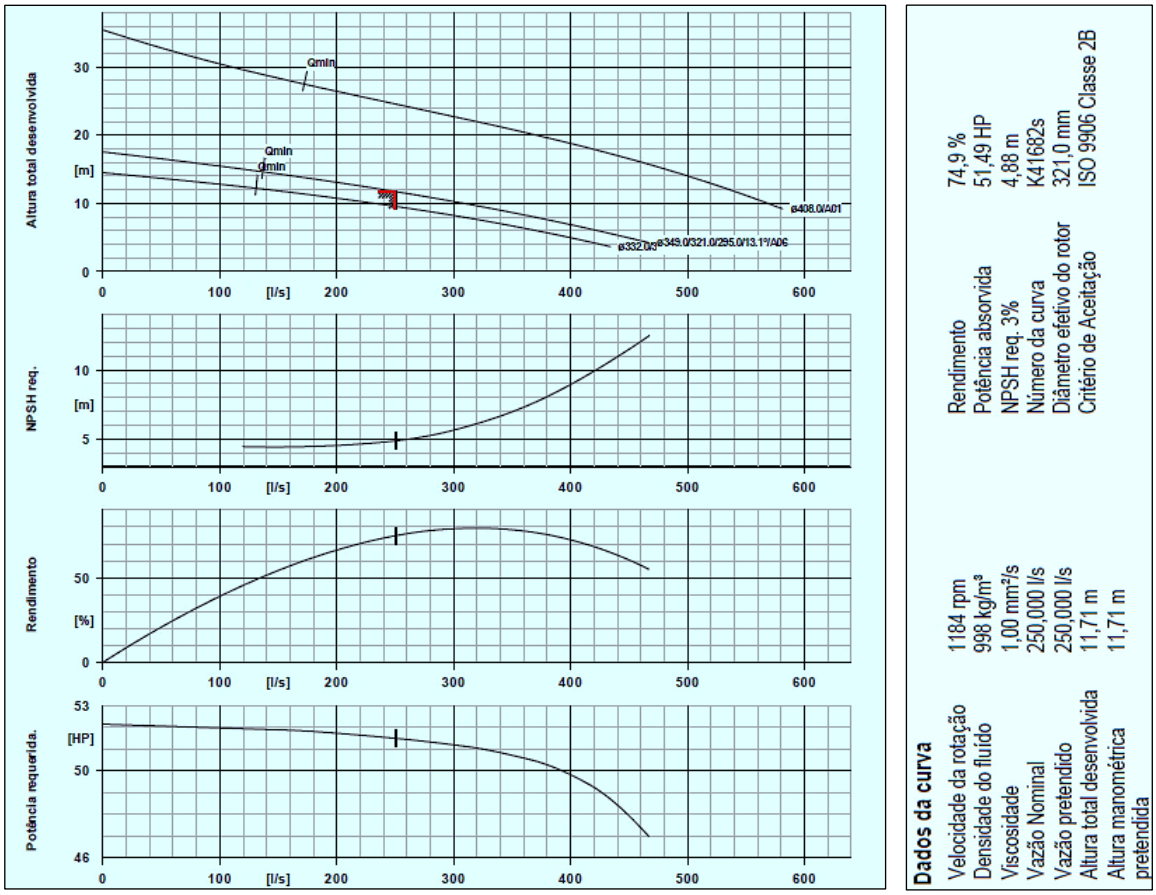

Figure S2.1. Performance curve for KRKT 300-400/506XG-S pumps

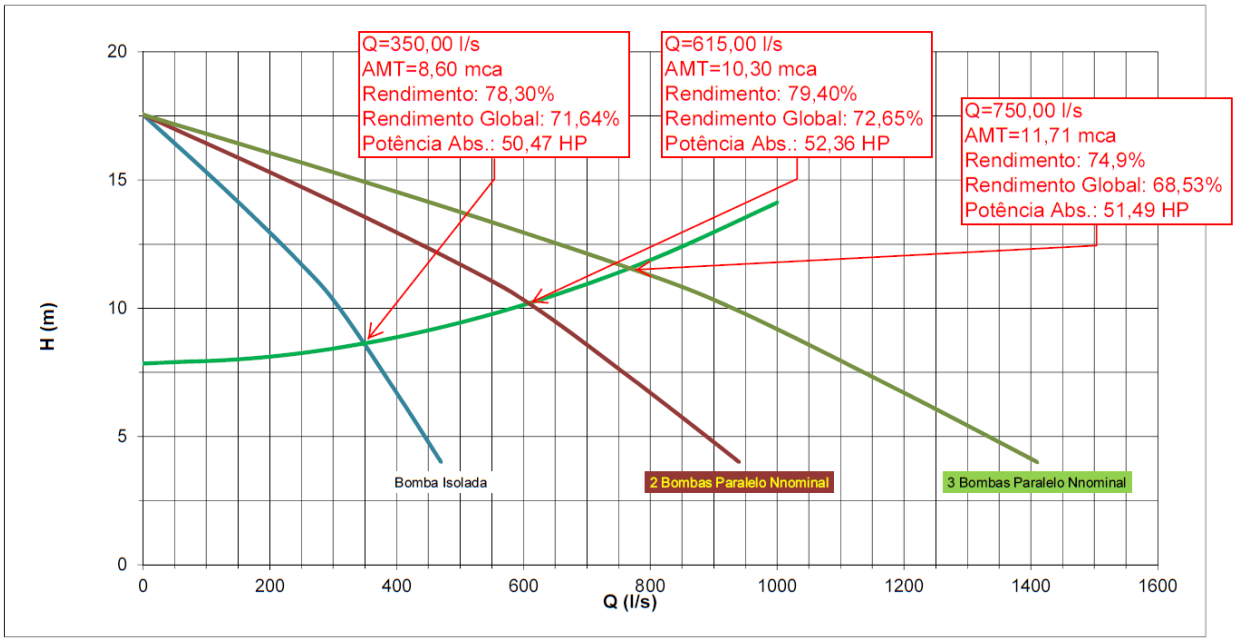

Figure S3.1. System curve for pumps in parallel. Pumps selected for the operating point with three pumps, two in operation and one on standby, all meeting the system curve, including flow rates higher than specified.

2.5 Pump and electric motor selection for RWPS EAB.RBN.002

CONDIÇÕES DE OPERAÇÃO DA BOMBA

Descrição	Equipamentos para serem utilizados na obra de implementação da Elevatória Número 2 de Água Bruta do Ribeirão Bananal EAB.RBA.RB2.RESERVA	
Vazão para uma bomba	275	l/s
Vazão para uma bomba	990	m³/h
AMT para uma bomba	152,62	mca
Rendimento bomba p/ uma bomba	80,3	%
BHP para uma bomba	696,89	hp
NPSH req. Para uma bomba	3,9	mca
Vazão total p/ duas bombas em paralelo	530	l/s
Vazão total p/ duas bombas em paralelo	1908	m³/h
Vazão unitária p/ duas bombas em paralelo	265	l/s
Vazão unitária p/ duas bombas em paralelo	954	m³/h
AMT para duas bombas em paralelo	156	mca
Rendimento bomba p/ duas bombas em paralelo	80,1	%
BHP para duas bombas em paralelo	688,00	hp
NPSH req. para duas bombas em paralelo	3,5	mca
Vazão total p/ três bombas em paralelo	750	l/s
Vazão total p/ três bombas em paralelo	2700	m³/h
Vazão unitária p/ três bombas em paralelo	250	l/s
Vazão unitária p/ três bombas em paralelo	900	m³/h
AMT para três bombas em paralelo	160,17	mca
Rendimento bomba p/ três bombas em paralelo	79,2	%
BHP para três bombas em paralelo	674,12	hp
NPSH req. para três bombas em paralelo	3,2	mca
Vazão mínima admissível da bomba p/ rotor de projeto	460	m³/h

DADOS CONSTRUTIVOS E MAIORES INFORMAÇÕES

Bocais	Diâmetro Nominal (mm)	Posição
Sucção	350	Horizontal
Recalque	250	Horizontal

Bomba centrífuga horizontal, tipo bi-partida, rotor apoiado entre mancais, sendo o mesmo fechado.

Tipo de mancal: Rolamentos.

Vedação por Selo Mecânico.

Lubrificação/refrigeração do próprio conjunto moto-bomba.

Rotor da bomba: tipo fechado com dupla sucção e balanceado hidraulicamente;

Ø Rotor máximo : 654 mm

Ø Rotor de projeto: 633 mm

Ø Rotor mínimo: 550 mm

Rendimento global para 01 bomba operando individualmente : 77,35 %;

Rendimento global para 02 bombas operando em paralelo : 79,4 %;

Rendimento global para 03 bombas operando em paralelo : 75,4 %;

Redução Concêntrica DN250 x DN350 no bocal de recalque da bomba.

Figure S4.1. RWPS EAB.RBN.002 injection pump systems. IMBIL brand pumps, model BP 250-700 C, arrangement (3+1), inverter start.

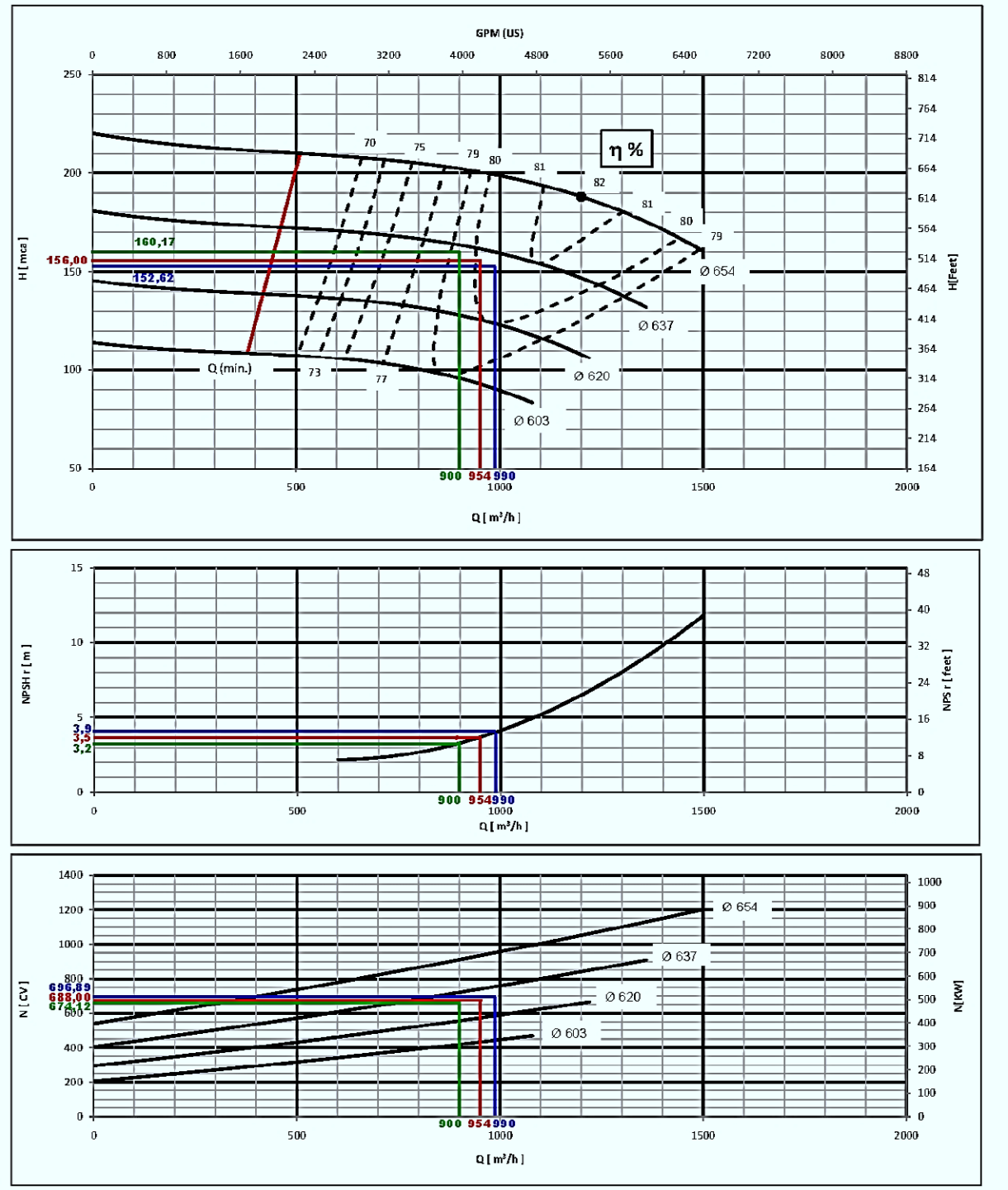

Figure S5.1. Performance curve for IMBIL brand pumps, Model BP 250-700 C, maximum impeller diameter 654 mm, and minimum diameter 603 mm.

Selected motor to motor pump assembly: WEG brand, rated power 800HP (588.4kW), 60Hz, 1,790 RPM, Insulation class F (155 C), protection degree IP-55, operating voltage 4,160 V

SM2 - SECOND ARTICLE

1 Abstract

This Supplementary Material provides the full descriptive context and the complete tabular data that support the analyses reported in the manuscript “Exergy Loss and Optimization in Brazilian Urban Wastewater Treatment: A Study of the Urban Water-Exergy-Environment Nexus”.

Each subsection explains data measurement, how the operating conditions relate to the system topology, and how the values should be interpreted inside the study boundaries.

2 Methodology

2.1 Sanitation Systems in Brasília: Structure and Operation

2.1.1 Treatment Process Overview

Table S1.2. Description of the dataset of the Study.

Data Category	Description/Parameter	Source/Reference	Data Type
Influent flow rate	Average daily inflow	CAESB Operational Report [a]	Primary
Electricity consumption	Monthly energy use	CAESB Energy Billing Records [a]	Primary
Sludge production	Dewatered sludge	WWTP Monthly Performance Report [a]	Primary
Methane flaring	Volume flared	Technical Site Inspection	Primary / Calculated
Biogas production	Total biogas generated	Technical Site Inspection	Primary / Calculated
Chemical consumption	Polymer and coagulant use	Internal Operational Logs	Primary
Treated effluent quality	BOD, TSS, TN, TP	Laboratory Analysis (CAESB)	Primary
Temperature (air/water)	Monthly average	INMET Meteorological Station [b]	Primary
GHG emissions	CH_4, N_2O from sludge and effluent	Estimated using IPCC and literature [c]	Secondary / Calculated
	CO_2 from energy use (Scope 2)	Emission factor approach [c]	Secondary / Calculated

Primary = Directly measured from WWTP or CAESB operational records and meteorological stations. Secondary = Derived from external literature. Calculated = Estimated using standardized models or emission factors based on 2020–2023 data. [a] (CAESB, 2024) , b (INMET, 2024); [c] (Chernicharo, 2016; Daudt, 2019; Daudt et al., 2019; IPCC, 2006; Ribeiro, R. P., 2017; Ribeiro et al., 2018; WRI & WBCSD, 2004).

2.2 Determination of the exergy of organic matter

Table S2.2. Input operational data for calculating the exergy of organic matter compounds (E^0_{ch,n_e}) in wastewater and dewatered sludge at the North and South WWTPs.

Phase	Influent wastewater (524.4 L s^{-1})			Effluent wastewater (524.4 L s^{-1})			Dewatered sludge (0.683 L s^{-1})		
Units	(mg L^{-1})	MW (mg mol^{-1})	(mol L^{-1})	(mg L^{-1})	MW (mg mol^{-1})	(mol L^{-1})	(mg L^{-1})	MW (mg mol^{-1})	(mol L^{-1})
North WWTP									
COD	656.00	200,254.80	3.28E-03	31.50	200,254.80	1.57E-04	1,370.00	97,120.00	1.41E-02
Nitrogen	65.10	18,040.00	3.61E-03	8.00	18,040.00	4.43E-04	52.72	18,040.00	2.92E-03
Phosphorus	7.04	97,995.20	7.18E-05	0.30	97,995.20	3.37E-06	73.40	97,995.20	7.49E-04
Iron	2.59	55,845.00	4.64E-05	0.40	55,845.00	6.49E-06	0.64	55,845.00	1.15E-05
South WWTP									
COD	533.50	200,254.80	2.66E-03	23.50	200,254.80	1.17E-04	1.10E+03	97,120.00	1.13E-02

Nitrogen	64.30	18.040.00	3.56E-03	7.80	18,040.00	4.32E-04	59.13	18,040.00	3.28E-03
Phosphorus	6.66	97,995.2	6.80E-05	0.23	97,995.20	2.35E-06	45.09	97,995.2	4.60E-04
Iron	2.11	55,845.00	3.78E-05	0.30	55,845.00	5.29E-06	0.58	55,845.00	1.04E-05

MW: molecular weight.

Table S3.2. Exergy of main compounds in the mixture at the North and South WWTPs.

Parameters	a_i	x_i	$E^0_{ch.n_e}$ [a]	(1) $\sum_i(\mu_i - \mu_{0.i})\, x_i$	RT_0	$ln(a_i)$	(2) $RT_0 \sum x_i\, ln(a_i)$	(1) + (2)	$(E_{ch.f} + E_{ch.c})$	
Units	(mol L^{-1})	(mol mol^{-1})	(kJ mol^{-1})	(kJ mol^{-1})	(kJ mol^{-1})		(kJ mol^{-1})	(kJ mol^{-1})	(kJ L^{-1})	(kW)
North WWTP										
Influent wastewater										
COD	3.28E-03	0.46802	2,704.63	1,265.8315	2.478	-5.7199	-6.6350	1,259.1965	4.1302	2,165.86
Nitrogen	3.61E-03	0.51511	337.21	173.7025	2.478	-5.6240	-7.1801	166.5224	0.6011	315.24
Phosphorus	7.18E-05	0.01025	870.26	8.9159	2.478	-9.5416	-0.2423	8.6736	0.0006	0.33
Iron	4.64E-05	0.00662	374.16	2.4773	2.478	-9.9782	-0.1637	2.3135	0.0001	0.06
Total	7.01E-03	1.00000	4,286.27	1,450.93			-14.2211	1,436.706	4.7320	2,481.48
Effluent wastewater										
COD	1.57E-04	0.25744	2,009.87	517.414	2.478	-8.7593	-5.5888	511.8250	0.0804	42.14
Nitrogen	4.43E-04	0.72640	337.21	244.951	2.478	-7.7219	-13.9021	231.0487	0.1024	53.67
Phosphorus	3.37E-06	0.00553	870.26	4.809	2.478	-12.6006	-0.1726	4.6363	0.0000	0.01
Iron	6.49E-06	0.01064	374.16	3.9817	2.478	-11.9452	-0.3151	3.6667	0.0000	0.01
Total	6.10E-04	1.00000	3,591.50	771.155			-19.9786	751.1768	0.1828	95.83
Dewatered sludge										
COD	1.41E-02	0.79300	1,322.91	1,049.071	2.478	-4.2616	-8.3758	1,040.6948	14.6738	9.98
Nitrogen	2.92E-03	0.16422	337.21	55.3789	2.478	-5.8362	-2.3755	53.0034	0.1548	0.11
Phosphorus	7.49E-04	0.04212	870.26	36.6594	2.478	-7.1968	-0.7514	35.9080	0.0269	0.02
Iron	1.15E-05	0.00065	374.16	0.2420	2.478	-11.3732	-0.0182	0.2238	0.0000	0.00
Total	1.78E-02	1.00000	2,904.54	1,141.3509			-11.5209	1,129.8300	14.8555	10.10
South WWTP										
Influent wastewater										

COD	2.66E-03	0.42050	2,704.12	1137.081	2.478	-5.9294	-6.1775	1,130.9039	3.0082	3,762.66
Nitrogen	3.56E-03	0.56277	337.21	189.775	2.478	-5.6380	-7.8613	181.9141	0.6476	810.04
Phosphorus	6.80E-05	0.01075	870.26	9.355	2.478	-9.5960	-0.2556	9.0994	0.0006	0.77
Iron	3.78E-05	0.00598	374.16	2.236	2.478	-10.1832	-0.1508	2.0850	0.0001	0.10
Total	6.33E-03	1.00	4,285.75	1338.45			-14.4452	1324.0024	3.6565	4573.57
Effluent wastewater										
COD	1.17E-04	0.21019	1,760.26	369.988	2.478	-9.0533	-4.7147	365.2731	0.0427	53.46
Nitrogen	4.32E-04	0.77609	337.21	261.707	2.478	-7.7471	-14.8965	246.8101	0.1066	133.36
Phosphorus	2.35E-06	0.00422	870.26	3.674	2.478	-12.9611	-0.1356	3.5384	0.0000	0.01
Iron	5.29E-06	0.00950	374.16	3.556	2.478	-12.1497	-0.2861	3.2697	0.0000	0.02
Total	5.57E-04	1.00	3,341.89	638.924			-20.0328	618.8914	0.1494	186.85
Dewatered sludge										
COD	1.13E-02	0.75081	1,323.36	993.595	2.478	-4.4830	-8.3393	985.2555	11.1334	14.99
Nitrogen	3.28E-03	0.21793	337.21	73.490	2.478	-5.7199	-3.0885	70.4020	0.2309	0.31
Phosphorus	4.60E-04	0.03056	870.26	26.599	2.478	-7.6843	-0.5819	26.0166	0.0120	0.02
Iron	1.04E-05	0.00069	374.16	0.259	2.478	-11.4737	-0.0196	0.2389	0.0000	0.00
Total	1.51E-02	1.00000	2,905.00	1,093.942			-12.0294	1,081.9130	11.3763	15.31

[a] $E^0_{ch.n_e}$ × molecular weight.

2.3 Biogas Recovery Potential

The estimation of methane production in anaerobic reactors and its associated exergy begins with the calculation of the daily influent COD load theoretically converted into methane (CH_4), as expressed in Eq. (S1.2). This relationship considers the daily sewage flow rate and the difference between influent and effluent COD concentrations, accounting for the COD used in biomass synthesis.

$$COD_{CH_4} = \dot{Q}.(COD_a - COD_e) - Y_{COD}.\dot{Q}.COD_a \quad \text{(S1.2)}$$

Where COD_{CH_4} is the daily COD load convertible into methane (kg day^{-1}); $\dot{Q}$ is the daily influent flow rate (m^3 day^{-1}); COD_a and COD_e are the influent and effluent COD concentrations, respectively (kg m^{-3}); Y_{COD} is the COD-to-biomass conversion coefficient, ranging from 0.11 to 0.23 kg COD_{sludge} kg^{-1} $COD_{influent}$. A value of 0.15 was adopted, as recommended by (Chernicharo, 2016) for systems with similar treatment technologies to the WWTPs North and South.

The daily methane production rate is then calculated using Eqs. (S2.2) and (S3.2):

$$\dot{Q}_{CH_4} = \frac{COD_{CH_4}}{f(T)} \quad \text{(S2.2)}$$

$$f(T) = \frac{(P\ .\ K_{COD})}{(R(273 + T))} \quad \text{(S3.2)}$$

Here, $\dot{Q}_{CH_4}$ is the daily methane flow rate (m^3 day^{-1}); $f(T)$ is the temperature correction factor (kg COD m^{-3}); P is the local atmospheric pressure (atm), with an annual average of 1.006662 atm in Brasília (1020 mbar); K_{COD} is the COD equivalent per mole of CH_4 (64 g COD mol^{-1}); R is the universal gas constant (0.08206 atm L mol^{-1} K^{-1}); T is the average operational temperature of the reactors, assumed as 21 °C. Therefore, $f(T)$ = 2.67045 kg COD m^{-3}.

According to Possetti et al. (2021), under average operational conditions of WWTPs, approximately 30% of the methane produced is lost dissolved in the treated effluent, 5% is present in the residual gas phase, and an additional 5% is lost through leaks and condensate purges. The total daily biogas production can be estimated using Eq. (S4.2):

$$\dot{Q}_{biogas} = \frac{\dot{Q}_{CH_4}}{C_{CH_4}} \quad \text{(S4.2)}$$

Here, $\dot{Q}_{biogas}$ is the biogas production rate (m^3 day^{-1}); C_{CH_4} is the methane concentration in the biogas, assumed as 60%.

2.4 GHG Estimation in WWTPs

2.4.1 Emission Categories and Mechanisms

Table S4.2. Key gas-generating reactions in WWTPs.

Condition	Reaction	GHG
Aerobic	$CH_2O + O_2 \rightarrow CO_2 + H_2O$	CO_2
Anoxic (denitrification)	$NO_3^- + CH_2O \rightarrow N_2 + CO_2 + H_2O$	N_2O, CO_2
Anaerobic (sulfate reduction)	$SO_4^{2-} + CH_2O \rightarrow H_2S + CO_2$	CO_2
Anaerobic (hydrogenotrophic methanogenesis)	$CO_2 + 4H_2 \rightarrow CH_4 + 2H_2O$	CH_4
Anaerobic (acetoclastic methanogenesis)	$CH_3COOH \rightarrow CH_4 + CO_2$	CH_4

Table S5.2. Life cycle inventory data for the wastewater treatment systems in WWTP North and WWTP South, under two scenarios (with and without biogas flaring).

Flow	Unit	North WWTP			South WWTP		
		S1	S2	S3	S1	S2	S3
Transport							
Diesel consumption	L h^{-1}	5.71	5.71	5.71	8.73	8.73	8.73
Wastewater transported	m^3 h^{-1}	1,887.85	1,887.85	1,887.85	4,502.44	4,502.44	4,502.44
Treatment – Inputs							
Inputs							
Electricity	kW	1,164.59	1,164.59	1,164.59	1,890.19	1,890.19	1,890.19
Process water	m^3 h^{-1}	4.52	4.52	4.52	8.87	8.87	8.87
Polyanionic polymer	kg h^{-1}	1.58	1.58	1.58	4.68	4.68	4.68
Polycationic polymer	kg h^{-1}	5.52	5.52	5.52	13.90	13.90	13.90
Aluminum sulfate	kg h^{-1}	218.70	218.70	218.70	472.56	472.56	472.56
Hydrated lime	kg h^{-1}	13.27	13.27	13.27	14.93	14.93	14.93
Outputs							
Dewatered sludge	m^3 h^{-1}	2.45	2.45	2.45	4.84	4.84	4.84

Flow	Unit	North WWTP			South WWTP		
		S1	S2	S3	S1	S2	S3
Effluent	$m^3\ h^{-1}$	1,889.92	1,889.92	1,889.92	4,506.47	4,506.47	4,506.47
N_2O emitted	$kg\ h^{-1}$	0.09	0.09	0.09	0.36	0.36	0.36
CH_4 (biogas) emitted	$kg\ h^{-1}$	162.64	16.3	16.3	312.2	31.2	31.2
CO_2 (biogas) emitted	$kg\ h^{-1}$	108.43	10.8	10.8	208.1	20.8	20.8
Biogas (CH_4+CO_2) collected	$kg\ h^{-1}$	0.00	243.97	243.97	0.00	468.34	468.34
Biogas flaring – only for "With flaring"							
Inputs							
Biogas combusted	$kg\ h^{-1}$	–	243.97	243.97	–	468.34	468.34
O_2 required for combustion	$kg\ h^{-1}$	–	585.52	585.52	–	1,124.01	1,124.01
Outputs							
CO_2 from CH_4 combustion	$kg\ h^{-1}$	–	500.13	500.13	–	960.09	960.09
H_2O from CH_4 combustion	$kg\ h^{-1}$	–	329.35	329.35	–	632.25	632.25
Electricity generated	MJ	–	0.00	7,337.28	–	0.00	14,085.21

2.3 Life Cycle Assessment - GHG in WWTPs

2.3.2 Life Cycle Inventory

(a) WWTP North

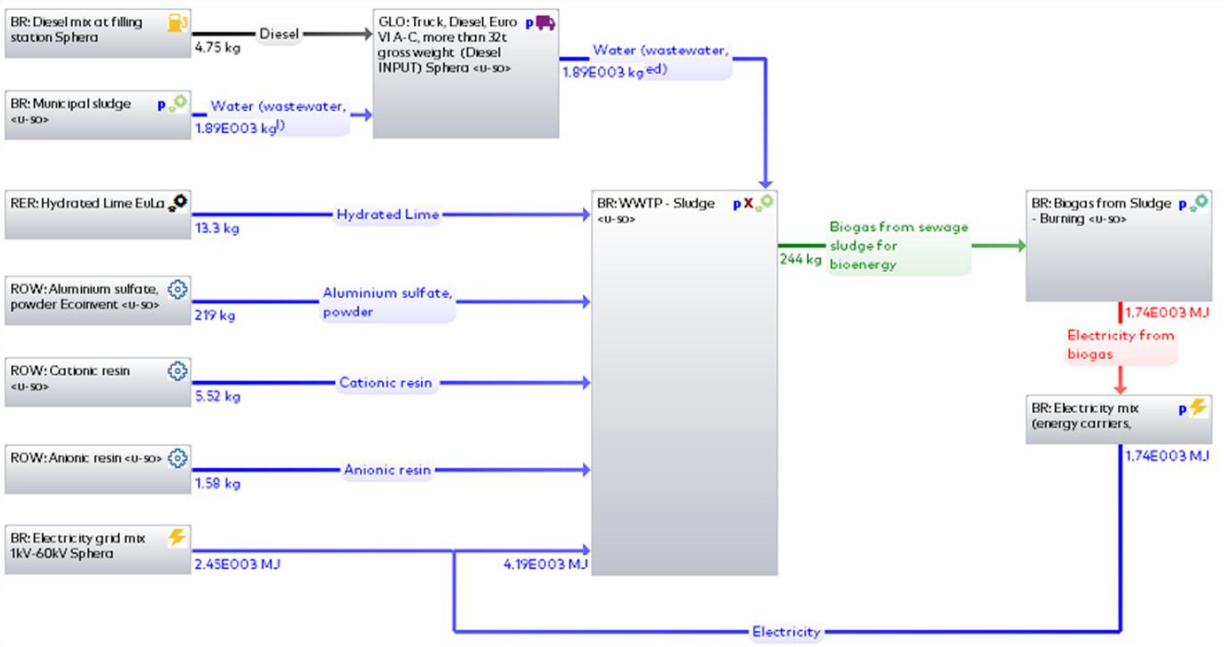

(b) WWTP South

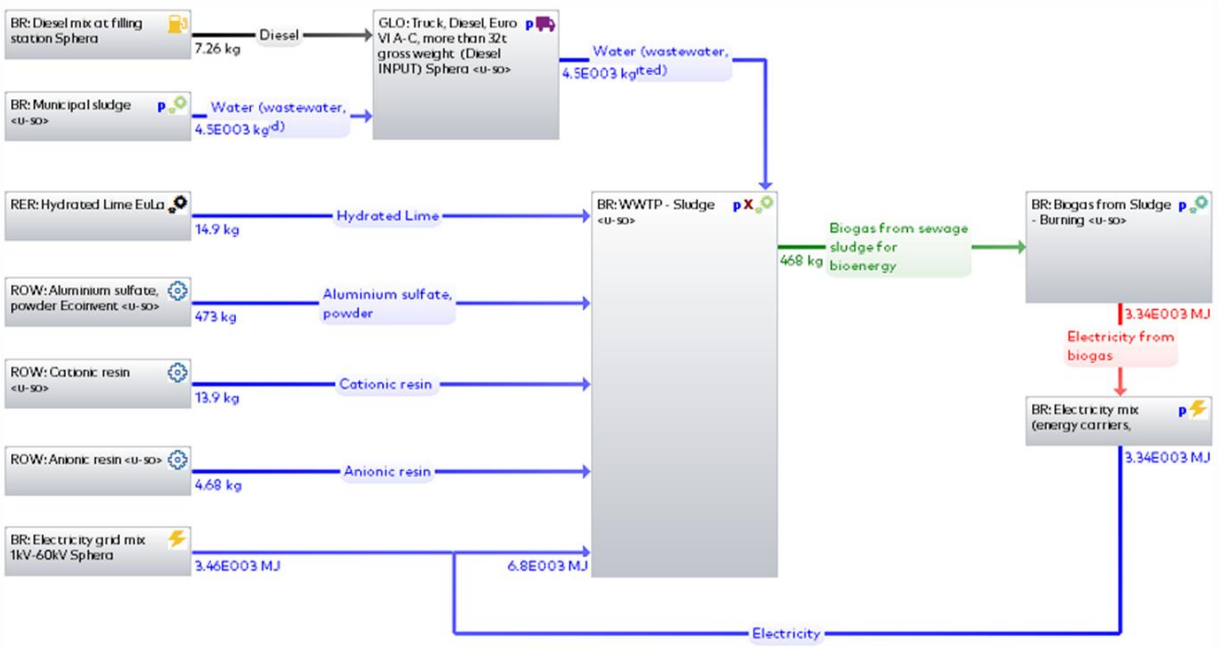

Figure S1.2. Life Cycle Inventory (LCI) flow diagrams of the technological model applied in WWTPs in Brazil, highlighting sludge treatment and biogas recovery. The diagrams represent two operational scenarios: the northern plant (a) and the southern plant (b), with different input loads and chemical consumption profiles.

3 Statistical analyses

3.1 Assessment of the North and South WWTPs

Table S6.2 presents a statistical comparison between the North and South WWTPs based on the mean values and standard deviations of 18 operational and performance parameters. The results highlight significant differences ($p < 0.05$) across most indicators, particularly in influent flow rates, energy consumption, and chemical usage.

Table S6.2. Statistical comparison of operational inputs and removal performance at the North and South WWTPs (2020–2023) based on Mann–Whitney U tests.

Parameter	North Mean	North Std	South Mean	South Std	$p - value$
Inputs and outputs [a]					
Influent wastewater flow ($m^3\ day^{-1}$)	45,478.80	2,903.87	108,058.40	12,326.62	>0.001
Power ($kWh\ day^{-1}$)	27.950.06	1,389.25	45,364.49	2,505.74	>0.001
Process water ($m^3\ day^{-1}$) [c]	37.98	4.95	112.22	17.33	>0.001
Polyanionic ($kg\ day^{-1}$)	132.57	12.90	333.56	26.87	>0.001
Polycationic ($kg\ day^{-1}$)	5,248.70	612.01	11,341.42	985.75	>0.001
Aluminum sulfate ($kg\ day^{-1}$)	318.44	49.44	358.42	78.27	0.13
Hydrated lime ($kg\ day^{-1}$)	58.69	4.59	116.13	11.53	>0.001
Removed compounds and removal rates [a]					
Total Nitrogen Influent ($mg\ L^{-1}$)	65.12	3.71	64.35	7.61	0.93
Total Nitrogen Effluent ($mg\ L^{-1}$)	8.02	1.85	7.78	1.06	0.89
Phosphorus Influent ($mg\ L^{-1}$)	7.04	0.51	6.66	0.98	0.26
Phosphorus Effluent ($mg\ L^{-1}$)	0.33	0.07	0.23	0.06	>0.001
Suspended Solids Influent ($mg\ L^{-1}$)	307.32	31.45	221.84	23.01	>0.001
Suspended Solids Efluent ($mg\ L^{-1}$)	6.30	0.62	4.47	0.80	>0.001
COD Influent ($mg\ L^{-1}$)	655.99	43.31	533.45	80.30	>0.001
COD Efluent ($mg\ L^{-1}$)	31.50	3.02	23.46	2.93	>0.001
BOD Influent ($mg\ L^{-1}$)	350.06	33.39	332.32	46.33	0.34
BOD Efluent ($mg\ L^{-1}$)	6.16	1.43	7.62	1.64	0.01
E. coli Influent (MPN 100mL) [b]	1.57E+07	7.62E+06	1.07E+07	2.39E+06	0.02
E. coli Efluent (MPN 100mL)	1.05E+05	3.76E+04	5.11E+04	3.37E+04	>0.001

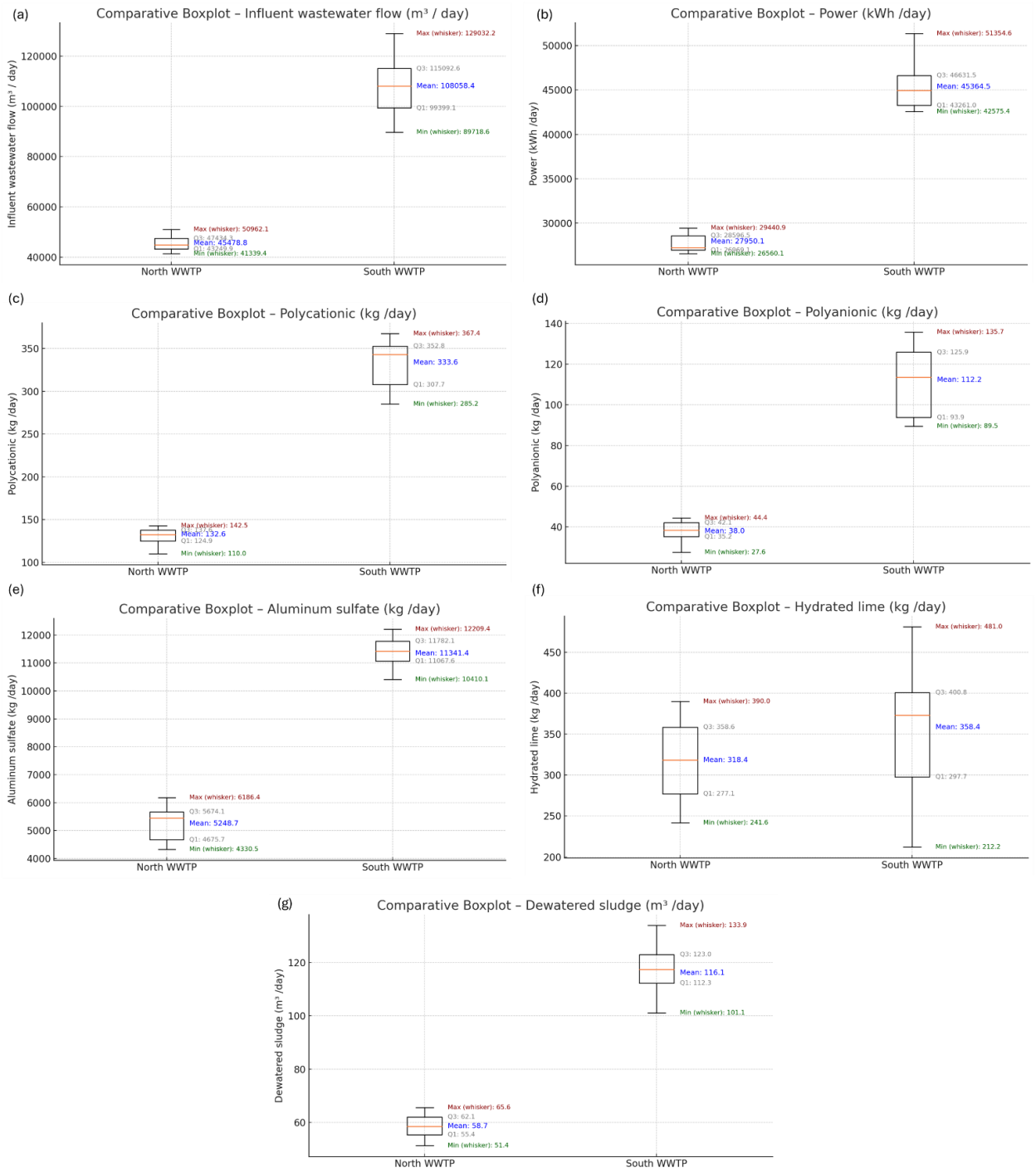

Figure S2.2. Comparative boxplots of operational parameters for the North and South WWTPs.

Each subplot shows the distribution of monthly data from 2020 to 2023, including the mean (blue), first and third quartiles (gray), and whisker limits (green for minimum, red for maximum). (a) Influent wastewater flow ($m^3\ day^{-1}$), (b) Power consumption ($kWh\ day^{-1}$), (c) Polycationic coagulant dosage ($kg\ day^{-1}$), (d) Polyanionic coagulant dosage ($kg\ day^{-1}$), (e) Aluminum sulfate dosage ($kg\ day^{-1}$), (f) Hydrated lime dosage ($kg\ day^{-1}$), (g) Dewatered sludge production ($m^3\ day^{-1}$).

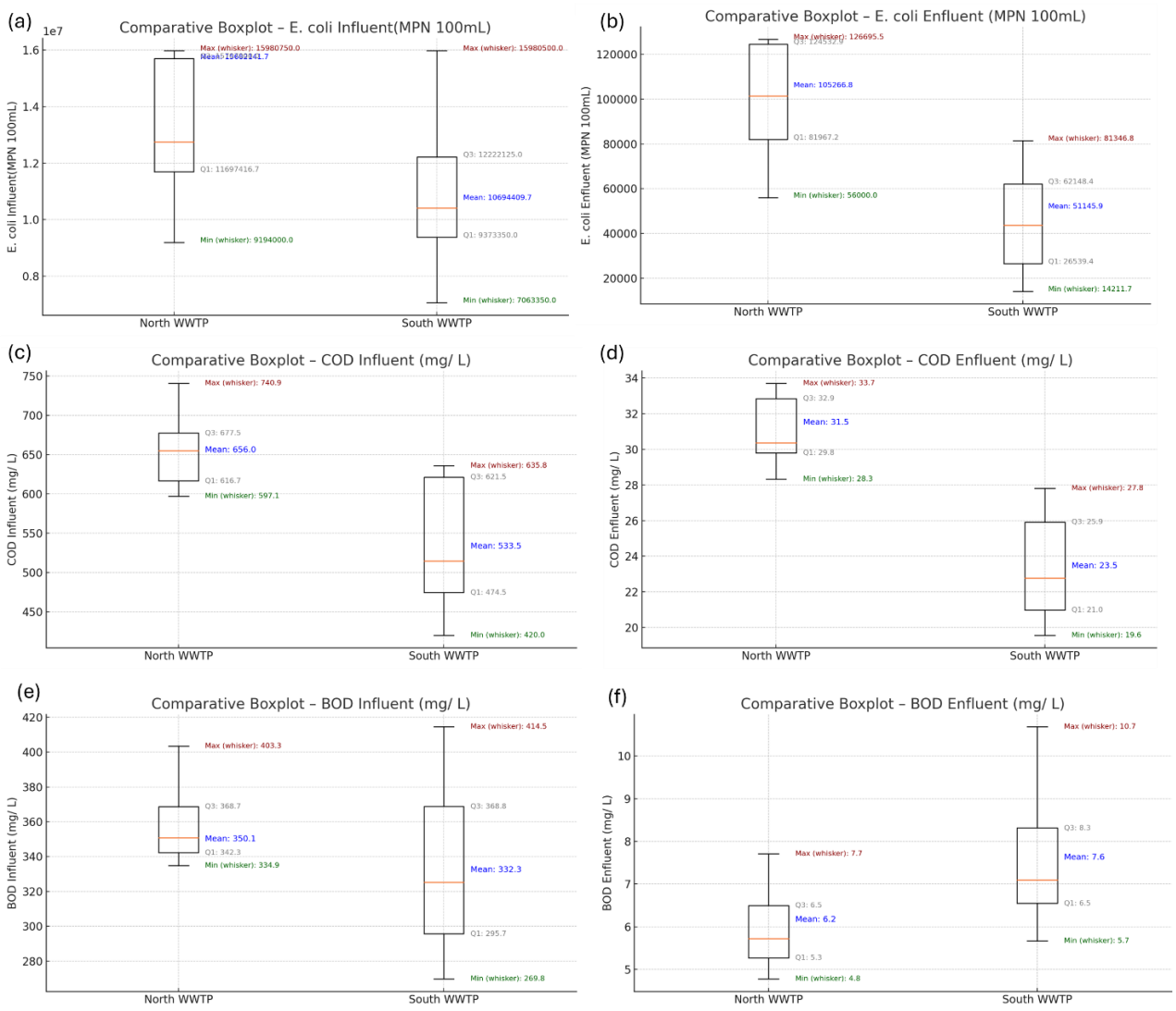

Figure S3.2. Comparative boxplots of operational parameters for the North and South WWTPs.

Each subplot shows the distribution of monthly data from 2020 to 2023, including the mean (blue), first and third quartiles (gray), and whisker limits (green for minimum, red for maximum). (a) E. coli Influent (MPN 100 mL^{-1}), (b) E. coli Effluent (MPN 100 mL^{-1}), (c) COD Influent (mg $^{-1}$ L), (d) COD Effluent (mg L^{-1}), (e) BOD Influent (mg L^{-1}), (f) BOD Effluent (mg L^{-1}).

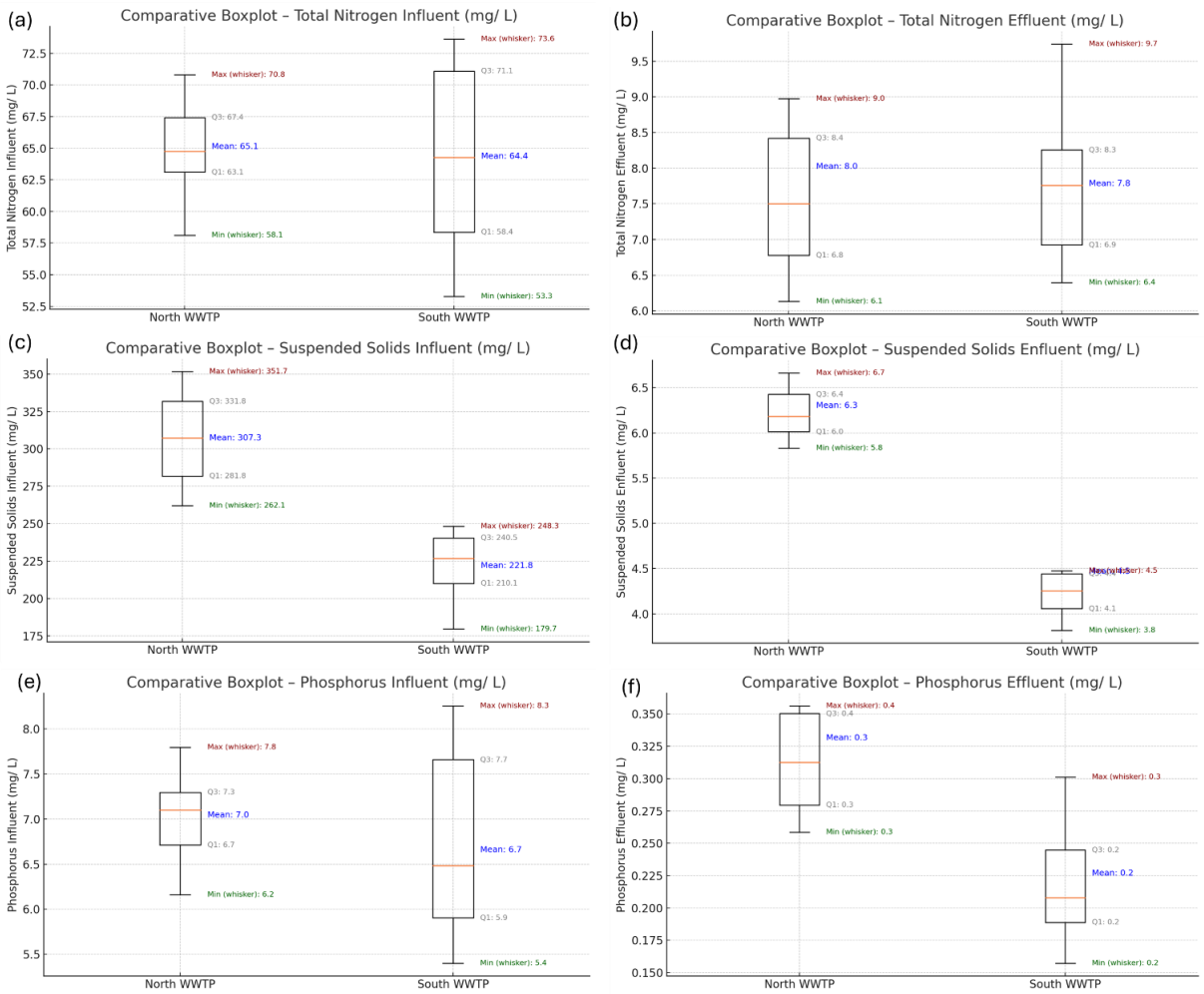

Figure S4.2. Comparative boxplots of operational parameters for the North and South WWTPs.

Each subplot shows the distribution of monthly data from 2020 to 2023, including the mean (blue), first and third quartiles (gray), and whisker limits (green for minimum, red for maximum). (a) Total Nitrogen Influent (mg L^{-1}), (b) Total Nitrogen Effluent (mg L^{-1}), (c) Suspended Solids Influent (mg L^{-1}), (d) Suspended Solids Effluent (mg L^{-1}), (e) Phosphorus Influent (mg L^{-1}), (f) Phosphorus Effluent (mg L^{-1}).

4 Methane exergetic calculations in WWTP'S

4.1 Methodology of calculation

Using the simplified method of Chernicharo (2016).

a) Methane produced in anaerobic reactors and estimation of associated exergy.

i) Equation (S5.2) gives the daily COD influent load to the WWTP reactors theoretically converted into CH_4 relating the daily sewage flow to COD removal.

$$DQO_{CH4} = \dot{Q}(DQO_i - DQO_e) - Y_{DQO}\dot{Q}DQO_i \quad \text{(S5.2)}$$

where, DQO_{CH4} is the daily load of COD convertible to methane (kg day^{-1}); Q˙ is the daily influent flow rate of sewage (m³ day^{-1}); DQO_i e DQO_e are, respectively, the influent and effluent COD concentrations (kg m^{-3}); Y_{DQO} is the solids production coefficient in the system in terms of COD (0.11 to 0.23 kgCODsludge kg COD_influent^{-1}). Y_{DQO} = 0.15 was adopted, an average value used by Chernicharo (2016) for reactors with characteristics and treatment technologies like those of the North and South WWTPs.

ii) Using Equations (S6.2) and (S7.2), the daily flow rate of methane produced is determined.

$$\dot{Q}_{CH_4} = DQO_{CH4}/f(T) \quad \text{(S6.2)}$$

Where f(T) is the correction factor for the reactor's operating temperature (kgCOD/m³):

$$f(T) = PK_{DQO}/R\,(273+T) \quad \text{(S7.2)}$$

where, $\dot{Q}_{CH_4}$, the daily flow rate of methane produced (m³ day^{-1}); P, local atmospheric pressure (atm). In Brasilia, the annual average is 1,020 mbar (1.006662 atm); K_{DQO} the COD corresponding to one mole of CH_4 (64 gCOD mol^{-1}); R the gas constant (0.08206 atm.L mol^{-1}.K^{-1}); T the operating temperature of the reactors (ºC), in the North and South Brasilia WWTPs on average T≈ 21 ºC. Therefore, $f(T)$ = 2.67045 kgCOD m^{-3}.

According to Posseti et al (2021), in an average scenario, approximately 30% of the CH4 produced in wastewater treatment plants is lost dissolved in the treated effluent, 5% in the gaseous phase of the residual gas, and another 5% through leaks and condensate purges. These values are reasonable for the operational conditions of the Brasilia WWTPs.

iii) With these data and considerations, the total biogas production at the stations is determined using Equation (S8.2).

$$\dot{Q}_{biogas} = \dot{Q}_{CH_4}/C_{CH_4} \quad \text{(S8.2)}$$

where $\dot{Q}_{biogas}$ is the daily flow rate of biogas produced (m³ day^{-1}); C_{CH_4} is the concentration of CH4 in the biogas (70%), based on Tables (S7.2) and (S8.2).

Table S7.2. Typical composition of biogas generated in anaerobic reactors at WWTPs.

Compound	Unit	Typical volumetric concentration
$\mathbf{CH_4}$	(%)	60 - 85
$\mathbf{CO_2}$	(%)	5 – 15
CO	(%)	0 – 0.3
$\mathbf{N_2}$	(%)	10 – 25*
$\mathbf{H_2S}$	(ppm)	1,000 – 2,000

* Due to dissolved N_2 in sewage. Source: Chernicharo (2016); Lobato (2011).

Table S8.2. Constants and input data for calculating biogas flow rate.

Values	Units	Value
$\boldsymbol{Y_{COD}}$	(COD sludge (kg) CODapplied (kg^{-1}))	0.15
P	(Atm)	1,004
$\boldsymbol{K_{COD}}$	COD (mo^{-1} L)	64
R	(atm.m^3 mol^{-1} K)	$8.206\ 10^{-5}$
T	(ºC)	26
Additional CH_4 losses	(%)	35
CH_4 concentration in biogas	(%)	70

Source: Chernicharo (2016); Lobato (2011)

iv) The available lower heating value of biogas is calculated using the Equation (S9.2).

$$LHV_d = \gamma b\ LCv_m\ 0{,}00116222 \quad \text{(S9.2)}$$

where, LHV_d is the available lower calorific value of biogas (kWh Nm^{-3}); γb specific weight of the biogas (kg Nm^{-3}); LHV_m lower calorific value of methane (kcal kg^{-1}) contained in the biogas, in the average composition highlighted in Tab. (S9.2); 0.00116222 is the conversion factor from kcal to kWh.

Table S9.2. LHV_d values of biogas relative to biogas composition

Chemical composition of biogas	Specific weight (kg Nm^{-3})	LHV (kcal kg^{-1})
10% CH_4 – 90% CO_2	1.84	465.43
40% CH_4 – 60% CO_2	1.46	2,338.52
60% CH_4 – 40 % CO_2	1.21	4,229.98
65% CH_4 – 35% CO_2	1.15	4,831.14
75% CH_4 – 25% CO_2	1.03	6,253.01
95% CH_4 – 5% CO_2	0.78	10,469.60
99% CH_4 – 1% CO_2	0.73	11,661.02

Source: Chernicharo (2016); Lobato (2011)

v) Finally, using Equation (S10.2), the electrical power available from the combustion of biogas in a generator driven by an Otto cycle engine is determined.

$$\text{Pow} = \dot{Q}_{biogas}\ LHV_d\ \eta_m \quad \text{(S10.2)}$$

where Pow is the electrical power available (kW); $\dot{Q}_{biogas}$ is the total biogas production ($Nm^3 h^{-1}$); LHV_d, lower calorific value of biogas (kW m^{-3}); η_m is the average overall efficiency of Otto cycle engines (approximately 25%).

b Determination of the exergy associated with organic compounds in sewage and dewatered sludge.

The methodology of the exergy analysis of the North and South WWTPs observes, where applicable, the considerations and simplifications applied by Mora Bejarano (2009) to the Barueri WWTP (SP):

a) Operating conditions occur in steady state. The control volume boundary for the wastewater treatment process is around the process. The manufacturing exergy of the chemical substances ($FeCl_3$, CaO and polymers) or other products used in the different stages of treatment is not calculated. The exergy considered is that of the compound and the product itself.

b) In the exergy analysis of the wastewater treatment process, the input data are the actual average monthly/annual operating values. The dilution of chemical compounds or the exergy of clean water is not considered (Huang et al., 2007; Hellström, 1997).

c) The chemical exergy of organic matter ($E_{org,mat}$) is calculated using Equation (S11.2), proposed by Kosravi, Panjeshay and Atei (2013), modified from the equation by Tai; Matsushige and Goda (1986), related to the chemical oxygen demand (COD).

$$E_{org,mat.} = 13.7\ COD - 116 \qquad (S11.2)$$

d) According to Mora Bejarano (2009), the exergy of the workforce operating WWTPs is not significant compared to flows such as the theoretical exergy of organic matter, as stated in a). Therefore, the calculations only involve the exergy flows of organic and inorganic compounds and nutrients contained in the sewage, byproducts generated such as dewatered sludge (biosolids), methane, chemical compounds used in the sludge stabilization process, in improving the primary sedimentation process, and electricity consumption. The exergy associated with the buildings is not also considered.

e) Sewage is considered a fluid with a pollutant load, and the exergy of the pollutants is their chemical exergy, a measure of the potential of pollutants in the body of water to cause damage to the aquatic environment, according to Huang *et al.* (2007). Wastewater is composed of approximately 99.9% water and 0.1% dissolved suspended solids, which can

be removed by appropriate treatment, according to Von Sperling (1996).

f) Mora Bejarano (2009) and Owen (1982) considered the molecular mass of sewage to be that of the substance $C_{10}H_{18}O_3N$.

g) The exergy of NO_3^- is calculated by interpolating data for NO and NO_2 (Ayres; Ayres; Martinás, 1997).

h) The chemical exergy of the influent and effluent flows in the wastewater treatment process and in the dewatered sludge are determined by Equation (S12.2) on a total molar basis of a mixture composed of *i* chemical species.

$$\bar{b}_{chi} = \sum \left(\mu_i - \mu_{0,i}\right) x_i + RT_0 \sum x_i \ln\left(a_i\right) \qquad \text{(S12.2)}$$

The following simplifying assumptions are considered in the calculation:

I. Non-ideal mixing (activity ≠ molar fraction, $a_i \neq x_i$) for the influent and effluent flows of the WWTPs

II. Ideal mixture (activity = molar fraction, $a_i = x_i$) for the dewatered sludge produced in WWTPs.

III. The activity (a_i) of organic and inorganic substances in the influent and effluent flows of the processes is calculated by the formula: $a_i = r_i\, m_i$; where r_i is the activity coefficient and mi is the molality of substance i.

IV. The activity coefficient is determined by Equation (S13.2) applying the Debye–Huckel theory for aqueous solutions (Mora Bejarano, 2009).

$$\text{Ln}\,(r_i) = (-A_{DH}\, z_i^2\, I^{1/2})/(1 + B_{DH}\, \Phi_i\, I^{1/2}) \qquad \text{(S13.2)}$$

where, A_{DH} = 0,51 (kg $mol^{-1})^{1/2}$ (Debye-Huckel constant, for water at 25 °C); B_{DH} = 3.287 10^9 (kg $mol^{-1})^{1/2}$ m (Debye-Huckel constant, for water at 25 °C); z_i = ionic charge or valence; $\Phi_i = (2\ 10^{-8} - 5\ 10^{-8})$ m (effective diameter of the ion in the solution); $I = 0.5 \sum m_i\, z_i^2$ (ionic strength, which considers the effects of other ions in the solution calculated by the equation).

And so,

$$\text{Ln}\,(r_i) = \{[-0.51\, z_i^2\, I^{1/2}]/(1 + 3.287\ 10^9\, 3.5\ 10^{-8}\, I^{1/2}\} \qquad \text{(S14.2)}$$

5 Exergy balance

Equation (S15.2) gives the exergy balance

$$(\Sigma \dot{E}_e - \Sigma \dot{E}_s) = (\Sigma \dot{E}_p + \dot{E}_d) \quad \text{(S15.2)}$$

Where, $\Sigma \dot{E}_e$ - incoming exergy flow, or exergy of the influent sewage (including COD of the influent sewage) and the exergy of electrical energy; $\dot{E}_s$ - outgoing exergy flow, or exergy of the final effluent (including COD of the final effluent); $\Sigma \dot{E}_p$ – lost exergy flow, or exergy of the dewatered sludge, considering that the sludge is not currently used for agricultural or other purposes, but disposed of in a sanitary landfill. $\dot{E}_d$ - Destroyed exergy, or exergy associated with the burning of the methane produced and the irreversibilities in sewage treatment.

Table S10.2 shows a summary of Mora Bejarano's (2009) study on the specific chemical exergy of the Barueri WWTP, whose treatment process is like that of the North and South WWTPs in Brasília. Except for dewatered sludge, COD and NH_3 account for the largest percentage of the specific chemical exergy of organic matter. The chemical exergy of the other compounds, mainly metals, is not quantitatively significant, even though the plant treats industrial wastewater with a considerably higher iron content.

Table S10.2 – Chemical exergy of sewage from the city of São Paulo treated at the Barueri WWTP.

Composition	Chemical exergy specific		
	(kJ L^{-1}	(%) partial	(%) total
Sewage affluent			
COD	2.6400	92.47	97.51
NH_3.	0.2012	7.04	
Others*	0.0139	0.49	0.49
Sewage effluent)			
COD	0.1660	64.84	93.47
NH_3.	0.0733	28.63	
SO_4.	0.0123	4.80	4.80
Others*	0.0044	1.73	1.73
Dewatered sludge			
COD	44.8000	20.55	99.45
Iron	172.0000	78.90	
Other metals	1.20000	0.55	0.55

* NO_2, S_2, SO_4, phenols, surfactants, and iron and other metals. Source: Mora Bejarano (2009).

6 Organic matter exergies in sewage and dewatered sludge.

6.1- Sewage and dewatered sludge for Brasilia North WWTP

Table 11.2 – Input data for calculating the exergy of organic matter compounds in sewage and dewatered sludge.

Phase	Sewage affluent (524.4 L s^{-1})			Sewage effluent (524.4 L s^{-1})			Dewatered Sludge (0.68 L s^{-1})		
Units	mg L^{-1}	MW (mg mol^{-1})	Mol L^{-1}	mg L^{-1}1	MW (mg mol^{-1})	Mol L^{-1}l	mg L–1	MW (mg mol^{-1})	Mol L^{-1}
Operational data									
COD	656.00	200,254.80	3.28E-03	31.50	200,254.80	1.57E-04	1370.00	97,120.00	1.41E-02
Nitrogen	65.10	18,040.00	3.61E-03	8.00	18,040.00	4.43E-04	52.72	18,040.00	2.92E-03
Phosphor	7.04	97,995.20	7.18E-05	0.30	97,995.20	3.37E-06	73.40	97,995.20	7.49E-04
Iron	2.59	55,845.00	4.64E-05	0.40	55,845.00	6.49E-06	0.64	55,845.00	1.15E-05

Table S12.2 - Exergy of the main compounds in the mixture

Phase	a_i	x_i	E^0_{ch,n_e}*	$\sum_i(\mu_i - \mu_{0,i})$ x_i (1)	RT_0	$ln(a_i)$	$RT_0 \sum x_i \ln(a_i)$ (2)	(1) + (2)	$(E_{ch,f} + E_{ch,c})$	
Units	(mol L^{-1})	(mol mol^{-1})	(kJ mol^{-1})	(kJ mol^{-1})	(kJ mol^{-1})		(kJ mol^{-1})	(kJ mol^{-1})	(kJ L^{-1}	(kW)
	Sewage affluent									
COD	3.28E-03	0.46802	2,704.63	1,265.8315	2.478	-5.7199	-6.6350	1,259.1965	4.1302	2,165.86
Nitrogen	3.61E-03	0.51511	337.21	173.7025	2.478	-5.6240	-7.1801	166.5224	0.6011	315.24
Phosphor	7.18E-05	0.01025	870.26	8.9159	2.478	-9.5416	-0.2423	8.6736	0.0006	0.33
Iron	4.64E-05	0.00662	374.16	2.4773	2.478	-9.9782	-0.1637	2.3135	0.0001	0.06
Total	7.01E-03	1.00000	4,286.27	1,450.9271			-14.221	1,436.71	4.732	2,481.48
	Sewage effluent									
COD	1.57E-04	0.25744	2,009.87	517.41	2.478	-8.759	-5.589	511.8250	0.0804	42.14
Nitrogen	4.43E-04	0.72640	337.21	244.95	2.478	-7.722	-13.902	231.0487	0.1024	53.67
Phosphor	3.37E-06	0.00553	870.26	4.809	2.478	-12.601	-0.173	4.6363	0.0000	0.01
Iron	6.49E-06	0.01064	374.16	3.982	2.478	-11.945	-0.315	3.6667	0.0000	0.01
Total	6.10E-04	1.00000	3,591.50	771.15			-19.979	751.177	0.1828	95.83
	Dewatered sludge									
COD	1.41E-02	0.79300	1,322.91	1,049.0706	2.478	-4.2616	-8.3758	1,040.6948	14.6738	9.98
Nitrogen	2.92E-03	0.16422	337.21	55.3789	2.478	-5.8362	-2.3755	53.0034	0.1548	0.11
Phosphor	7.49E-04	0.04212	870.26	36.6594	2.478	-7.1968	-0.7514	35.9080	0.0269	0.02

Iron	1.15E-05	0.00065	374.16	0.2420	2.478	-11.3732	-0.0182	0.2238	0.0000	0.00
Total	1.78E-02	1.00000	2,904.54	11,41.351			-11.521	11,29.83	14.856	10.10

*(E^0_{ch,n_e} x MW (Molecular Weight)

5.2 – Sewage and dewatered sludge for Brasilia South WWTP

Table S13.2 - Input data for calculating the exergy of organic matter compounds in sewage and dewatered sludge.

Phase	Sewage affluent (1,250.8 Ls^{-1})			Sewage effluent (1,250.8 l/s^{-1})			Dewatered sludge (1.346 l/s^{-1})		
Units	mg L^{-1}	MW (mg mol^{-1})	Mol L^{-1}	mg L^{-1}	MW (mg mol^{-1})	Mol L^{-1}l	mg L^{-1}	MW (mg mol^{-1})	Mol L^{-1}
Operational data									
COD	533.50	200,254.80	2.66E-03	23.50	20,0254.80	1.17E-04	1,100.00	97,120.00	1.13E-02
Nitrogen	64.30	18,040.00	3.56E-03	7.80	18,040.00	4.32E-04	59.13	18,040.00	3.28E-03
Phosphor	6.66	97,995.2	6.80E-05	0.23	97,995.20	2.35E-06	45.09	97,995.2	4.60E-04
Iron	2.11	55,845.00	3.78E-05	0.30	55,845.00	5.29E-06	0.58	55,845.00	1.04E-05

Table S14.2 - Exergy of the main compounds

Calculation step	a_i	x_i	E^0_{ch,n_e}*	$\sum_i(\mu_i - \mu_{0,i})\,x_i$ (1)	RT_0	$ln(a_i)$	$RT_0 \sum x_i \ln(a_i)$ (2)	(1) + (2)	$(E_{ch,f} + E_{ch,c})$	
Units	(mol L^{-1})	(mol mol^{-1})	(kJ mol^{-1})	(kJ mol^{-1})	(kJ mol^{-1})		(kJ mol^{-1})	(kJ mol^{-1})	(kJ l^{-1})	(kW)
Sewage affluent										
COD	2.66E-03	0.42050	2,704.12	1,137.081	2.478	-5.9294	-6.1775	1,130.9039	3.0082	3,762.66
Nitrogen	3.56E-03	0.56277	337.21	189.775	2.478	-5.6380	-7.8613	181.9141	0.6476	810.04
Phosphor	6.80E-05	0.01075	870.26	9.355	2.478	-9.5960	-0.2556	9.0994	0.0006	0.77
Iron	3.78E-05	0.00598	374.16	2.236	2.478	-10.1832	-0.1508	2.0850	0.0001	0.10
Total	6.33E-03	1.00	4,285.75	1,338.45			-14.4452	1,324.0024	3.6565	4,573.57
Sewage effluent										
COD	1.17E-04	0.21019	1,760.26	369.988	2.478	-9.0533	-4.7147	365.2731	0.0427	53.46
Nitrogen	4.32E-04	0.77609	337.21	261.707	2.478	-7.7471	-14.8965	246.8101	0.1066	133.36
Phosphor	2.35E-06	0.00422	870.26	3.674	2.478	-12.9611	-0.1356	3.5384	0.0000	0.01
Iron	5.29E-06	0.00950	374.16	3.556	2.478	-12.1497	-0.2861	3.2697	0.0000	0.02

Total	5.57E-04	1.00	3,341.89	638.924			-20.0328	618.8914	0.1494	186.85
Dewatered sludge										
COD	1.13E-02	0.75081	1,323.36	993.595	2.478	-4.4830	-8.3393	985.2555	11.1334	14.99
Nitrogen	3.28E-03	0.21793	337.21	73.490	2.478	-5.7199	-3.0885	70.4020	0.2309	0.31
Phosphor	4.60E-04	0.03056	870.26	26.599	2.478	-7.6843	-0.5819	26.0166	0.0120	0.02
Iron	1.04E-05	0.00069	374.16	0.259	2.478	-11.4737	-0.0196	0.2389	0.0000	0.00
Total	1.51E-02	1.00000	2,905.00	1,093.942			-12.0294	1,081.9130	11.3763	15.31

*(E^0_{ch,n_e} x MW).